ROLE OF ACTIVIN RECEPTOR-LIKE KINASE 1 (ALK1) IN REGULATION OF ANGIOGENESIS

By

EUN-JUNG CHOI

A DISSERTATION PRESENTED TO THE GRADUATE SCHOOL
OF THE UNIVERSITY OF FLORIDA IN PARTIAL FULFILLMENT
OF THE REQUIREMENTS FOR THE DEGREE OF
DOCTOR OF PHILOSOPHY

UNIVERSITY OF FLORIDA

2009

To my loving mom, husband and sister

ACKNOWLEDGMENTS

There have been so many people who have helped me complete my graduate work. I would like to give my great thanks to all of them from the bottom of my heart. I am sure that I would never follow my queries in science this far without them.

I thank my loving family for their unconditional and endless love, encouragement and support. Especially, my mom, In-Sook Kim, always cheers, inspires and strengthens me in the ups and downs throughout my life. I am so grateful to my wonderful and lovely husband, Koo Yung Jung. He is always my big brother who constantly loves, cares and motivates me. I also thank my sister, Su-Jung Choi for her lifetime friendship with me sharing good and bad times.

I would like to give my special thanks to my mentor Dr. S. Paul Oh for his outstanding support and guidance. I have been inspired and awed by his persistent passion toward science. Dr. Oh helped me gain an understanding of critical thinking and creativity that are absolutely needed in the field of research. He also helped me build my enthusiasm and knowledge to succeed in science. I also thank my dissertation committee members, Dr. Satya Narayan, Dr. Daiqing Liao and Dr. Chen Liu for their constructive comments, assistance and encouragement. I also truly acknowledge professors from my undergraduate study, Drs. Tae-Young Jung, Chang-Won Kang, Gil-Saeng Jung, Hong-Yang Park and Hoon-Taek Lee for being continuously mentors and supporters.

I am also indebted to all past and current Oh lab members for providing great companionship. I am especially grateful to Naime Fliess for not only her help in research but also her kindness and support. Her pleasant personality, generosity and great sense of humor made our lab a friendly and warm place. I would like to acknowledge Dr. Young-Jae Lee and Melissa Chen for their advice and assistance in working with cells. I truly thank Dr. Chastity Bradford for her helpful discussions, Ha-Long Nguyen and Jairo Tabora for their generous helps

in preparation of presentations and writings. I would also like to thank Kwon-Ho Hong and Chul Han for their great friendship and helps scientifically and personally. Lastly, I would like to express my gratitude to Kimberly Hodges for her kind assistance and concern on handling all administrative works properly and timely.

TABLE OF CONTENTS

LIST OF TABLES

LIST OF FIGURES

Abstract of Dissertation Presented to the Graduate School
of the University of Florida in Partial Fulfillment of the
Requirements for the Degree of Doctor of Philosophy

ROLE OF ACTIVIN RECEPTOR-LIKE KINASE 1 (ALK1) IN REGULATION OF ANGIOGENESIS

By

Eun-Jung Choi

August 2009

Chair: S. Paul Oh
Major: Medical Sciences—Molecular Cell Biology

Hereditary hemorrhagic telangiectasia (HHT), also known as Rendu-Osler-Weber syndrome, is a genetic vascular disease inherited in an autosomal dominant manner. Its clinical manifestations are recurrent nosebleeds, multiple mucocutaneous hemorrhages and arteriovenous malformations (AVMs) in multiple organs including the brain, lung, liver and gastrointestinal tract. Three distinctive types of HHT have been categorized depending on their different disease-causing genes. The HHT type 1 (HHT1), type 2 (HHT2) and a combined syndrome of HHT and Juvenile Polyposis (JP-HHT) are predisposed by various homozygous mutations in *ENDOGLIN* (*ENG*), *Activin receptor-Like Kinase 1* (*ACVRL1*; *ALK1*) and *SMAD4* genes, respectively. Interestingly, all of these genes encode proteins that are implicated in the transforming growth factor (TGF)-β superfamily signaling. Therefore, HHT has been considered as a TGF-β disease.

Previously, our *in vivo* studies have demonstrated that conditional deletion of the *Alk1* gene in endothelial cells (ECs) is sufficient for development of AVMs in various vascular beds. In order to investigate the molecular mechanism by which endothelial Alk1-deficiency leads to AVM formation, we have characterized *Alk1*-null pulmonary endothelial cell lines at the biochemical and cellular levels. We found that *Alk1*-null pulmonary ECs displayed significantly

increased migratory properties *in vitro* and *in vivo* in response to an angiogenic factor. In tube forming assays on Matrigel, *Alk1*-null ECs formed a vascular network with higher density, length, and thickness compared to corresponding control ECs, indicating that ALK1 may modulate responses to an angiogenic stimulus during angiogenesis. Interestingly, while an inhibitory effect of BMP-9 in tube formation was blunted in *Alk1*-null ECs, BMP-9-mediated downstream SMAD1/5 phosphorylation was unaffected. Taken together, this data suggest that ALK1 is an important cellular modulator for angiogenic stimuli during angiogenesis via a SMAD-independent pathway.

Since ALK1-deficient ECs form AVMs in angiogenic environment, we examined whether ALK1-deficiency can impact tumor formation or growth by inducing non-productive blood vessels feeding to tumor. We observed that *Alk1*-deletion considerably inhibited formation and growth of Lewis lung carcinoma (LLC). We found numerous AVMs in the peripheral tumor microcirculation and disorganized blood vessels in the tumor. This data indicate that ALK1 can be a novel target of tumor angiogenic therapy.

CHAPTER 1
INTRODUCTION

Organization of Vascular Network

The development and maintenance of blood circulation are essential processes for the vertebrate life. The blood circulation throughout the body is achieved through blood vessels which roughly consist of arteries, veins and capillaries. The hierarchical vascular system is organized into a functional vascular network required and established by a fine-tuned orchestration of the cross-talk between numerous molecular signaling pathways and several different cell types during the developmental stages (1). It functions mainly to deliver adequate supplies including oxygen and nutrients and eliminate wastes.

Anatomy and Function of Blood Vessels

Capillaries are the thinnest and most ample blood vessels (1). The structure of their walls consists of a single layer of endothelial cells (ECs; endothelium) surrounded by a layer of a basement membrane (BM) and pericytes. Such a structure allows the exchange of molecules between blood and tissues. As compared to capillaries, arterioles and venules are sheathed with more mural cells (1), acting as a bridge between arteries and veins with capillary beds. Arteries and veins share the same fundamental structure (1). The walls of these large vessels are comprised of three layers from the inner most layer to the outer most layer: an intima, media and adventitia. The intima and media are sheets containing endothelial cells and smooth muscle cells (SMCs), respectively, while the adventitia is a zone comprised of fibroblasts, an extracellular matrix (ECM) and elastic laminae. The vascular diameter, vessel tone and blood flow are modulated by SMCs and elastic laminae.

Vascular Circulatory System

The circulation is a tightly regulated and closed system that delivers blood throughout the body. It starts from the left ventricle of the heart from which oxygenated blood enters into arteries. The arteries are connected to arterioles that lead arterial blood into the capillary bed. The capillary bed is a network of the smallest and the thinnest blood vessels where the blood supplies oxygen, water and nutrients to surrounding tissues as well as removes local carbon dioxide and waste products. The deoxygenated blood flows from the capillary bed through venules into the veins and returns to the heart. As capillaries provide actual conduits enabling blood to supply all tissues of the body, its sustained permeability is crucial for ensuring molecular exchanges and maintaining vascular homeostasis.

Angiogenesis

Nascent blood vessels are formed by two processes: vasculogenesis and angiogenesis. Vasculogenesis occurs mainly during embryonic development in which a primary capillary plexus is established from the differentiation of endothelial progenitor cells (2). On the other hand, angiogenesis refers the formation of new blood vessels by sprouting or splitting from pre-existing vessels during both development and in postnatal life (3). In the adult, angiogenesis is usually initiated in response to either physiological or pathological stimuli. Physiological angiogenesis takes place during wound healing, inflammation(4, 5), in the female reproductive system (6) and is tightly regulated. However, in pathological conditions, such as proliferative retinopathy, rheumatoid arthritis and tumorigenesis (4, 5), it is uncontrolled.

Types of Angiogenesis

Two distinctive types of angiogenesis have been described (7). One is sprouting angiogenesis, which is the true branching of capillaries from pre-existing vessels. It begins with degradation of ECM by proteolytic enzymes, followed by migration and proliferation of ECs

towards an angiogenic stimulus. After formation of the vascular lumen, the vascular endothelium is stabilized and functionally mature (7). On the other hand, non-sprouting angiogenesis, also known as intussusception, is initially seen in the embryonic lung (7, 8). It occurs when the vessel lumen widens and pre-existing vessels are subsequently split by transcapillary pillars, following proliferation of vascular ECs (7). It is also caused by coalescence and division of capillaries.

Overview of Angiogenesis

Angiogenesis is a multiple step process that is roughly divided into two phases of activation and resolution (9-12). The activation phase is characterized by initiation and progression steps. Upon angiogenic stimuli, permeability of pre-existing capillaries or post-capillary venules is increased. EC migration and sprouting into ECM follows basement membrane degradation. ECs then proliferate and form a capillary lumen. Conversely, during the resolution phase, EC proliferation and migration are inhibited and BM is reconstituted. ECs then differentiate and recruit perivascular cells to promote maturation and stabilization of newly formed vessels.

Angiogenic Signaling Pathways

Many signaling pathways underlying angiogenesis have been identified from genetic studies of animal models (7, 11). The most extensively investigated ones are the vascular endothelial growth factor (VEGF), fibroblast growth factor (FGF) and transforming growth factor (TGF)-β receptors and their ligands families. Recently, more angiogenic pathways have been discovered (13), such as the Notch/Delta(14-16) ,Eph/Ephrin (17, 18), Hedgehog (19), Sprouty (20) and Roundabout/Slit (19, 21, 22) families. These were initially found to play crucial roles in embryonic vascular development and differentiation. Thus, finding these involved in postnatal angiogenesis allows us to broaden our understanding of developmental blood vessel establishment as well as physiological and pathological angiogenesis.

Vascular Endothelial Growth Factor (VEGF) Family Signaling

The VEGF family includes three tyrosine kinase receptors (VEGFR-1, -2 and -3), seven ligands (VEGF-A, -B, -C, -D, -E, placenta growth factor (PLGF)-1 and -2) and two co-receptors (neuropilin (NRP)-1 and -2) (13, 23). Several of the VEGF ligands exert various angiogenic effects depending on their different binding specificities for each of three receptors. The signal is then tranduced through several identified secondary pathways, such as the Akt and MAPK pathways (13).

Originally, two receptors, VEGFR-1 (24) and VEGFR-2 (25) , were discovered on ECs (23). VEGFR-1, also known as FLT-1 (fms-like tyrosine kinase 1), binds to VEGF-A, VEGF-B and PLGF. It functions differently depending on developmental stages, physiological and pathological conditions and cell types (23). It is known as a potent VEGF antagonist for VEGF activity either by binding to VEGF with high affinity (26) or by inhibiting VEGFR-2-regulated signaling (27). VEGFR-2, also known as KDR (kinase insert domain receptor), is a receptor for VEGF-A, VEGF-C and VEGF-E (13, 23). It is known as the main receptor mediating effects of VEGF-A on EC proliferation, migration, invasion, survival (28, 29) and permeability of microvessels (30) during angiogenesis. It has been reported that activation of VEGFR-2 alone could efficiently induce angiogenesis *in vitro* and *in vivo* (23, 31). Lastly, VEGFR-3, also known as FLT-4 (fms-like tyrosine kinae 4), binds to VEGF-C, VEGF-D (13, 23) and is highly expressed in embryonic developmental vasculature (13). In the adult, it is present in lymphatic vessels and implicated in lymphangiogenesis (23, 32, 33). However, its persistent role in the vasculature regulating VEGFR-2 signaling to maintain vascular integrity has been also suggested (23, 34).

Fibroblast Growth Factor (FGF) Family Signaling

In vertebrates, there are 22 polypeptide growth factor (FGF1-14 and 16-23) and four tyrosine kinase receptor (FGFR-1, -2, -3, and -4) members of the FGF family (35). They have multiple functions on various cell types that are strictly modulated by the activity and receptor specificity of FGF (35). In the embryonic development, their functions are involved in patterning, limb formation, brain development as well as mesoderm and neural induction (36) via control of cell proliferation, migration and differentiation (35). In adult stages, they regulate wound healing and angiogenic processes. During angiogenesis, acidic FGF (FGF1) and basic FGF (FGF2) play significant roles in elevating EC proliferation and tube formation (37). They are believed to be more potent angiogenic factors than VEGF or platelet-derived growth factor (PDGF) (37).

Transforming Growth Factor (TGF)-β Superfamily Signaling

The TGF-β superfamily is consisted of three types of serine/threonine kinase transmembrane receptors, including type I (RI), type II (RII), type III (RIII), and several ligands (TGF-βs, activins, bone morphogenetic proteins (BMPs), growth and differentiation factors (GDFs) and nodal) (38, 39). They control various biological processes such as embryogenesis, embryonic patterning, growth, cell cycle regulation and immunosuppression (38, 40, 41) through their influence on proliferation, migration, differentiation and survival of several cell types (39, 42, 43). Furthermore, from genetic studies of mice lacking different TGF-β members, the importance of TGF-β family for vascular development and homeostasis maintenance has been well established (7, 11, 38).

The cellular effects of TGF-β superfamily are diversified by combinatorial associations between its receptors and ligands (38, 39, 44). In general, dimeric type II receptors are associated with one of ligands and recruit a specific type I receptor, forming a heteromeric complex. The

auto-phosphorylated type II receptor phosphorylates the type I receptor. The activated type I receptor then transduces the signal by phosphorylating as series of intracellular signaling molecules, the SMADs. Depending on the ligand/receptor activated, there are two TGF-β SMAD-dependent pathways distinguished by the type of receptor-regulated SMADs (R-SMADs) mediating the signal. SMAD 2/3 is involved with the TGF-β pathway, while SMAD1/5/8 modulate BMP signals (45-48). After their phosphorylation by the type I receptor, R-SMADs make heteromeric complexes with the common-SMAD (co-SMAD), named SMAD4. Finally, these complexes translocate into the nucleus where they interact with transcription factors and co-factors (co-activators and co-repressors) to control target gene expression (49, 50). Additionally, this signaling transduction can be enhanced by auxiliary co-receptors (type III receptors), like ENDOGLIN and β-GLYCAN, at the cell surface (48) or impeded by the binding of inhibitory-SMAD6 and SMAD7 (I-SMADs) to the heterodimeric receptor complex (39) (Figure 1-1).

Notch/Delta Family Signaling

Notch signaling was originally identified in the development of *Drosophila* (15). It consists of four Notch receptors (Notch-1, -2, -3 and -4) and five ligands (Jagged-1, -2, Delta-1, -3 and -4) (13, 16) and transduces the signal through the association between one cell-bound ligand and another nonautonomous cell containing a receptor (13). Upon the activation of Notch, its intracellular domain is cleaved, released and subsequently translocated into the nucleus to activate target genes that inhibit differentiation of cells and cause cells to proliferate. All members are widely present in at least one type of blood vessels (e.g. arteries, veins or capillaries) or vascular structures, like VSMCs or pericytes (13). However, only Notch-4 and Delta-4 are expressed in capillaries (51). Moreover, Notch-4 is arterial specific (52), while Delta-like 4 is specifically expressed in ECs (53, 54).

It was shown that Notch signaling plays an important negative role on endothelial functions during angiogenesis (55). Recently, it has been suggested that VEGF signaling regulates Notch receptor and Delta ligand gene expression (56, 57). It was shown that VEGF through VEGFR-1 and VEGFR-2, but not basic FGF (FGF2), induced expression of Notch-1 and its ligand Dll4 (Delta-4) in human arterial endothelial cells (HAECs) (56). Another study further demonstrated that in capillary-like network formation and in activation of Notch-1, Notch-4, VEGFR-2 was downregulated, resulting in inhibition of EC proliferation in response to VEGF, but not bFGF (57). It is noteworthy to mention that expression of Dll4 is almost absent in adult tissues; however, it is highly expressed in the areas where angiogenesis is active and in the tumor vasculature (13, 51, 53). And upon the activation of Dll4 by VEGF signaling, it makes a negative feedback loop to block VEGF-induced tumor angiogenesis (57, 58).

Eph/ephrin Family Signaling

Similar to the Notch/Delta family members, Eph receptors and ephrin ligands are both membrane-bound proteins (13, 51). Eph receptors are transmembrane molecules containing a tyrosine kinase activity and divided into two groups, EphA and EphB. Depending on how they are inserted into the plasma membrane, ephrin ligands are classified into A and B types and show remarkable indiscrimination towards receptor binding (13, 51). These family members are present in a broad range of tissues during embryonic and adult stages. Nonetheless, several Eph receptors and ephrin ligands, including the EphB3 and EphB4 receptors and ephrinA1, ephrinB1 and ephrinB2 ligands, have been identified to be specifically expressed in vascular endothelium (13, 51). It has been suggested that ephrinA1 is involved in inflammatory angiogenesis activated by tumor necrosis factor-α (TNF-α) (13, 51, 59), while ephrinB1 increases endothelial capillary-like network formation and cell attachment *in vivo* (13, 51, 60).

Other Family Signaling

There are three human homologues of the *Drosophila hedgehog* gene; *sonic hedgehog* (*SHH*), *desert hedgehog* (*DHH*) and *Indian hedgehog* (*IHH*) (13, 51). These associate with the Patched1 receptor to activate the transcription factors Gil1, Gil2 and Gil3. Hedgehog signaling is important for the formation of limb, bone, lung, gut and hair follicles (51). The expression patterns of three hedgehog proteins are different and deficiency of each one results in distinct phenotypic defects (13, 51). A role for the Hedgehog signaling in angiogenesis was implied by evidence showing that its dysregulation causes vascular defects. SHH did not affect EC proliferation or migration *in vitro* (19). However, it induced expression of VEGF, angiopoietins-1 and -2 from interstitial mesenchymal cells, suggesting an indirect role in angiogenesis by exerting its upstream function on angiogenic factors (19). Furthermore, in mice, administration of SHH resulted in unique enlarged vessels in ischemic hind limbs, indicating its potent angiogenic activity *in vivo* (19).

In mammals, four intracellular isoforms of Spry have been identified. Sprouty (Spry) was initially discovered as an inhibitor of FGF signaling in the development of *Drosophila* tracheal system (13, 51). Because of many similarities between mammalian angiogenesis and *Drosophila* tracheal development, a role of Spry in angiogenesis was expected (13, 51). The first *in vivo* evidence was reported to show an inhibitory role for Spry during angiogenesis (20). It was found that overexpression of the mouse Spry4 (mSpry4) derived by a recombinant adenoviral vector in the endothelium of a developing mouse embryo resulted in reduced branching of small vessels from large vessels (20). Moreover, in human umbilical vein endothelial cells (HUVECs), *in vitro* mSpry4 transfection led to decreased cellular migration and cell cycle arrest at the G1/S phase through receptor tyrosine kinase pathways such as bFGF (FGF2)- or VEGF-induced MAPK signaling (13, 20, 51).

Lastly, there are two Roundabout receptors and three Slits in human (51). The expression of these family members was believed to be restricted to cells of neuronal lineage and they are implicated in regulation of repulsive axonal guidance (21, 61). However, a novel Roundabout receptor, magic roundabout (ROBO4), has been recently identified to be exclusively expressed in ECs (62). Under physiological conditions, it is absent in adult tissues, however, it is strongly expressed in some tumor vasculature including bladder, brain, and colon-metastatic liver tumors (22). In this respect, ROBO4 is emerging as a promising antiangiogenic therapeutic target (13, 51).

Hereditary Hemorrhagic Telangiectasia (HHT)

Disrupted TGF-β signaling has been implicated in a diversity of diseases including cancer, autoimmune diseases, fibrosis and vascular disorders (44, 63, 64). HHT, also known as Osler-Rendu-Weber syndrome, is an autosomal dominant vascular disease characterized by epistaxis (spontaneous and recurrent nosebleeds), mucocutaneous telangiectases and arteriovenous malformations (AVMs) in internal organs such as brain, lung, liver and gastrointestinal tract (38, 44, 65, 66). It affects 1 in 5,000 - 10,000 individuals (67-69) worldwide. Various types of mutation have been mostly identified in three genes. *ENDOGLIN* (*ENG*) is responsible for HHT type 1 (HHT1) (70-73), *Activin receptor-Like Kinase 1* (*ALK1*) is accountable for the HHT type 2 (HHT2) (74-76) and *SAMD4* is associated with a combined syndrome of HHT and Juvenile Polyposis (JP-HHT) (77).

Clinical Features of HHT

The clinical symptoms of HHT are highly variable even within the same HHT family. HHT is diagnosed by clinical and molecular methods (78). In terms of clinical evaluation, the affected individual is initially diagnosed to have HHT by the presence of at least three manifestations according to the Curacao criteria: 1) spontaneous recurrent nosebleeds

(epistaxes), 2) multiple mucocutaneous telangiectasias on the lips, tongue, oral mucosa, or fingertip, 3) visceral involvement (AVM in the brain, lung, liver, gastrointestinal tract, or spine) and 4) appropriate family history (65). Confirmation by molecular testing is by a genetic test for mutations in the *ENDOGLIN*, *ALK1* and *SMAD4* genes (78). Spontaneous recurrent nosebleeds are the earliest and most common clinical indications of HHT (78). On average, telangiectases of the skin and mucosa typically appear when a person is in their 30's and worsen with age. Many patients suffer mild symptoms and live a normal life span (78). A majority of patients possess AVMs in at least one of following: pulmonary (~50%), hepatic (~30%), cerebral (~10%), spinal (~1%) circulations, but are usually asymptomatic (78, 79). Complications that arise from HHT symptoms involve chronic and severe anemia, stroke and brain abscess. Rarely, more severe complications can lead to deep venous thromboses, symptomatic liver disease, severe pulmonary hypertension, pregnancy-related death and spinovascular accidents (78).

Arteriovenous Malformation (AVM)

AVM is the hallmark vascular lesion of HHT. It is a focal pathological condition where arteries and veins are interconnected without intervening capillaries (38). In a histopathological view, these lesions contain dilated and fused vessels with thin walls. Therefore, they tend to be easily ruptured, bleed and cannot nurture surrounding tissues well. Moreover, AVMs in certain internal organs, such as the brain and lung, can be life-threatening due to direct arteriovenous (AV) shunts (80, 81). An overview of the establishment of these vascular anomalies was offered by a systemic electron microscopic study (38, 82). It started on the dilation of post-capillary venules followed by the enlargement of their lumen. Arterioles became dilated, and then the venules progressively enlarged and expanded, resulting in two to four AVMs that accompanied disappearance of the capillary bed.

Clinical Management and Treatment

Since each HHT patient has variable and differential clinical manifestations, treatment options should be designed specifically for each patient (83). Therapeutic options for nosebleeds are tranexamic acid treatments, estrogen/progesterone preparations, use of vasodilators, laser photocoagulation, dermoplasty of the nasal mucosa and embolization of nasal arteries (65, 83-86). Telangiectasias of the skin and the mucosae are commonly treated by medical or laser therapy (84). The gastrointestinal hemorrhages is treated with estrogen/progesterone, danazol or octreotide (83). Thermic cauterization and laser photocoagulation using endoscopy are performed if there is multiple GI hemorrhaging. Severe anemia caused by recurrent nosebleeds and gastrointestinal bleeding is managed by blood transfusion and/or iron replacement therapy (83). Transcatheter embolotherapy with balloon or stainless-steel coils and surgery are used for the treatment of pulmonary AVMs (PAVMs) (83-85, 87). Stereotaxic radiotherapy and transcatheter embolotherapy are performed to treat cerebral fistula (84). Severe liver insufficiency requires organ transplantation (83, 88).

Transgenic Mouse Models for HHT2

ALK1 is one of seven type I receptors of TGF-β superfamily (89, 90). Biochemical studies suggested that Activin A (90, 91), TGF-β1 and TGF-β3 are putative physiological ligands for ALK1 (92). Recently, BMP-9 and BMP-10 have been further identified (93-95). In general, upon its stimulation, ALK1 phosphorylates and activates the BMP-induced SMAD-dependent intracellular pathway (38) that is mediated by R-SMAD1/5/8 (96-98).

To investigate the role of ALK1 in HHT pathogenesis, genetically modified mouse models have been generated and utilized (38, 44, 97, 99). The *Alk1* knockout (KO) was embryonic lethal during mid-gestation (E10.5 - E11.5). *Alk1*-KO embryos displayed vascular defects due to the elevated activation phase of angiogenesis and the failure of differentiation and recruitment of

vascular smooth muscle cells (VSMCs) (97). Furthermore, hyper-dilated and -fused blood vessels as well as AVMs were found. Despite all of these findings that clearly demonstrate the importance of ALK1-regualted TGF-β signaling for the proper vascular development, the *Alk1* KO lethality makes it not suitable for studying the pathogenesis of HHT. On the other hand, heterozygous *Alk1* mice developed HHT-like phenotypes (38, 100); age-dependent subcutaneous and mucocutaneous vascular lesions as well as hemorrhages in the lung, intestine, liver, brain and spleen (100). All of these pathological conditions are strikingly similar to clinical indications observed in human HHT patients. In that respect, they have been a valuable animal model for elucidating the crucial role of ALK1 for the vascular homeostasis maintenance and the HHT manifestation.

Aim and Significance of the Study

The genes that are responsible for a majority of cases of the inherited vascular disorder HHT had been known for over a decade now. However, the exact pathogenic mechanism(s) of the HHT remains obscure. Treatment options for HHT largely depend on management of symptoms, but the dependable and consistent therapy is currently unavailable. Thus, the primary goal of this study was to determine ALK1-mediated endothelial signaling pathway(s) that may be responsible for AVM development seen in HHT. To study ALK1 endothelial signaling during angiogenesis, pulmonary endothelial cells were molecularly and cellulary characterized in response to various angiogenic stimuli using *in vivo* as well as *in vitro* assays. The results from this study will provide the potential therapeutic target(s) that can prevent or cure vascular lesions in HHT patients.

So far, there is no study examining whether *de novo* ALK1 deficiency causes AVMs in the established vasculature of the adult. Recently, our laboratory generated a transgenic mouse line, using the Cre/LoxP system, in which the *Alk1* gene was deleted after tamoxifen treatment. These

conditional knockout (cKO) mice developed AVMs in adult vessels undergoing angiogenesis. Employing this mouse line, the next aim of this study was to investigate a novel physiological effect of AVMs in tumor vasculature *in vivo*. The main purpose of tumor-induced angiogenesis is to meet the elevated metabolic needs of tumors as they grow. Since microcirculation of AVMs is non-productive due to the lack of capillaries and AV shunts, their formation in blood vessel surrounding tumors will starve tumor mass, thereby leading to tumor growth inhibition and/or regression.

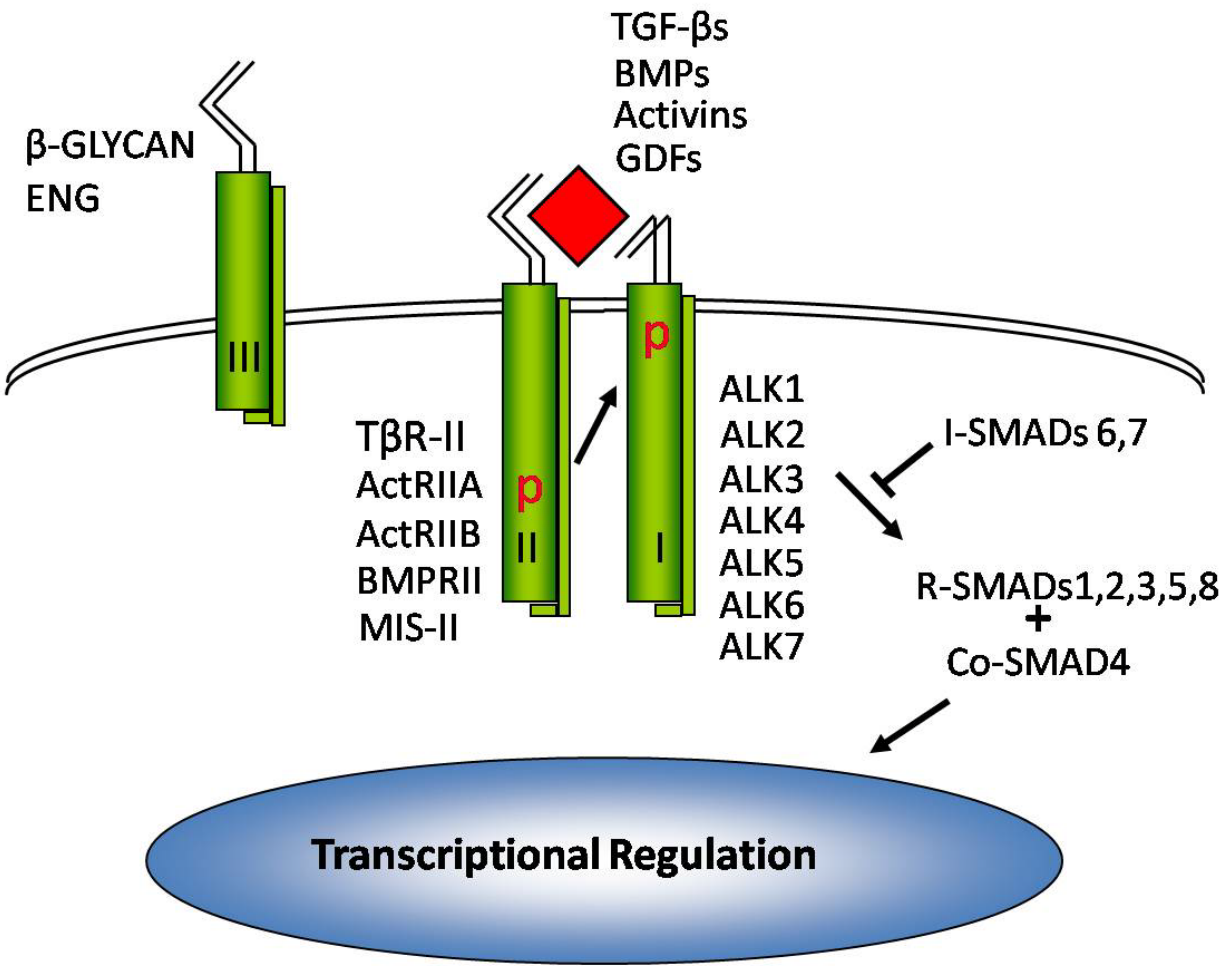

Figure 1-1. TGF-β signal transduction through ALK1. The TGF-β superfamily contains more than 30 known ligands that are roughly divided into TGF-β and BMP ligands. There are seven type I (R-I), five type II (R-II) and two type III (Co-R) receptor family members. Its signal transduction starts with the binding of a ligand to specific type II receptors. The activated type II receptor then recruits and phosphorylates a type I receptor. This R-II and R-I complex propagates the signal through intracellular signaling molecules, SMADs. In general, depending on ligands, the receptor (R)-SMAD2/3 pathway mediates TGF-β ligands-activated signaling, whereas BMP ligands utilize the R-SMAD1/5/8 pathway. At the end of the signal transduction, the complex of R-Smad and common (co)-SMAD4 enters into the nucleus and regulates expression of many target genes which are involved in various cellular events such as cell proliferation, migration, differentiation and apoptosis. The signal is positively regulated by co-receptor binding or negatively controlled by inhibitory (I)-SMADs 6 and 7 interaction with the R-I and R-II complex. ALK1 is one of seven TGF-β type I receptors (ALK1-7). It has been reported that among numerous TGF-β superfamily ligands, TGF-β1, TGF-β3, Activin A, BMP-9 and BMP-10 are putative physiological ligands for ALK1. Additionally, *in vitro* studies indicated that ALK1 transduce the signal through the SMAD1/5/8-regualted BMP pathway.

CHAPTER 2
MOLECULAR AND CELLULAR CHARACTERIZATION OF ALK1-DELETED PULMONARY ENDOTHELIAL CELLS (ECS)

Background

Overview of Hereditary Hemorrhagic Telangiectasia (HHT)

HHT (also known as Rendu-Osler-Weber syndrome) is a genetic vascular disease that is inherited in an autosomal dominant manner and affects 1 in 5,000 -10,000 people worldwide (67-69). A person is diagnosed with HHT when he/she possesses at least three of the following four criteria: 1) a related family history, 2) epistaxes (spontaneous and recurrent nosebleeds), 3) multiple mucocutaneous telangiectases, and 4) AVMs (arteriovenous malformations) in major visceral organs including the brain, lung and liver (65). Depending on the different genetic loci encoding HHT-causing autosomal genes, HHT is categorized into five different types. Several heterozygous mutations in *ENDOGLIN* (*ENG* on chromosome 9) and *Activin receptor-Like Kinase 1* (*ACVRL1*; *ALK1* on chromosome 12) genes cause the HHT type 1 (HHT1) (70-73) and HHT type 2 (HHT2) (74-76), respectively. A subset of HHT patients showing mutations in the *SMAD4* gene on chromosome 18 develop a combined syndrome of HHT and Juvenile Polyposis (JP-HHT) (77). Additionally, two other genetic loci were recently identified and mapped to chromosomes 5 (101) and 7 (102). These contribute to HHT types 3 (HHT3) and 4 (HHT4), respectively. Interestingly, the most commonly mutated genes (*ENG*, *ALK1* and *SMAD4*) in HHT encode proteins that are components of the transforming growth factor-β (TGF-β) signal transduction pathway. Therefore, HHT has been considered a disease caused by dysregulation of TGF-β subfamily signaling.

Signal Transduction for TGF-β Superfamily

The TGF-β superfamily consists of a large number of secreted pleiotropic cytokine ligands and several receptors (38, 39). There are roughly four different subfamilies containing TGF-β,

activin/inhibin, myostatin/growth and differentiation factors (GDF) and bone morphogenetic proteins (BMP) ligands and three distinctive types of receptor (41, 64). In mammals, seven type I (RI; ALK1-7), five type II (RII; TGF-βRII, ActRIIA, ActRIIB, BMPRII, and MIS-II) and two type III (RIII; ENDOGLIN and β-GLYCAN) transmenbrane receptors have been identified (39, 44). Type I and type II receptors are serine/threonine kinases, whereas type III receptors have short intracellular domains lacking a kinase domain (44). As compared to type II receptors, type I receptors contain a unique glycine/serine (GS) domain followed by the kinase domains (39). The TGF-β signaling pathway is very complicated by various combinations among these members and redundant in the association between ligands and type II receptors as well as type II and type I receptors. Its signaling affects cellular proliferation, differentiation, migration and apoptosis (39, 42, 43). Many genetic studies in mice have described the importance of the TGF-β subfamilies for normal vascular development and maintenance (7, 11, 38). This pathway is also implicated in a variety of physiological processes such as development, embryogenesis, embryonic patterning, immunological regulation and growth (38, 40, 41).

In the resting state of TGF-β signaling, type II and type I receptors are present as homodimers on the cell surface (39). Its signal transduction is initiated by the binding of ligand(s) to specific autophosphorylated type II receptors (38, 39, 44). The activated type II receptor recruits a type I receptor, forming a heteromeric complex, and transphophorylates the GS motif of the type I receptor (39). The signal is propagated via phosphorylation at the C-terminal serines of the cytoplasmic mediators, SMAD proteins, by the type I receptors (39). There are three distinctive types of SMADs, receptor-regulated (R)-SMADs (SMAD1, 2, 3, 5 and 8), common (co)-SMAD (SMAD4) and inhibitory (I)-SMADs (SMAD6 and 7). R-SMAD2 and 3 are TGF-β ligands-specific, whereas R-SMAD1, 5 and 8 are BMP-specific (45-48). All

signals (phosphorylated R-SMADs) by the SMAD-dependent pathways converge with SMAD4, resulting in heteromeric complexes. Upon their entrance into the nucleus, these complexes are associated with transcription factors, co-factors and regulate various target genes (49, 50). Additionally, it is believed that the interaction between type II receptors with their ligands are modulated by type III receptors (66, 103). Also, the association of heteromeric receptor complexes with R-SMADs are hindered by I-SMAD6 and 7, resulting in a negative feedback loop (39). There are also SMAD-independent pathways that have been identified to mediate TGF-β signaling, including the MAPK and PI3K pathways (39, 104).

Vascular Endothelial-Specific ALK1 Signaling

ALK1 is one of seven transmembrane type I receptors for the TGF-β superfamily, exerting serine/threonine kinase activity (89, 90). Because of the uncertainty of its specific ligand(s) and downstream target(s), ALK1 had been considered an orphan receptor (90). Biochemical studies have suggested that ALK1 is a putative physiological receptor for some TGF-β ligands including Activin A (90, 91), TGF-β1 and TGF-β3 (92) based upon its binding ability. More recently, BMP ligands such as BMP-9 and BMP-10 have been reported to bind to ALK1 and elicit the ALK1 signaling as well (93-95).

Alk1 is primarily expressed in vascular endothelial cells (ECs) (105-107). A dynamic spatiotemporal expression of Alk1 had been described by using *Alk1-LacZ* knockin (KI) mice (106). Developmental expression of Alk1 was predominant in arterial ECs up to postnatal growth stages, while its expression was reduced in the adult stage. However, when angiogenesis was initiated by either wounding or tumorigenesis in the adult, its expression reappeared in nascent and remodeling arteries. Furthermore, another study reported that in the embryos, Alk1 expression was confined to sites where angiogenesis was active in endothelium (108).

Animal Models for HHT

The clinical onset and progression of HHT is highly variable, implying a significant role for modifying factors (38). To investigate genetic as well as environmental factors for the pathogenesis of the HHT, numerous groups have generated and studied several genetically modified mouse models (38, 44, 108, 109). Homozygous null mutations in the *Eng* (110-112) and *Alk1* (97, 99) genes were embryonic lethal between E10.5-11.5 due to severe vascular defects. Since heterozygous mice for each gene developed HHT-like vascular lesions and HHT is a dominantly inherited genetic disease, they have been valuable animal models for studying the HHT. $Eng^{+/-}$ mice exhibited telangiectases, recurrent nosebleeds and AVMs (111, 113, 114). $Alk1^{+/-}$ mice showed age-dependent subcutaneous and mucocutaneous vascular lesions and hemorrhages in organs involving lung, intestine, liver, brain, and spleen (100). This data suggest haploinsufficiency of ENG and ALK1 is responsible for HHT1 and HHT2 manifestations, respectively (66). However, these heterozygous mice also had limitations for investigating the molecular pathogenesis of HHT. They were highly variable in their onset of vascular lesions and HHT-like phenotypes. Additionally, penetrance varied among mouse strains (100, 111, 113, 114). To overcome embryonic lethality and these limitations, a conditional knockout (cKO) strategy has been developed by taking advantages of the the Cre/LoxP system, producing mouse models in which recapitulation of HHT vascular lesions can be created in a desired location predictably and consistently (78, 115).

Is ALK1 Signaling Independent from TGF-β Subfamily Pathway?

HHT has been considered a TGF-β subfamily disease. However, our most recent *in vivo* studies in mice and zebrafish (115) indicated that neither ALK5 nor TGFBR2 is required for the ALK1 signaling, suggesting that HHT might not be a TGF-β subfamily disease (115). In this study, cKO alleles for *Alk1*, *Alk5* or *Tgfbr2* were deleted specifically in the vascular endothelium

using a novel Cre deleter line in which Cre recombinase was predominantly expressed in pulmonary ECs from E13.5. Severe vascular defects included excessive, convoluted, dilated blood vessels and thin vessel walls as well as AVMs, which are very similar to vascular lesions seen in HHT, resulted from the *Alk1*-deletion. These mice were embryonic lethal between E16.5-18.5. In contrast, mice with *Alk5*- or *Tgfbr2*-conditional deletion did not exhibit such abnormal vascular phenotypes. Furthermore, recent biochemical data suggested that BMP9 might be a physiological ligand for ALK1 (93-95). In that respect, the functions of ALK1 signaling might be exerted via the BMP subfamily pathway involving BMP ligand(s) and type II receptors (ActRIIA, ActRIIB, or BMPR2). All of these studies strongly suggest that ECs are the primary cell type affected by the ALK1 deficiency and EC-specific *Alk1*-deletion is sufficient for the development of the vascular abnormality.

HHT-Like Vascular Lesions Induced by *Alk1*-Deletion at the Adult Stages

In our most recent preliminary study, we investigated the role of the ALK1 signaling in the adult vasculature. To induce the global *Alk1* conditional allele-deletion, we employed the ROSA26-CreER knockin deleter strain in which Cre recombinase is ubiquitously expressed and can be activated upon tamoxifen (TM) treatment. Between 9 to 21 days after a single TM injection, the adult mice carrying homozygous *Alk1*-deletion died. An autopsy revealed hemorrhages in the lungs and gastrointestinal tract, while no other organs showed such features. To explain why only these organs were affected by the *Alk1*-deletion, we speculated that ongoing angiogenesis might be required for the formation of abnormal blood vessels in response to *Alk1*-deletion, based upon our previous observations. Firstly, Alk1 is persistently expressed in the pulmonary vasculature in the adult stage. Both pulmonary and gastrointestinal blood vessels showed severe vascular defects upon *Alk1*-deletion at embryonic and adult stages. Secondly, expression of the *Alk1* gene was reinitiated by wound- or tumorigenesis-induced angiogenesis

during adulthood (106). To test this hypothesis, we performed an *in vivo* wound-induced angiogenesis assay and found that homozygous *Alk1*-deletion and proangiogenic cues are required and sufficient for the formation of HHT-like vascular abnormalities in the adult mice. Interestingly, we could not observe these pathological features in *Alk1*-heterozygous mice with wounding, indicating that homozygous deletion of the *Alk1* gene in ECs might be required for development of such vascular lesions in the adult angiogenesis.

Here, we examined how *Alk1*-deletion affected molecular and cellular traits of pulmonary ECs upon angiogenic challenges. Our next hypothesis was that the ALK1 signaling in ECs controls cellular responses to angiogenic factors during angiogenesis. Thus, when there is a deficiency in ALK1, the appearance of dilated, thin-walled, excessive, tortuous blood vessels and formation of AVMs (115) may result due to angiogenic dysregulation in ECs. To test this, we isolated and established two new pulmonary EC lines that were either *Alk1*-heterozygous or -homozygous. We found that *Alk1*-deleted ECs exhibited increased migratory and sprouting properties in response to proangiogenic cues both *in vitro* and *in vivo*. Furthermore, *Alk1*-null ECs formed an irregular, disorganized and enlarged tube-like structure. Next, we investigated which ligand and intracellular pathway, TGF-β or BMP, would be relevant for such cellular behaviors. In the absence of ALK1, the tubular network was significantly regressed by TGF-β1 treatment. However, this inhibitory effect was not seen with BMP-9 treatment of *Alk1*-null pulmonary ECs, indicating that the BMP pathway is more specific for ALK1 signaling. Consistent with this data, our Western blot analysis suggested that the activation of ERK in *Alk1*-null pulmonary ECs was greater in BMP-9 treatment than TGF-β1 treatment. However, the induction of SMAD-dependent pathways was unchanged with or without ALK1, implying that the cytoplasmic pathway(s) mediating the ALK1 signaling may be SMAD-independent.

Results

Establishment of Genetically Modified Pulmonary EC Line

The overall experimental scheme is summarized in Figure 2-1. Pulmonary ECs were isolated from the whole lung of a *R26*$^{+/CreER}$*; Alk1*$^{2f/1f}$ mouse. The *2f* means that exons 4 to 6, which encode the transmembrane domain of the *Alk1* gene, are floxed with two LoxP sequences within the *Alk1*-cKO allele, while *1f* refers the *Alk1*-nulle allele (Figure 2-3A). Thus, *R26*$^{+/CreER}$*; Alk1*$^{2f/1f}$ ECs are equivalent to heterozygous *Alk1*-null (*Alk1*$^{+/-}$) ECs. Additionally, in this mouse line, cDNA encoding a Cre-ER fusion protein is inserted into the ROSA26 locus (*R26*$^{+/CreER}$). And upon treatment with the tamoxifen (TM), a chemical compound that recognizes and binds specifically mutated estrogen receptor (ER), Cre recombinase becomes active. Therefore, when *R26*$^{+/CreER}$*; Alk1*$^{2f/1f}$ ECs are treated with TM, activated Cre recombinase recognizes two LoxP sequences and deletes the *Alk1*-cKO allele, resulting in homozygous *Alk1*-null (*Alk1*$^{1f/1f}$*; Alk1*$^{-/-}$*)* ECs lacking the transmembrane region of ALK1 (Figure 2-3A).

After isolation and immortalization, ECs were fluorescently and endothelial-specifically labeled with Dio-Ac-LDL and then sorted by the fluorescent activated cell sorting (FACS) system. Typically, the culture is enriched with more than 95% ECs (Figure 2-2A). Subsequently, endothelial-specific properties of sorted ECs were further evaluated by their morphology and desired biomarker genes expression. Morphologically, isolated ECs exhibited the EC-characteristic cobble-stone shape and cell-cell contact inhibition at confluency (Figure 2-2B). And the expression of various known EC-specific marker genes, such as *Flk1*, *Tie2*, *Endoglin (Eng)*, *Endothelin (Edn)* and *Alk1*, was confirmed by RT-PCR analyses. To obtain more homogeneous populations of ECs, several clones were isolated and further analyzed by methods described above. Based on its typical polygonal shape and high expression of *Alk1* and *Edn*

(Figure 2-2C), clone #28 was chosen and used for further analyses. Finally, the parental EC line carrying the *R26*$^{+/CreER}$*; Alk1*$^{2f/1f}$ transgene was established.

Development of *Alk1*$^{2f/1f}$ (*Alk1*-Null Heterozygote)-Derived *Alk1*$^{1f/1f}$ (*Alk1*-Null Homozygote) ECs

To obtain the *R26*$^{+/CreER}$*; Alk1*$^{1f/1f}$ (*Alk1*-null homozygote) EC line, the parental *R26*$^{+/CreER}$*; Alk1*$^{2f/1f}$ ECs were treated with 1 μM hydroxy (OH)-TM (Figure 2-3A). After a 2-days TM treatment, the *2f Alk1*-cKO allele was deleted and thereby undetectable, but only the resulting *1f Alk1*-null allele was detected by genomic PCR (Figure 2-3B) and Southern blot (Figure 2-3C) analyses. This genetic modification was maintained in normal endothelial cell medium (ECM) for at least 7 days without additional TM treatment (Figure 2-3B). By culturing ECs in normal ECM for a week, we could avoid any possible side effects from the TM treatment. Furthermore, RT-PCR analysis showed that *Alk1* transcripts were observed in TM-untreated parental cells, but were undetectable in TM-treated cells (Figure 2-3D). The TM treatment did not affect morphology nor cellular and molecular characteristics of ECs. Hereafter, *R26*$^{+/CreER}$*; Alk1*$^{2f/1f}$ and *R26*$^{+/CreER}$*; Alk1*$^{1f/1f}$ are denoted as control (*Alk1*$^{2f/1f}$) and mutant (*Alk1*$^{1f/1f}$), respectively.

Alk1-Null ECs Showed Increased Migratory Index in Response to an Angiogenic Challenge *in vitro*

Migratory property is one of the important features to focus on when studying the cellular phenotypes of ECs. Two well-established migration assays are widely used: two-dimensional (2D) wound-induced migration (116) and three-dimensional (3D) modified Boyden chamber (117) assays. In a previous study, in agreement with our preliminary data from the *in vivo* wound-induced angiogenesis, we found that without angiogenic stimulation, there was no difference in migration between control (*Alk1*$^{2f/1f}$) and mutant (*Alk1*$^{1f/1f}$) ECs. Thus, basic fibroblast growth factor (bFGF, 50 ng/ml), a well-known angiogenic factor, was added into the normal ECM containing 20% fetal bovine serum (FBS). In the 2D wound-induced migration

assay, we observed that *Alk1*-null mutant ECs migrated faster than control ECs (Figure 2-4A). The rate of change (mean ± SE; 0.079 mm/hr ± 0.0016; n=9) in migratory distance of mutant cells was significantly higher than that (mean ± SE; 0.062 mm/hr ± 0.0016; n=9) of control cells ($p < 0.0001$). The overall change (mean ± SE; 0.99 mm ± 0.024; n=9) in migration of mutant cells for 12 hours was significantly higher than that (mean ± SE; 0.77 mm ± 0.024; n=9) of control cells ($p < 0.0001$) (Figure 2- 4B, C). Consistent with the results, in the 3D migration chamber assay, the average (mean ± SE; 29.94 ± 0.14; n=6) number of migrating mutant cells for 48 hours was significantly higher than that (mean ± SE; 17.33 ± 1.57; n=6) of control cells ($p<0.0002$) (Figure 2-4F).

However, there is a possibility that unknown factor(s) in ECM containing 20% FBS may be influencing some of the migratory property of the ECs. Consequently, we repeated both migration assays in chemically defined growth factor- and serum-free ECM containing bFGF (50 ng/ml). We obtained the same results in that mutant cells exhibited a significantly higher rate of change (mean ± SE; 0.077 mm/hr ± 0.0015; n=9) and overall change (mean ± SE; 0.95 mm ± 0.019; n=9) in migration as compared to control cells (mean ± SE; 0.062 mm/hr ± 0.0015 and 0.76 mm ± 0.019; n=9) ($p < 0.0001$) (Figure 2-4D, E). Furthermore, in the 3D modified Boyden chamber assay, a significantly more number of mutant cells (mean ± SE; 17.29 ± 4.96; n=6) migrated than control cells (mean ± SE; 7.75 ± 2.87; n=6) ($p < 0.0001$) (Figure 2-4G).

Alk1-Deficient ECs Resulted in Excessive, Disorganized and Enlarged Tubular Network Formation upon an Angiogenic Challenge *in vitro*

To study endothelial outgrowth or sprouting during the activation phase of angiogenesis *in vitro*, several gel systems such as basement membrane, collagen and fibrin matrices have been developed (117). These contain components of extracellular matrix (ECM) that are important for the cellular physiology of ECs (118). We employed Matrigel, a basement membrane-rich ECM

(119) to examine branching morphogenesis of *Alk1*$^{2f/1f}$ control and *Alk1*$^{1f/1f}$ mutant pulmonary ECs.

bFGF (50 ng/ml) was added to the culture to determine the ECs' behavior during an angiogenic stimulation. After the control (*Alk1*$^{2f/1f}$) or mutant (*Alk1*$^{1f/1f}$) cell suspensions in chemically defined growth factor- and serum-free ECM were seeded onto the Matrigel, the morphological changes in their sprouting were photographed every 3 hours up to 12 hours and terminated at 24 hours. Overall, the appearance of resulting tube-like networks was quite different between control and mutant ECs cultures in response to bFGF treatment (Figure 2-5A). A tubular network formed by control ECs consisted of slowly sprouting, thin and few tubes between 3 and 6 hours (Figure 2-6A). In contrast, *Alk1*-null mutant ECs developed an excessive and disorganized tubular network due to fast branching and thick tubes during the same period (Figure 2-6B). In addition, between 9 to 12 hours (Figure 2-6C) cord-like structures in the control culture began to regress and many of them disappeared after 24 hours (Figure 2-6E). However, similar structures formed by mutant cells were resistant to regression during this time period (Figure 2-6D and F).

To quantify and statistically analyze these data, all images from the assay were processed by imaging software. By doing so, we could obtain quantitative readouts such as coverage area of tube-like structures on the Matrigel (Figure 2-6A-F), total length of these structures (Figure 2-7A and B) and number of sprouting tubes from each nodule (Figure 2-7D and E) to examine differing cellular phenotypes between control and mutant cells during *in vitro* induced angiogenesis. Statistical analyses confirmed that *Alk1*-null mutant cells formed significantly more and thicker tube-like structures, indicated by an increased area of coverage at all time points in response to bFGF (Figure 2-6G). On the other hand, the tubular network developed by

control cells showed less area of coverage largely due to thin tube-like structures (Figure 2-6G). Although tube-like structures in both control and mutant cultures showed significant regression between 12 to 24 hours, *Alk1*$^{2f/1f}$ control cells showed significantly rapid regression compared to their counterpart *Alk1*-deleted mutant cells (Figure 2-6G). This data indicates that ALK1-deficiency prevented endothelial tubes from regression in an angiogenic condition. In terms of total length (Figure 2-7C) and total number (Figure 2-7F) of sprouting tubes, there was no significant difference between control and mutant ECs by 12 hours. However, mutant ECs showed a considerable increase in both readouts after 24 hours (Figure 2-7C and F), further confirming that ALK1-deficiency leads to an enhanced resistance to tubular regression.

Antiangiogenic Effect of BMP-9 was Blunted, But That of TGF-β1 was Present in *Alk1*-null ECs

Based on *in vitro* data, it was believed that ALK1 propagates the TGF-β ligand (TGF-β1, TGF-β3 and Activin A) signal through the BMP-specific SMAD1/5/8 intracellular pathway in a combination with the TGF-β type II (TGFBR2) receptor. However, the existence of an unidentified ligand different from TGF-β1 and -β3 in serum has been implied (92). In three recent studies, two BMP ligands (BMP-9 and -10) have been reported to specifically bind to ALK1 and activate the SMAD1/5/8 pathway. One group showed that BMP-9 and BMP-10 induced phosphorylation of SMAD1/5/8 in microvascular ECs. They also activated expression of genes, such as *ID1*, *ID2*, *SMAD6*, *SMAD7*, *ENG* and *BMPRII*, which was previously suggested to be derived by caALK1 (94). And these two factors were antiangiogenic by inhibiting growth and migration of ECs. However, this activation was abrogated when Alk1 and Bmpr2 were silenced. The same group also found that in human serum only the BMP-9 neutralizing antibody could inhibit serum-induced SMAD1/5 phosphorylation (95). Furthermore, from two *in vivo* angiogenesis assays, it was demonstrated that BMP-9 potently prevented sprouting angiogenesis.

Thus, they argue that BMP-9 might be a circulating specific ligand for ALK1 and drive a physiological effect of ALK1. The conclusion from another group further supported these findings (93). In their study, it was observed that BMP-9 bound to ALK1 and BMPR2 with high affinity in ECs. They also found that SMAD1/5 and caALK1-responsive genes were activated by BMP-9. Additionally, BMP-9 suppressed proliferation and migration of bFGF-stimulated bovine aortic endothelial cells (BAECs) as well as vascular endothelial growth factor (VEGF)-derived angiogenesis.

Thus, we examined whether these previous data showing an antiangiogenic function of the ALK1 signaling by BMP-9 stimulation would be true in our pulmonary ECs. Moreover, in comparison with the TGF-β1 treatment, we tested which ligand is more specific or relevant to activate antiangiogenic effects of ALK1 signaling in these ECs in an angiogenic condition. bFGF (50 ng/ml) was added in combination with either TGF-β1 (5 ng/ml) or BMP-9 (20 ng/ml) into chemically defined growth factor- and serum-free ECM. Depending on its different concentration, TGF-β1 exerts a biphasic effect in a variety of biological processes (11). bFGF- or VEGF-induced sprouting of bovine microvascular endothelial cells was promoted by 200 to 500 pg/ml of TGF-β1 and inhibited by 5 to 10 ng/ml of TGF-β1 during *in vitro* angiogenesis (11). The concentration of circulating BMP-9 in healthy human sera and plasma has been determined recently (95). The physiological concentration of circulating BMP-9 was varied between 2 and 12 ng/ml and its mean level was 6.2 ± 0.6 ng/ml (95). Here, to study a maximum inhibitory effect of BMP-9 during angiogenesis, we examined 20 ng/ml of BMP-9 that is much higher than its known biologically active concentration.

Endothelial sprouting was photographed at various time points (3, 6, 9, 12 and 24 hours) post-seeding on the Matrigel (Figure 2-5B and C). Control cells less branched and more

regressed over the time in response to TGF-β1 (Figure 2-5B) or BMP-9 (Figure 2-5C) as compared to observations with bFGF alone (Figure 2-5A), indicating that their inhibitory effects on endothelial outgrowth were maintained in the presence of the ALK1. By contrast, *Alk1*-deleted mutant cells did not appear to be affected by either TGF-β1 (Figure 2-5B) or BMP-9 (Figure 2-5C) treatments. There was an increase in capillary-like network density comparable to that of mutants ECs in response to bFGF alone (Figure 2-5A). Furthermore, such tube-like structures were resistant to regression despite the presence of TGF-β1 or BMP-9 (Figure 2-5A-C), indicating increased vessel stability due to the absence of ALK1.

Next, all of pictures were processed by imaging software to obtain quantitative parameters, and then these readouts were statistically analyzed. The surface area of tube formation by $Alk1^{2f/1f}$ control ECs was significantly less than that of $Alk1^{1f/1f}$ mutant ECs at all time points in response to TGF-β1 (Figure 2-8A) or BMP-9 treatments (Figure 2-8B). Moreover, tube-like structures in the control rapidly retreated over time (Figure 2-8A and B), indicating their inhibitory effects were present in control ECs. It is important to note that such antiangiogenic effects led to less surface area but more regression as compared to corresponding cultures with bFGF alone (Figure 2-6G), indicating that ALK1 in pulmonary ECs suppressed uncontrolled endothelial outgrowth upon a proangiogenic cue and its inhibitory effect was further improved by the addition of antiangiogenic factors (TGF-β1 and BMP-9). In contrast to control cells, *Alk1*-null mutant cells greatly induced tube-like structures despite the presence of TGF-β1 (Figure 2-8A) or BMP-9 (Figure 2-8B) by 3 hours. However, these structures significantly and rapidly regressed between 3 to 24 hours upon TGF-β1 treatment (Figure 2-8A), but slowly regressed and much longer sustained in the presence of BMP-9 (Figure 2-8B). This suggests that without ALK1, the inhibitory effect by BMP-9, and not TGF-β1, was blunted, indicating that BMP-9

might be a more specific or the relevant physiological ligand for the ALK1 signaling in pulmonary ECs. On the other hand, the total length of such tubular networks (Figure 2-8C and D) and the total number of sprouting from nodules (Figure 2-8E and F) in response to TGF-β1 or BMP-9 stimulation was not much different during early stages up to 12 hours between *Alk1*-heterozygous and *Alk1*-null ECs. However, at 24 hours, *Alk1*-deleted mutant ECs showed a higher index for these readouts (Figure 2-8C-F), further demonstrating that ALK1-deficiency resulted in increased vessel stability. Importantly, unlike results from coverage area readout, we did not observe either TGF-β1- or BMP-9-specific antiangiogenic effects depending on the presence of ALK1 in sprouting and elongating properties (Figure 2-8C-F). Therefore, our data from the *in vitro* tube formation assay were in agreement with previously reported conclusions (93-95) that BMP-9 might be a specific ligand for ALK1 and the BMP-induced ALK1 signaling exerted an antiangiogenic role during angiogenesis.

Alk1 Deletion Caused Higher Migratory Indication of ECs and Abnormal Blood Vessel Formation *in vivo*

Importantly, we found that *in vivo Alk1*-deletion also led to a higher migratory activity among ECs and abnormal nascent blood vessels. Two *Alk1*-cKO alleles in $R26^{+/CreER}$; $Alk1^{2f/2f}$ mice were deleted by intraperitoneal injection of TM, resulting in adult *Alk1*-null mutant mice. As a control, $R26^{+/+}$; $Alk1^{2f/2f}$ mice were used and also injected with TM. Subsequently, Matrigel containing bFGF (250 ng/ml) was subcutaneously injected into the dorsal region of mice. Between 7 to 10 days post-injection, mice were sacrificed and Matrigel plugs were collected for further histological analysis. To easily visualize migrating ECs and newly formed vessels into the Matrigel plug, we utilized control and mutant mice containing the $Flk1^{lacZ}$-KI allele. In these mice, expression of the *lacZ* gene can be easily detected by X-gal staining where the EC-specific *Flk1* gene is expressed.

Macroscopic observation of plugs from *Alk1*-deficient mutant mice revealed several vessels extending from the skin and penetrating into the Matrigel plug (n=5) (Figure 2-9B), while none of the plugs from control mice showed this (n=6) (Figure 2-9A). Histological analysis demonstrated that migrating cells were found only in the peripheral region of the Matrigel plug in the controls (Figure 2-9C, E, G). However, in the mutants, ECs significantly migrated into the center of the Matrigel plug (Figure 2-9D, F, H). Moreover, *Alk1*-null ECs formed several blood vessel structures (Figure 2-9D, F, H), as compared to just a few tiny vessels by control ECs at the edge of the Matrigel plug (Figure 2-9G). These newly formed blood vessels in the Matrigel plug from mutant mice were dilated, irregular and disorganized (Figure 2-7D, F, H). Thus, such findings further suggested that *Alk1*-deficient ECs were more migratory and pro-angiogenic in response to the angiogenic stimuli.

Biochemical Characterization of *Alk1*-Null Pulmonary ECs

To determine what intracellular downstream pathway is differentially regulated by ALK1 signaling in pulmonary ECs, *Alk1*-null ECs were biochemically studied by Western blot analysis. The canonical TGF-β superfamily signaling consists of two different SMAD-dependent intracellular pathways, TGF-β ligands-activated SMAD2/3 and BMP ligands-induced SMAD1/5/8 pathways (45-48). TGF-β1 and TGF-β3 was originally believed to be the TGF-β ligand that activate ALK1 signaling (92). However, recent studies have suggested BMP-9 and BMP-10 to be responsible for inducing ALK1 activation (93-95). In general, ligand-activated ALK1 propagates the signal through phosphorylation of SMAD1/5/8. Here, we examined which ligand, TGF-β or BMP-9, is more speific for the ALK1 signaling by measuring phosphorylation levels of either SMAD2/3 or SMAD1/5/8, respectively, in the presence or absence of ALK1. Furthermore, other SMAD-independent signal transduction pathways (104) were studied to see whether the ALK1 signaling may function in a SMAD-independent manner in our ECs.

For examination of SMAD-dependent TGF-β subfamily signaling pathways, after overnight serum starvation, both parental *Alk1*-heterozygous (*Alk1*$^{2f/1f}$) and TM-treated *Alk1*-null (*Alk1*$^{1f/1f}$) ECs were treated with either TGF-β1 (5 ng/ml) or BMP-9 (20 ng/ml) for 30 minutes. The total protein levels of SMAD2 were unchanged by ALK1 and each treatment (Figure 2-10A, B). As expected, in both the *Alk1*$^{2f/1f}$ and *Alk1*$^{1f/1f}$ ECs SMAD2/3 TGF-β pathway was greatly activated by TGF-β1 treatment, while its activation was almost unchanged by BMP-9 treatment. Interestingly, the basal level of phosphorylated SMAD2/3 was moderately decreased in *Alk1*-null ECs, indicating slightly reduced TGF-β pathway without ALK1 (Figure 2-10A, B). On the other hand, SMAD1/5/8 BMP pathway was markedly elevated by BMP-9, whereas a slight increase was observed by TGF-β1 (Figure 2-10C, D). The total protein levels of SMAD1 were constant with or without ALK1 and treatments. Surprisingly, despite the absence of ALK1, phosphorylation of SMAD1/5/8 was still considerably elevated by the BMP-9 treatment (Figure 2-10C, D). This result implied that SMAD1/5/8-mediated BMP pathway may not be a major intracellular pathway of the ALK1 signaling in lung ECs. Overall, signaling components for the canonical TGF-β superfamily signaling were present and intact in both *Alk1*$^{2f/1f}$ control and *Alk1*$^{1f/1f}$ mutant pulmonary ECs.

Next, we performed similar Western blot analyses to determine whether a SMAD-independent signaling pathway may be mediating the ALK1 signal. There have been numerous studies demonstrating SMAD-independent intracellular pathways, including MAPK and PI3K pathways, for the TGF-β family members (39, 104). A recent report proposed that constitutively active (ca) ALK1 negatively regulated the activation of ERK MAPK induced by human dermal microvascular endothelial cells (HMVEC-d) wounding, thereby inhibiting EC migration (120). Based on this finding, we expected that the activation of ERK1/2 MAPK pathway would be

increased in response to the absence of ALK1. The total amount of ERK1/2 was same regardless of ALK1 and stimulations (Figure 2-10E, F). Unexpectedly, basal and induced phospho-ERK1/2 levels were slightly decreased in the absence of ALK1, although not statistically significant (Figure 2-10E, F), indicating that the ERK MAPK pathway may be a ALK1-independent pathway in pulmonary ECs.

When these ECs were further stimulated by the pro-angiogenic factor bFGF (50 ng/ml) in combination with either TGF-β1 or BMP-9, similar trends were observed (Figure 2-10B, D, F). However, in response to angiogenic stimulation, the basal level of both phospho-SMAD2/3 and -SMAD1/5/8 was decreased (mean of controls: mean of mutants for Smad1; from 0.95: 1.02 to 0.30: 0.39 and for Smad2; from 0.59: 0.44 to 0.21: 0.16). Their changes in induction were also reduced as compared to those without bFGF treatment (mean of controls: mean of mutants for p-Smad1/5/8; from 3.24: 3.06 to 1.10: 1.18 and for p-Smad2/3; from 2.20: 2.10 to 1.41: 1.50). However, the activation pattern of ERK1/2 was opposite. In the presence of bFGF, its basal level (mean of controls: mean of mutants for ERK1/2; from 0.30: 0.25 to 0.45: 0.37) and change in induction (mean of controls: mean of mutants for p-ERK1/2; from 0.23: 0.18 to 0.48: 0.31 with TGF-β1; from 0.21: 0.24 to 0.43: 0.36 with BMP-9) were increased.

Overall, there was no obvious difference in SMAD-dependent pathways between parental control *Alk1*$^{2f/1f}$ and TM-treated mutant *Alk1*$^{1f/1f}$ pulmonary ECs. The activation of TGF-β-specific SMAD2/3 was greatly induced by TGF-β1, but not by BMP-9. On the other hand, the phospho-SMAD1/5/8 was significantly up-regulated by BMP-9, while it was slightly increased with TGF-β1. Interestingly, in *Alk1*$^{2f/1f}$ control ECs, the phosphorylation of ERK1/2 was unchanged or slightly decreased by TGF-β1 or BMP-9 treatments (Figure 2-10E, F). However, although not statistically significant, the reduction in the amount of phsopho-ERK1/2 in response

to TGF-β1 treatment in *Alk1*$^{1f/1f}$ mutant ECs was greater than that in response to BMP-9 (Figure 2-10E, F), implying that the negative function of BMP-9 on the activation of ERK1/2 was reduced in the absence of ALK1.

Discussion

Despite advances made in the elucidation of a crucial role for vascular endothelial ALK1 in the establishment and maintenance of vascular integrity, many issues remain unclear. Biological effect(s) and molecular target(s) of ALK1 in vascular ECs still need to be determined. Results have been contradictory because of limitations in the experimental approach. First, due to the complexity of the TGF-β superfamily signal transduction pathway, there are discrepancies in data depending on endothelial cell types and culture conditions used. Second, because of an absence of a physiological ligand for ALK1, the constitutively active (ca) ALK1 is mainly used to avoid the simultaneous activation of another TGF-β type I receptor, ALK5, in ECs. However, as the ligand-independent activation of ALK1 can induce a broad range of downstream signaling pathway, finding the specific ALK1-regualted intracellular signaling cascade which is likely relevant to the pathogenesis of HHT2 is limited.

Based on this background and our previous studies, the rationale for experimental approach presented can be summarized in three points. First, the expression of *Alk1* is persistent in vascular ECs of the lungs at the adult, while its expression is decreased in most systemic vascular ECs after neonatal periods. Furthermore, in mice, the pulmonary vasculature including gastrointestinal (GI) vascular system is affected by *Alk1* deletion at both embryonic and adult stages. Second, since primary cells could not be cultured *in vitro* for a long time with many passages, ECs were immortalized by the SV40 T-antigen transfection to avoid variability among the distinct EC batches from different isolation. More importantly, *R26*$^{+/CreER}$*; Alk1*$^{2f/1f}$ (equivalent to *Alk1*$^{+/-}$) and TM-treated *R26*$^{+/CreER}$*; Alk1*$^{1f/1f}$ (equivalent to *Alk1*$^{-/-}$) ECs have the

same origin. Therefore, we could reduce variation depending on age and genetic background of different mice. Third, unlike using siRNA to block the ALK1 signaling, our genetic approach would result in the complete blockage of the ALK1 signaling.

The primary goal of this study was to determine an endothelial-specific role for ALK1 signaling during angiogenesis. Based on our previous studies, ALK1 deficiency in vascular ECs is the most likely cause of HHT-like vascular lesions during embryonic and adult stages of mice. However, there was no evidence that explains why only the pulmonary and gastrointestinal vasculatures are consistently affected by the ALK1 deficiency in the adult mice. Our previous study hinted that diminished ALK1 expression during postnatal development was reactivated by active angiogenesis (106). Thus, we tested the relationship between *Alk1*-deletion and ongoing angiogenesis for the development of HHT-like vascular abnormalities. Our *in vivo* wound-induced angiogenesis assay showed both factors were necessary and sufficient for the formation of abnormal blood vessels that were disorganized, irregular, excessive, tortuous and AV shunted. Such results led us to investigate how ALK1 deficiency affects cellular and biochemical properties of vascular ECs during angiogenesis.

Another emerging issue was that ALK1 may not propagate signals in a TGF-β pathway-dependent manner, therefore, HHT might not be a TGF-β subfamily disease. Three recent *in vitro* reports demonstrated that ALK1 specifically bound to BMP-9 and BMP-10 in combination with BMPR2. This association induced activation of the BMP-specific SMAD1/5/8 pathway and resulted in inhibition of proliferation and migration of ECs as well as suppression of sprouting angiogenesis (93-95). This finding was further strengthened by our *in vivo* data suggesting that HHT-like pathological vascular features were caused by the endothelial *Alk1*-deficiency, but not by *Alk5* or *Tgfbr2*-deletion in vascular ECs (115). This raised the possibility that another TGF-β

superfamily signal transduction, most likely BMP ligands-implicated pathway, may be relevant for the ALK1 signaling, rather than the TGF-β lignads-induced signaling pathway. Although there has been no *in vivo* evidence showing that deletion of BMP-9 and/or BMP-10 cause HHT-like phenotypes, a recent study suggested that RNA interference-mediated silencing of Bmpr2 expression caused vascular abnormality including mucosal bleedings and the lack of mural cells on vessel walls (121). Thus, they conferred a possible link between the perturbation of BMP pathway induced by BMP ligands through BMPR2 and HHT pathological vessel lesions.

We initially examined endothelial-specific cellular phenotypes such as proliferation, migration and tube formation of *Alk1*-null lung ECs without pro-angiogenic cues. Consistent with our *in vivo* data, there was no difference in their phenotypes for migration and tube formation in the absence of an angiogenic factor, even in the media containing 20% FBS. However, we observed that during bFGF-induced *in vitro* angiogenesis, *Alk1*-deficient pulmonary ECs exhibited significantly higher migratory properties than *Alk1*-heterozygous ECs in both 2D wound-induced and 3D modified Boyden chamber assays. When these ECs were seeded onto the Matrigel, they organized into a tube-like structure in response to angiogenic bFGF. *Alk1*-null ECs rapidly developed an excessive, irregular and thick tube-like network. However, *Alk1*-heterozygous ECs contained less, long and thin cords. Moreover, the cord-like structures in the mutant cell culture was sustained much longer than those of control cell culture. Although we could not see any TGF-β1- or BMP-9-specific difference in migration properties between mutant and control cells, we observed BMP-9-mediated antiangiogenic effects were blunted in *Alk1*-deleted ECs in the tube formation assay, indicating higher specificity of BMP-9 over TGF-β1 for the ALK1 signaling. Further quantitative *in vivo* assay using subcutaneous implantation of Matrigel containing bFGF also demonstrated the elevated migratory and pro-

angiogenic characteristics of *Alk1*-deleted ECs. However, a drawback in our cell lines is that we could not see a significant difference in proliferation rates between *Alk1*-heterozygous and -homozygous ECs since they were immortalized.

It has been controversy regarding the role of ALK1 on ECs during angiogenesis. Previously, our group found that in *Alk1*-KO embryos, a number of genes that act in the activation phase of angiogenesis showed an increase in their mRNA levels. Thus, we suggested that ALK1 signaling was implicated in the resolution phase of angiogenesis and functioned to inhibit EC proliferation and migration as well as promoting VSMC recruitment (97). Another group supported our findings and reported that target genes of caALK1 inhibit proliferation and migration of human microvascular endothelial cells from the dermis (HMVEC-d), implying the role of ALK1 in the maturation phase of angiogenesis (122). Furthermore, it was demonstrated that interruption of the *acvrl1* gene increased endothelial cell number in cranial vessels of zebrafish (123). However, others suggested that ALK1 signaling enhances proliferation and migration of ECs, proposing ALK1 involvement in the activation phase of angiogenesis (98, 107, 124).

Our results from this study further support a significant role of endothelial-specific ALK1 signaling for the resolution phase of angiogenesis. *Alk1*-deficient ECs resulted in increased migration, excessive tube formation and resistance for regression, features of the activation phase of angiogenesis. Therefore, in ECs without ALK1, the transition of ECs from activation to resolution is perturbed and uncontrolled angiogenesis lead to the formation of an abnormal vascular network.

Taken together, our findings at the cellular level provide a hint for the pathogenic mechanism underlying HHT-like vascular lesions containing dilated, thin-walled, excessive and

tortuous blood vessels and AVMs. Mutations in the *Alk1* gene result in a decrease in ALK1 expression, causing perturbation in the functions of ECs during blood vessel development and remodeling. The *Alk1*-deficiency in ECs leads to persistent activation phase of angiogenesis, thereby superfluous blood vessels formed. Consequently, without proliferation termination and maturation, the vessels develop enlarged lumen and thin vessel walls. In addition, it was thought that dilated and fused blood vessels surrounding AVMs mainly resulted from hemodynamic forces during the pathogenesis of HHT. However, in our *in vitro* data from the tube formation assay, peculiar thick and fused capillary-like cords or tube developed solely by *Alk1*-deletion in ECs. These fragile blood vessels are prone to rupturing, causing recurrent bleedings from telangiectasia (focal dilation of blood vessels) within the mucocutaneous layers of the skin including lips, tongue, nose and finger tips of HHT patients. Moreover, due to the lack of a switch to the resolution phase of angiogenesis, the telangiectasias can worsen and the vessels can progress into AVMs. AV shunts may develop from AVMs, leading to dilated and tortuous veins as well as fusion of arterial and venous blood flow. It is noteworthy that perturbation of Notch/Delta signaling, another known important angiogenic signaling pathway, also developed AVMs in mice (125, 126). This pathway has been implicated in arteriovenous specification (14, 16, 127, 128).

Next, we searched which signaling pathway(s) may be responsible for these cellular phenotypes. The purpose of examining the mechanism would be to find potential therapeutic target(s) that could be designed to prevent or alleviate clinical symptoms of the HHT. The TGF-β signaling pathway is diverse and complex, and proceeds in numerous SMAD-dependent and -independent pathways (39). Two major SMAD-dependent pathways are stimulated by the ligand binding to the type II and Type I receptor complex (39, 44) (Figure 2-11A). The TGF-β ligand-

mediated pathway propagates signals via receptor-regulated (R)-SMAD2 and 3. These are phosphorylated by the structurally similar type I receptors ALK4, 5 and 7 (129-132). In contrast, R-SMAD1, 5 and 8 are specific for the BMP pathway and are induced by ALK1, 2, 3 and 6 (133). We found that the basic components for these two major SMAD pathways were present in both parental control and TM-treated mutant ECs based on our findings that phosphorylation of SMAD2/3 or SMAD1/5/8 were enhanced with TGF-β1 or BMP-9 treatment, respectively. Interestingly, the basal level of phospho-SMAD2/3 was slightly decreased in *Alk1*-null ECs with or without bFGF, suggesting that the inhibitory effects of TGF-β signaling on ECs were reduced in the absence of ALK1; thus, *Alk1*-deleted ECs were more migratory and pro-angiogenic in response to an angiogenic cue. The most interesting finding was that BMP pathway was intact despite the absence of ALK1. In RT-PCR analysis, the presence of BMP pathway-implicated type II receptors, including activin type II receptors (ActRII) and BMPR2 as well as other type I receptors such as ALK2, 3 and 6, was revealed, suggesting that the SMAD1/5/8-regualted BMP pathway was compensated by other receptors in the ALK1-deficient mutant pulmonary ECs (Figure 2-11B). This implied that distinctive cellular phenotypes of *Alk1*-null ECs might be resulted from unknown ALK1-specific downstream pathway(s) rather than SMAD-dependent signal transduction cascades.

Many studies have demonstrated that TGF-β family signaling can activate SMAD-independently MAPK and PI3K pathways (39, 104). It was found that the activation of JNK MAPK (134) and p38 MAPK (135) was observed in SMAD-defective cells with TGF-β treatment. Additionally, it was reported that TGF-β-induced signaling lead to phosphorylation of an intracellular component (Akt) of the PI3K pathway (136, 137). Among MAPK pathways including JNK, p38, and ERK, we focused on the ERK1/2 MAPK pathway. Previously, it was

suggested that the activated ERK signaling by TGF-β caused SMAD phosphorylation and modulated SMAD activation (134, 138-140). More importantly, a recent study showed a negative effect of caALK1 on the activation of ERK1/2 in human dermal microvascular ECs, resulting in inhibition of EC migration in response to wounding (120). However, results from our Western blot analysis contradicted conclusions. Although it was not statistically significant, the basal phosphorylation level of ERK1/2 was decreased in ALK1-deficient ECs. The induction of ERK1/2 in response to stimulation by either TGF-β1 or BMP-9 with or without pro-angiogenic bFGF was even further reduced in these ECs. Since activated ERK induces the SMAD phosphorylation and subsequent activation, it indicated that TGF-β signaling might be more inhibited upon stimulation in ALK1-defiecnt ECs. Thus, its negative effects on ECs were more repressed, leading to further elevated pro-angiogenic properties. Notably, although the difference was not significant, in the absence of ALK1, the reduction in phosphorylated ERK1/2 was greater by TGF-β1 than BMP-9 treatments. Therefore, it appears that BMP-9-induced inhibitory effects on the ERK MAPK pathway were reduced in *Alk1*-null ECs. In other words, BMP-9 may be more dependent on the ALK1 signaling than TGF-β1 in our pulmonary ECs. However, we could not rule out the possibility that immortalization by the SV40 T-antigen transfection could affect many signaling pathways in our ECs.

In summary, we established a pulmonary EC line containing a genetically modified *Alk1* allele from the $R26^{+/CreER}$; $Alk1^{2f/1f}$ mouse. After a 2-day TM treatment, we could obtain *Alk1*-null ECs from these parental ECs. As compared to $Alk1^{2f/1f}$ control ECs, the peculiar cellular phenotypes of *Alk1*-null ECs were increased migration and endothelial outgrowth or sprouting in response to the pro-angiogenic challenge, suggesting that the *Alk1*-deletion resulted in elevated angiogenic responses in lung ECs. Additionally, disorganized and dilated tube-like structures

developed exclusively due to *Alk1*-deficiency in ECs. Furthermore, this *in vitro* tube formation assay suggests that ALK1 may be more specific or the pertinent receptor for BMP-9, rather than TGF-β1. However, since we used a much higher concentration of BMP-9 than its known physiological concentration (approximately 5 ng/ml), it will be necessary to perform the same experiments with this concentration. Although we could not find a ALK1-specific intracellular downstream pathway, our results from Western blotting demonstrated that ALK1 signaling in ECs may be SMAD-independent and BMP-9 may be the more relevant ligand for its signaling. There are several other pathways such as JNK MAPK, p38 MAPK and PI3K which has been suggested to be regulated by the TGF-β superfamily members. Most recently, an *in vivo* study suggested functional redundancy between p38 and Smad4, the intracellular effector transducing the signal from all SMAD-dependent pathways into the nucleus, in mediating TGF-β signaling during tooth and palate development (141). Therefore, it will be interesting to investigate how the p38 MAPK as well as JNK MAPK and PI3K pathways are differentially modulated in our *in vitro* systems. Moreover, we have developed another parental EC line carrying the $R26^{+/CreER}$; $Alk1^{2f/2f}$ transgene. Using this EC line, we can compare cellular and molecular phenotypes of $Alk1^{2f/2f}$ equivalent to *Alk1*-wildtype and $Alk1^{1f/1f}$ equivalent to homozygote pulmonary ECs. The findings from this study will further broaden our insight into the EC-specific ALK1 signaling.

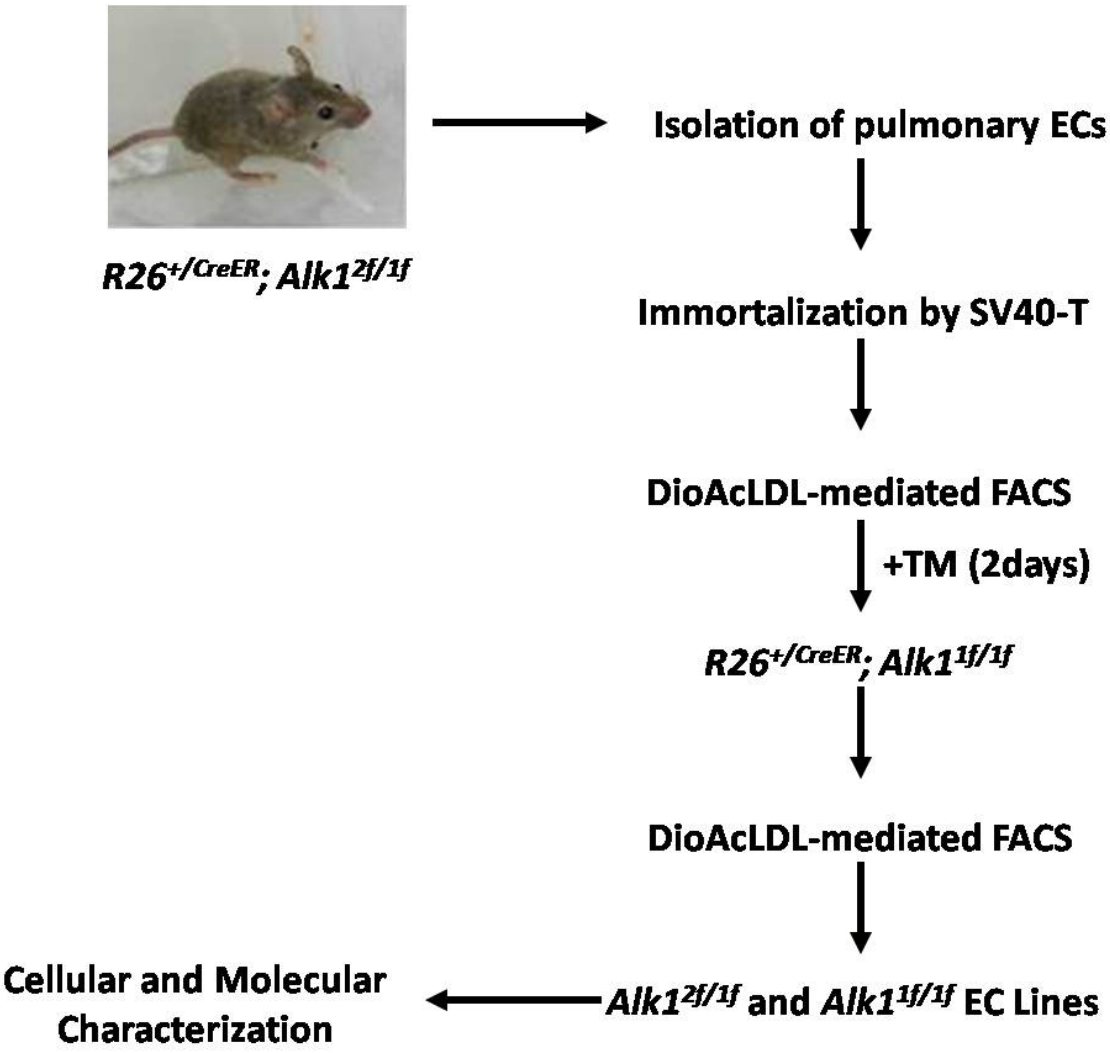

Figure 2-1. Experimental scheme for cellular and molecular characterization of *Alk1*-heterozygous (*Alk1*$^{2f/1f}$) and *Alk1*-homozygous (*Alk1*$^{1f/1f}$) pulmonary ECs. Parental pulmonary ECs were isolated from the *R26*$^{+/CreER}$*; Alk1*$^{2f/1f}$ mouse and immortalized by SV40-T antigen tranfection. A pure EC population was obtained by FACS. Endothelial properties were further examined by their morphology and EC-specific marker genes expression. Based on the desired characteristics, clone #28 was selected. Subsequently, *Alk1*-null ECs were derived from the parental cell line with a 2-day TM treatment. After another FACS, both *Alk1*$^{2f/1f}$ control and *Alk1*$^{1f/1f}$ mutant EC lines were established. Finally, they were cellularly and molecularly investigated.

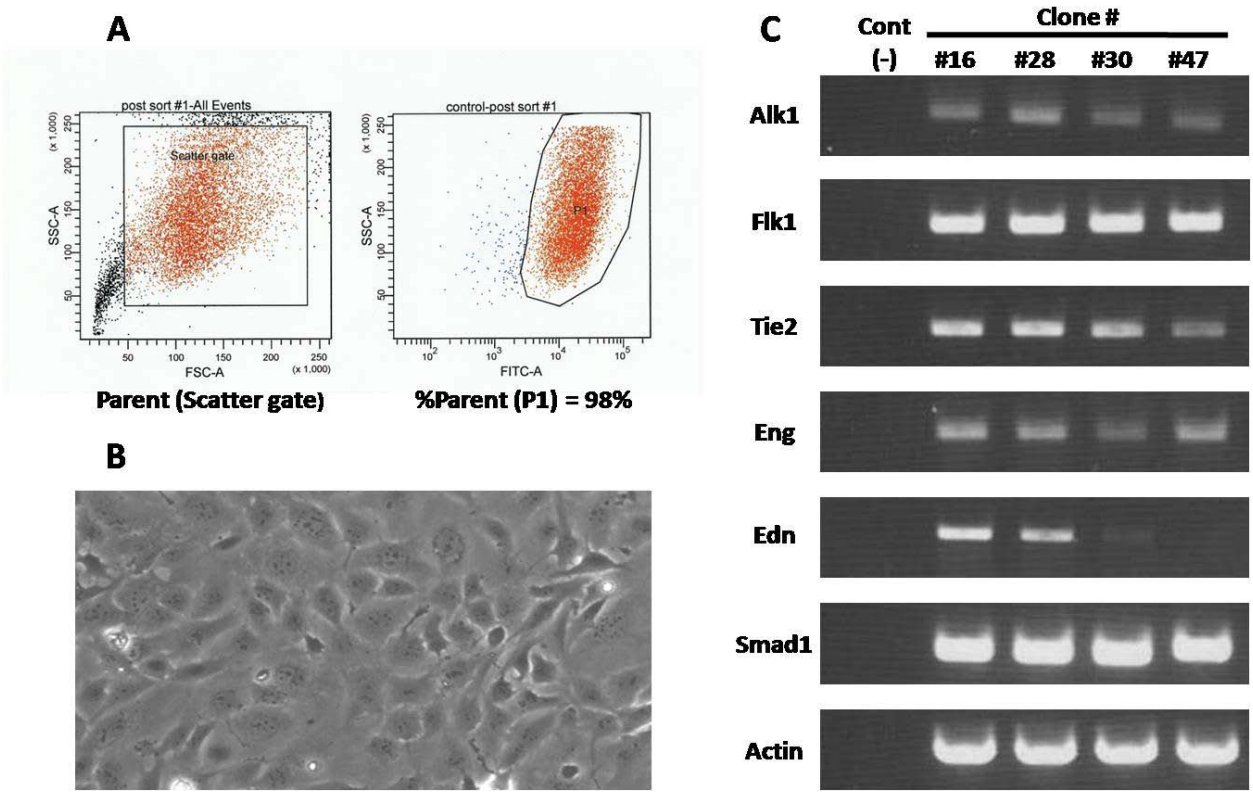

Figure 2-2. Establishment of *R26*$^{+/CreER}$*; Alk1*$^{2f/1f}$ (equivalent to *Alk1*-null heterozygote; *Alk1*$^{+/-}$) parental pulmonary endothelial cell line. A) After DioAcLDL-labeled FACS, representative data showed the culture containing about 98% purity for the EC population. Note that TM-treated *R26*$^{+/CreER}$*; Alk1*$^{1f/1f}$ (equivalent to *Alk1*-null homozygote; *Alk1*$^{-/-}$) ECs showed the similar pure population, indicating that TM did not affect endothelial properties of ECs. B) In morphological evaluation, isolated and immortalized ECs displayed endothelial-specific polygonal shapes and cell-cell contact inhibition at confluency. C) Amongst several isolated clones, the clone #28 showed the highest Alk1 and Endothelin (Edn) expression at the RNA level. Expression for EC-specific marker genes including Flk1, Tie2, and Eng was further confirmed by the RT-PCR analysis. The expression of Smad1 was examined to see whether this clone contained its representative downstream molecule. Actin was used as the loading control.

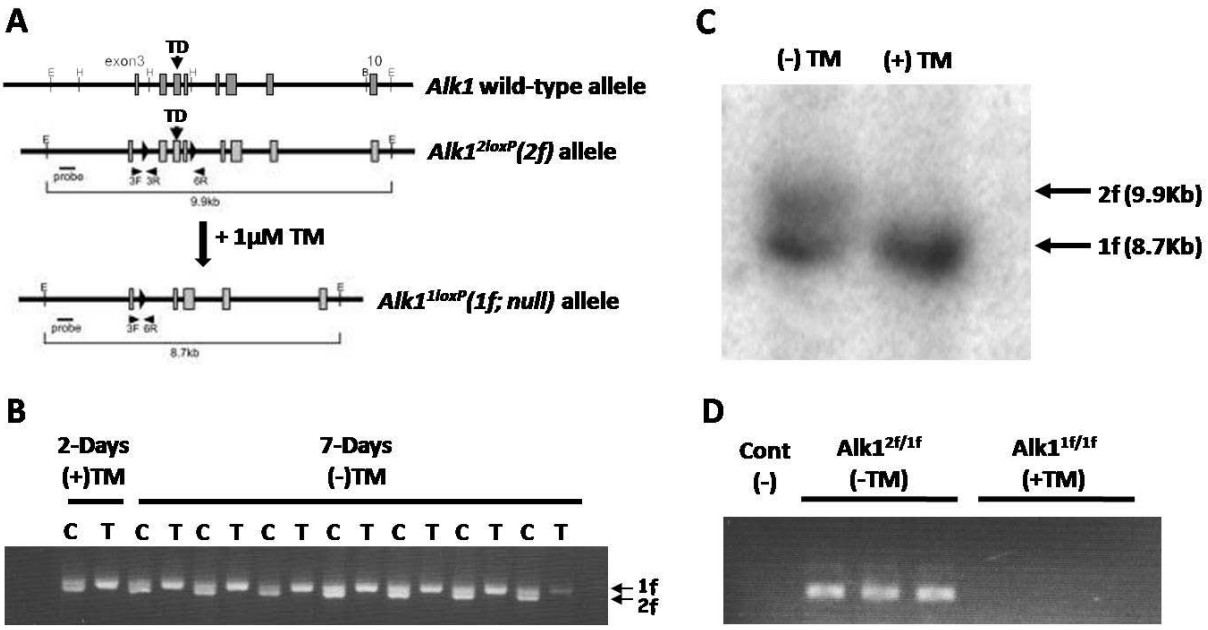

Figure 2-3. Derivation of *R26*$^{+/CreER}$*; Alk1*$^{1f/1f}$ (equivalent to *Alk1*-null homozygote; *Alk1*$^{-/-}$) ECs from parental EC line. A) Schematic diagram of the *Alk1* wild-type, *Alk1*^{2loxP} (2f) and *Alk1*^{1loxP} (1f) alleles. Exons and loxP sequences are denoted by boxes and arrowheads, respectively. Locations of primer pairs detecting specific regions containing loxP sequences for the genomic PCR analysis and sites of probes recognizing the 5' region of the *Alk1* gene which was used for the genomic Southern blot analysis are indicated. Note that since exon 5 encodes the transmembrane domain (TD) of the *Alk1* gene, the deletion of exons 4 to 6 results in a null allele. B) After a 2-day 1 μM TM treatment, the *2f Alk1*-cKO allele was undetectable due to Cre recombinase-mediated deletion. The resulting *1f Alk1*-null allele was maintained for 7 days without further TM addition. Note that for genomic DNA PCR analysis, genomic DNAs were collected at 2 days post-TM treatment and everyday for 7 days after transferring cells in normal ECM. C) Genetic modification of *Alk1*-null homozygote by a 2-day TM treatment was confirmed by the genomic Southern blotting. D) RT-PCR analysis verified the deletion of the *Alk1* gene at the RNA level. Alk1 transcripts were undetectable in the TM-treated *Alk1*$^{1f/1f}$ ECs. Negative control indicates no RT-PCR reaction. Note that PCR primers used for RT-PCR analysis detect exons 4 and 5 of the *Alk1* gene.

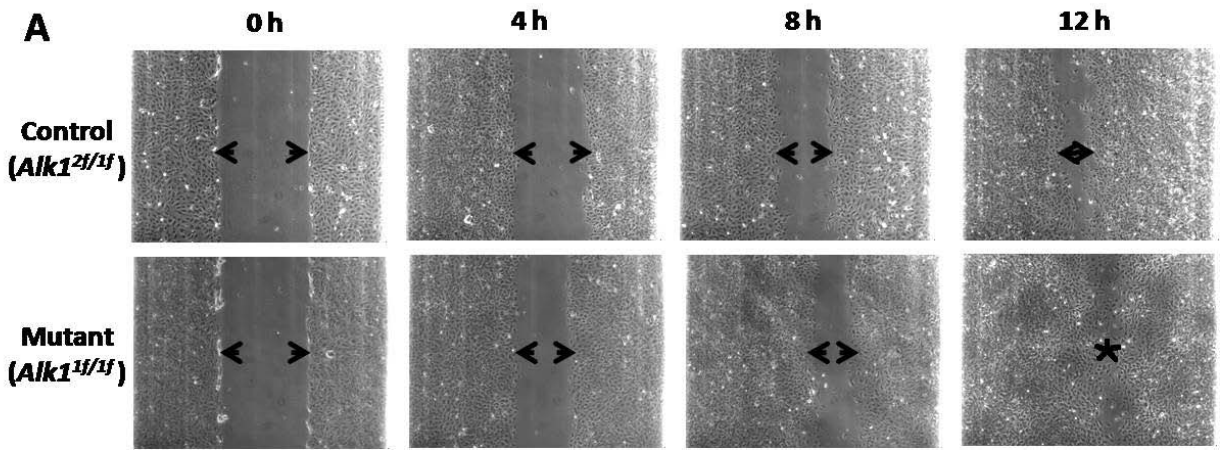

Figure 2-4. *Alk1*-null pulmonary ECs displayed elevated migratory index upon angiogenic factor challenge. A) After control and mutant ECs wounding, the closing of wounds in response to bFGF (50 ng/ml) stimulation was photographed every 4 hours. Mutant cells migrated much faster compared to control cells. At 12 hours post wounding, mutant cells almost completely closed the wound, while the wound was still present in the control culture. This observation was confirmed by the statistical analysis. B) and C) In the 2D wound-induced migration assay, $Alk1^{1f/1f}$ mutant ECs were significantly more migratory than $Alk1^{2f/1f}$ control ECs in ECM containing 20% FBS. D) and E) The same results were obtained in chemically defined growth factor- and serum-free ECM, indicating no FBS effects on the data in B and C. F) and G) In the 3D modified Boyden chamber assay, 48 hours after seeding (5×10^2 cells), significantly more number of migrating $Alk1^{1f/1f}$ mutant ECs were counted in six randomly chosen fields as compared to $Alk1^{2f/1f}$ control ECs F) with 20% FBS and G) without FBS. Note that all data represent means from three independent experiments. Error bars show standard errors.

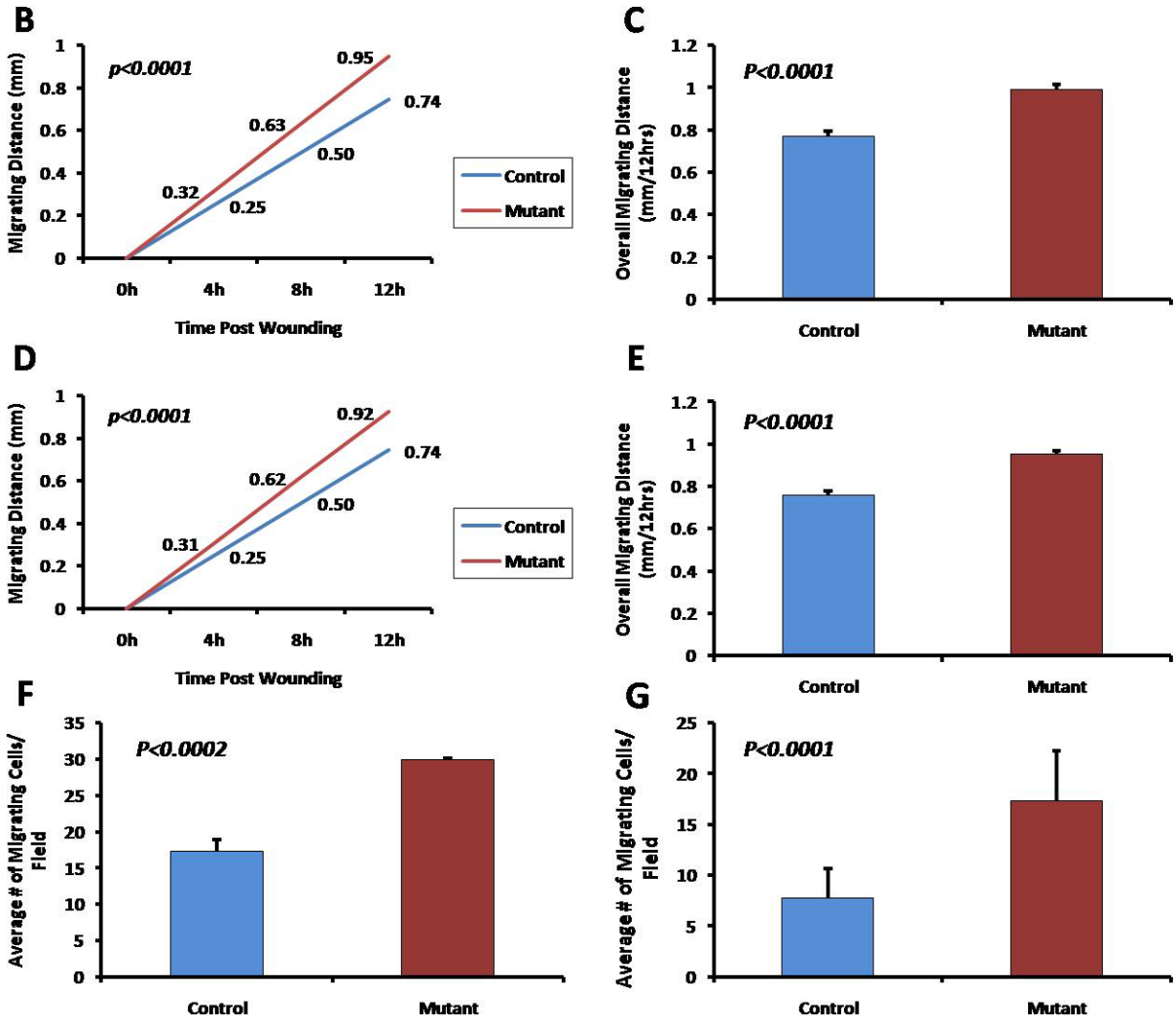

Figure 2-4. Continued.

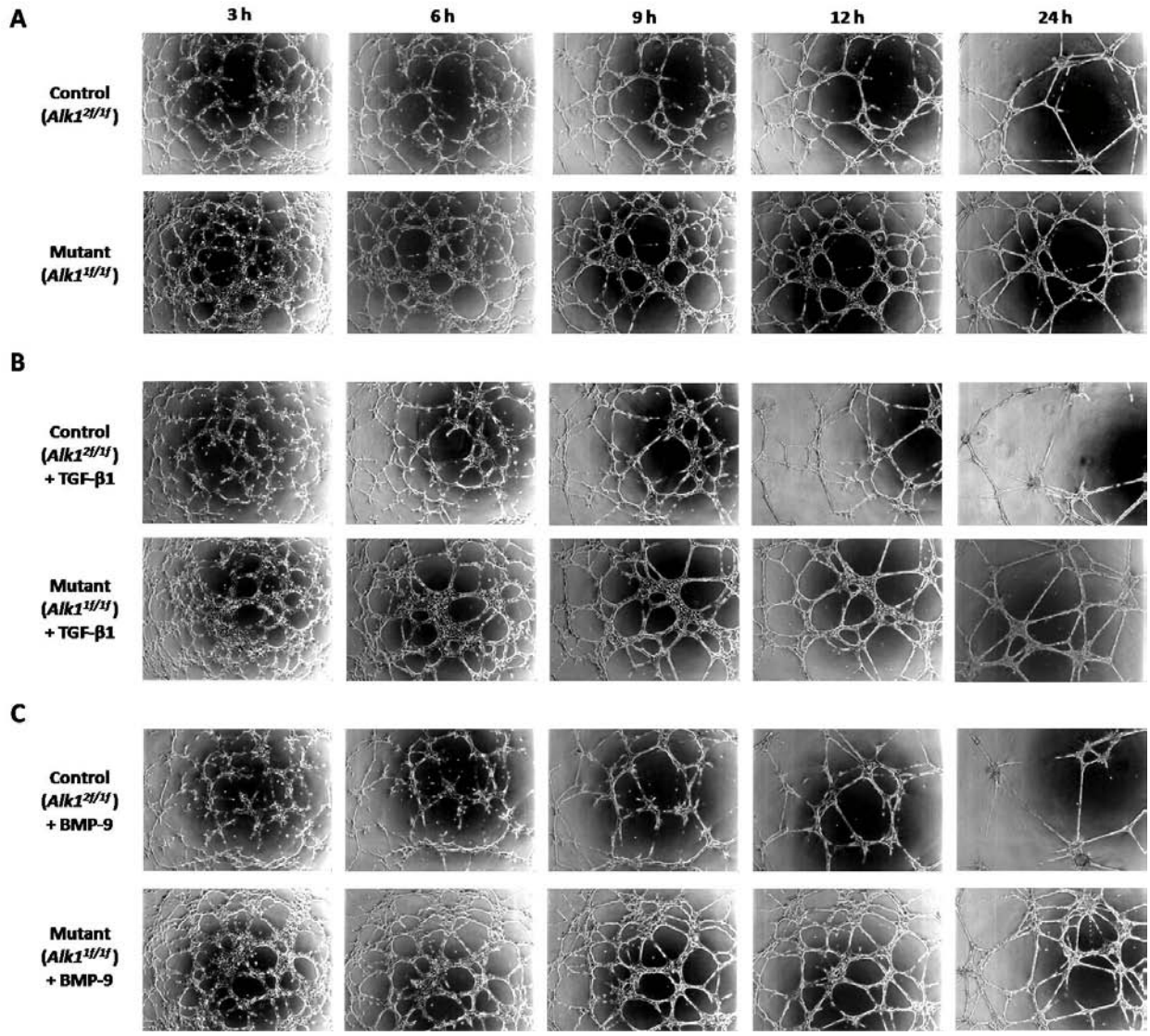

Figure 2-5. *in vitro* Matrigel tube formation assay. *Alk1*-heterozygous ($Alk1^{2f/1f}$) control and *Alk1*-homozygous ($Alk1^{1f/1f}$) mutant pulmonary ECs (1×10^5) were diluted into chemically defined growth factor- and serum-free ECM and seeded onto the Matrigel. To monitor their cellular traits in the tube formation during *in vitro* angiogenesis, pictures were taken every 3 hours (50X; height × width = 2.1 mm × 2.8 mm). A) Tube-like structures were formed by control or mutant cells in response to bFGF (50 ng/ml). B) In addition to bFGF, one known putative physiological ligand for ALK1, TGF-β1(5 ng/ml) was supplemented with culture medium. C) Another possible ligand for ALK1, BMP-9 (20 ng/ml) was added into medium containing bFGF. Note that all pictures are representatives of three independent experiments. *Alk1*-deleted ECs displayed an irregular, excessive and dilated capillary-like network formation as compared to control cultures.

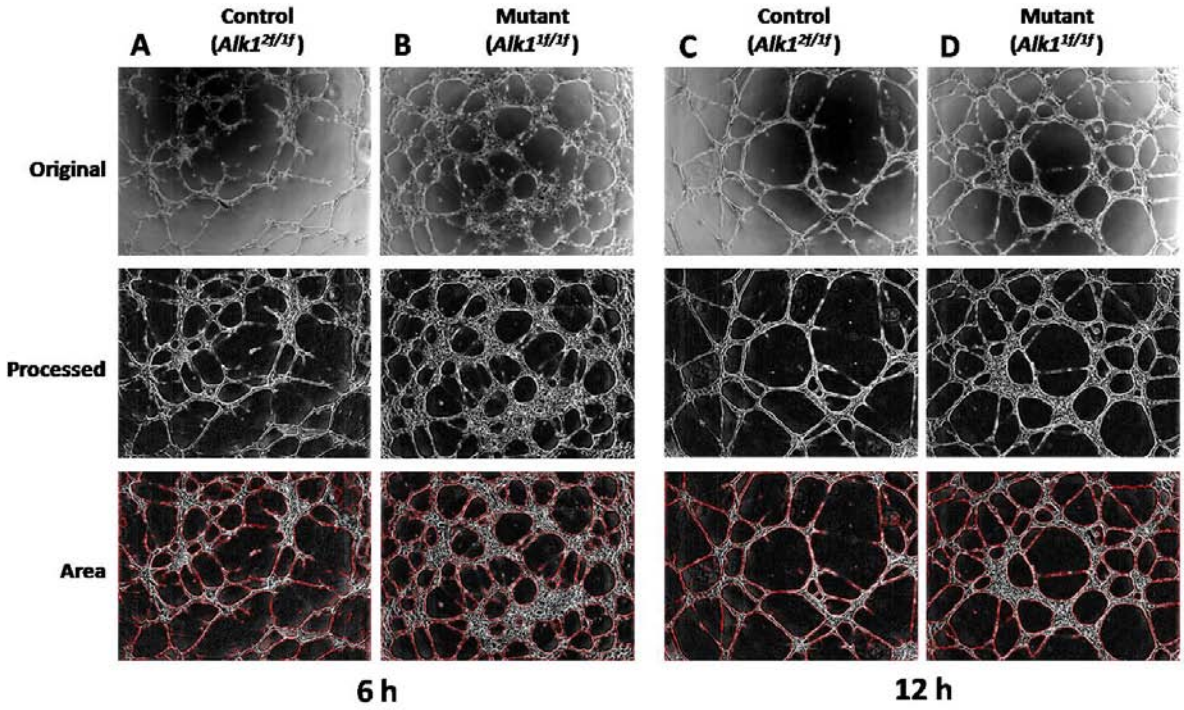

Figure 2-6. *Alk1*-null ECs formed thicker tube-like structures that are resistant to regression. A), C) and E) Original images of the control cultures at 6, 12, 24 hours after seeding (50X). All of original images were processed by the MatLab imaging program. Matrigel background is shown as black, while tube-like structures are presented as light gray. The processed images were used to calculate coverage area of capillary-like structures. The red solid line delineated boundaries of these structures. B), D) and F) Corresponding original, processed and coverage area-measured images of the mutant culture. G) Coverage areas of capillary-like structures formed by control or mutant cells in response to bFGF (50 ng/ml) were calculated as percentages of the whole field. Results from statistical analysis are shown. Note that pictures are representatives of three independent cultures. All data are means of three distinctive experiments. Error bars indicate SEM (+ $p<0.05$, ++ $p<0.01$ and +++ $p<0.001$).

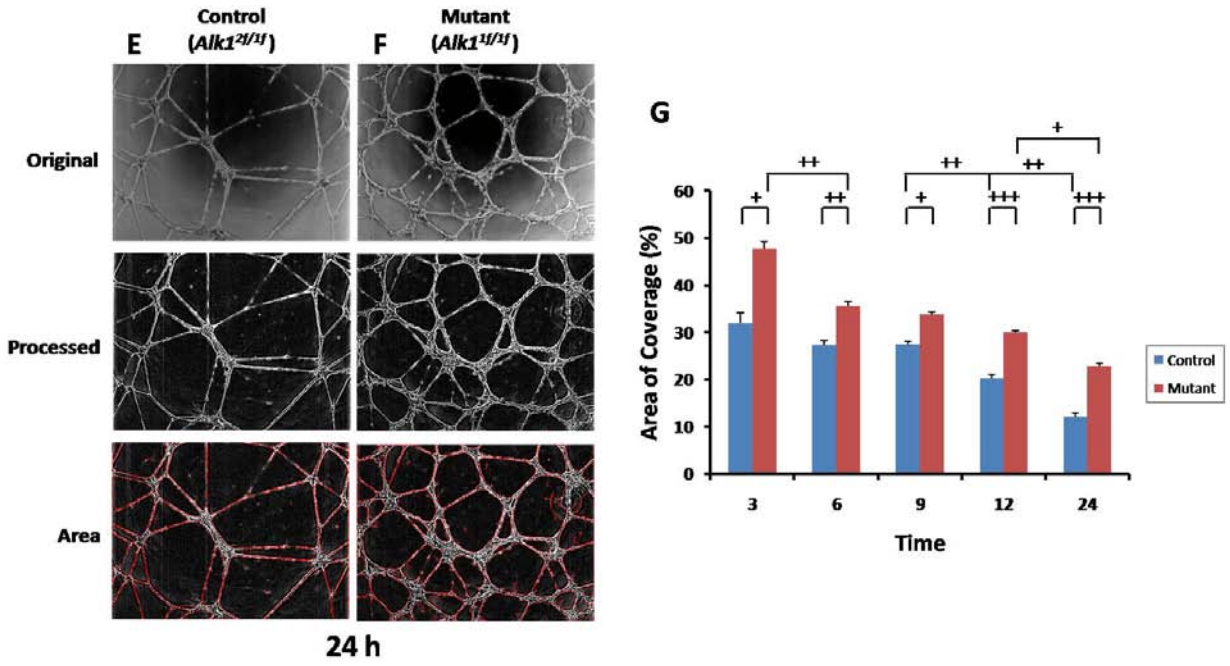

Figure 2-6. Continued.

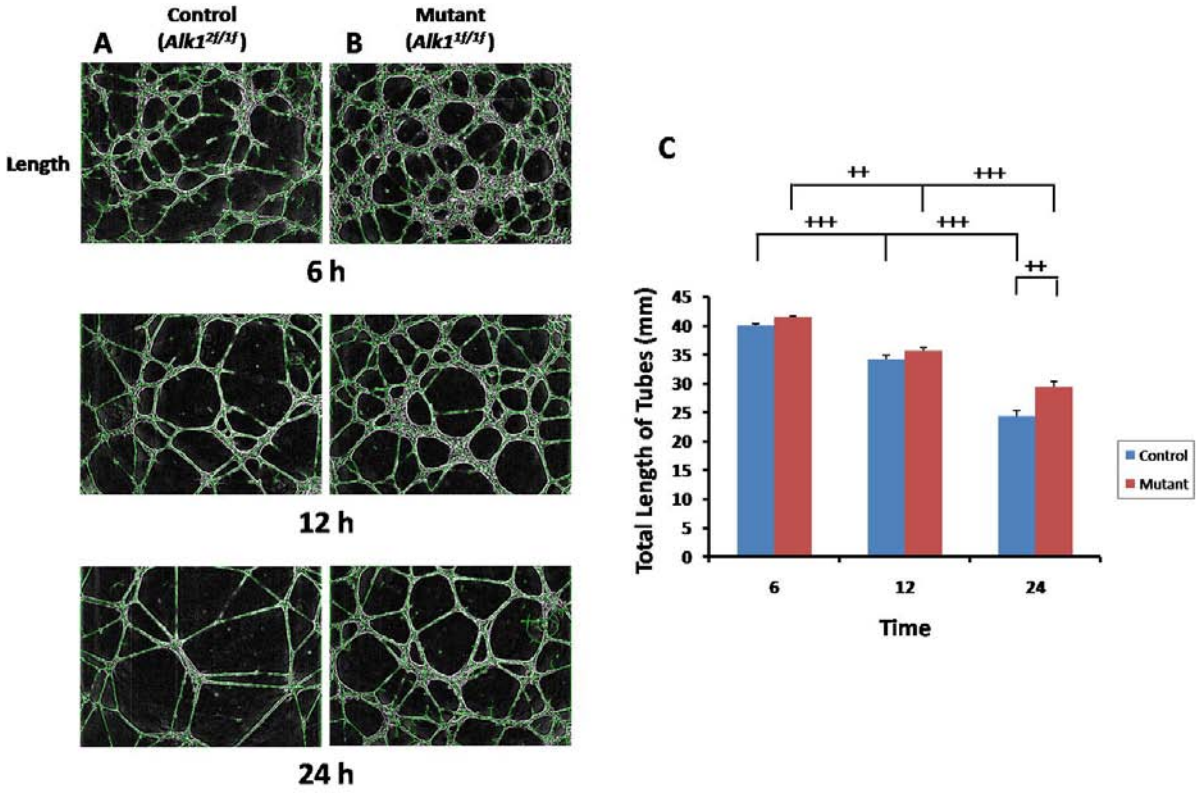

Figure 2-7. ALK1-deficiency resulted in an increase in length of tubes and sprouting of ECs. A) Processed images of control cells were used to calculate the total length of tubes. Tubular lines are shown in green solid lines. B) Corresponding images of mutant cells were used to measure the total length of tubes. C) Total length of endothelial tubes of the control and mutant were measured and statistically analyzed. D and E) Control and mutant ECs sprouts or outgrowth from nodules are represented as red dots on tubular networks which are shown in A and B, respectively. F) The number of endothelial sprouting from each nodule was counted. The difference in sprouting properties of control and mutant cells was examined by comparing total number of their outgrowth per field and statistically evaluated. Note that images are representatives of three distinctive cultures. All data are means of three independent experiments. Error bars indicate SEM (+ $p<0.05$, ++ $p<0.01$ and +++ $p<0.001$).

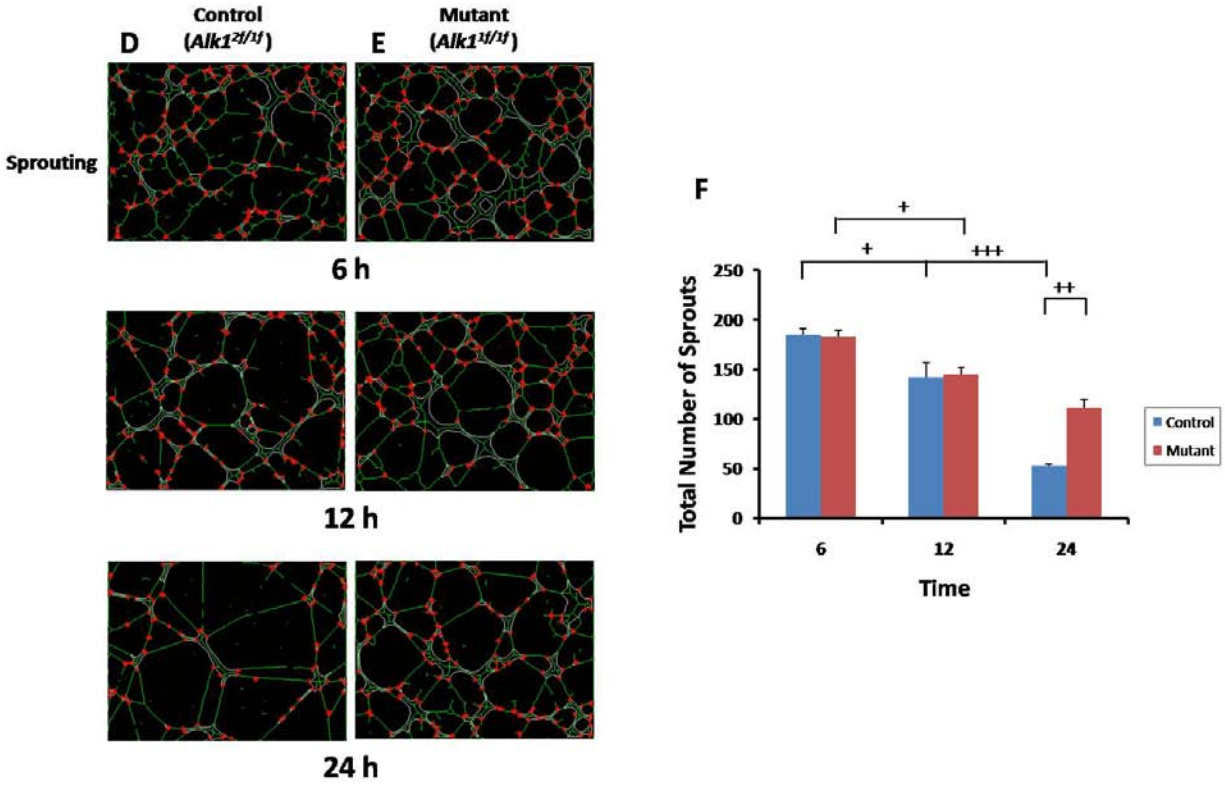

Figure 2-7. Continued.

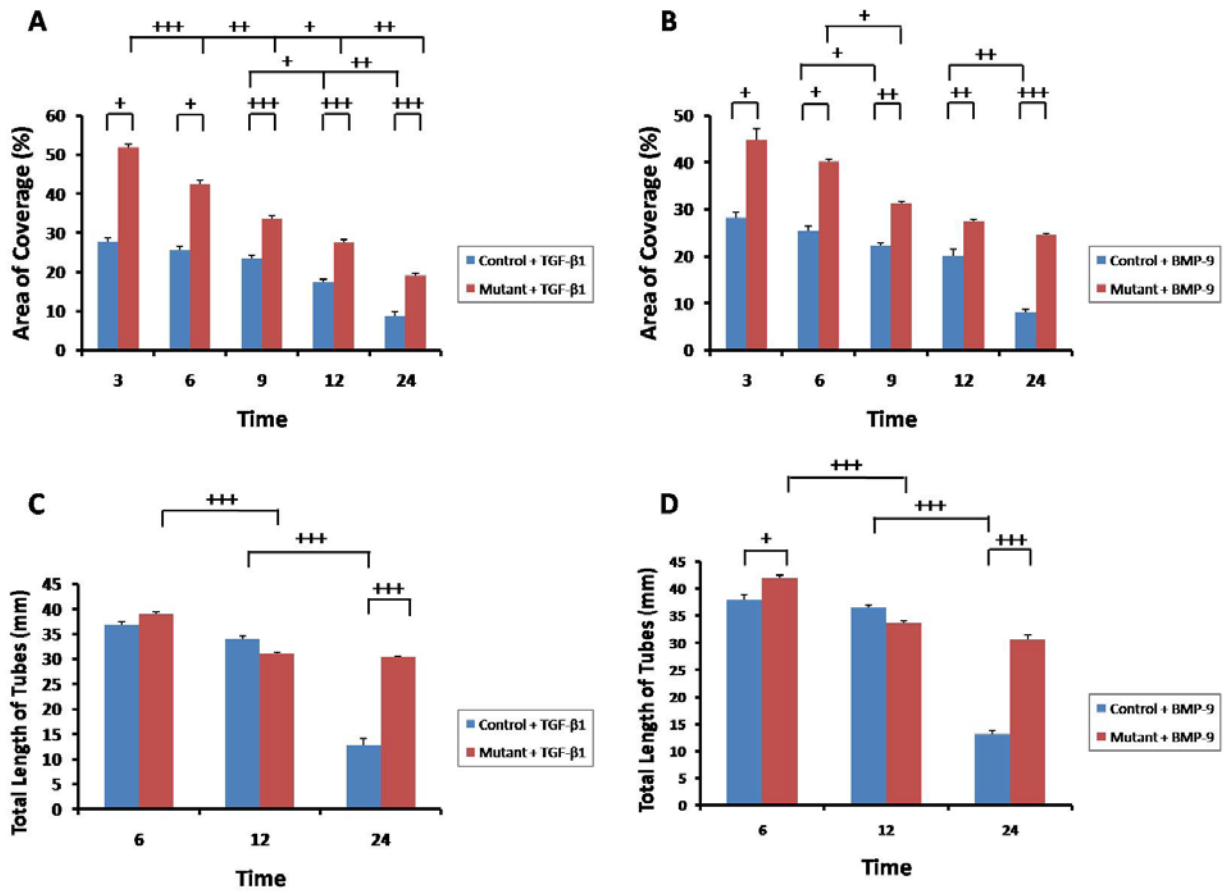

Figure 2-8. Inhibitory effect of BMP-9 on angiogenesis was diminished, whereas that of TGF-β1 existed in *Alk1*-null ECs. Pictures of control and mutant ECs cultures with bFGF (50 ng/ml) in combination with either A), C) and E) TGF-β1 (5 ng/ml) or B), D) and F) BMP-9 (20 ng/ml) taken at various time points were processed as described in Figures 6 and 7. Each parameter was measured by using processed images. A) and B) Surface area of capillary-like networks from the control and mutant was calculated and statistically analyzed. C) and D) The total length of these networks was statistically evaluated. E) and F) The total number of EC sprouting from nodules were counted and statistically analyzed. Note that all of calculations were performed as described in Figures 6 and 7. Images are representatives of three distinctive cultures. All data are means of three independent experiments. Error bars indicate SEM (+ $p<0.05$, ++ $p<0.01$ and +++ $p<0.001$).

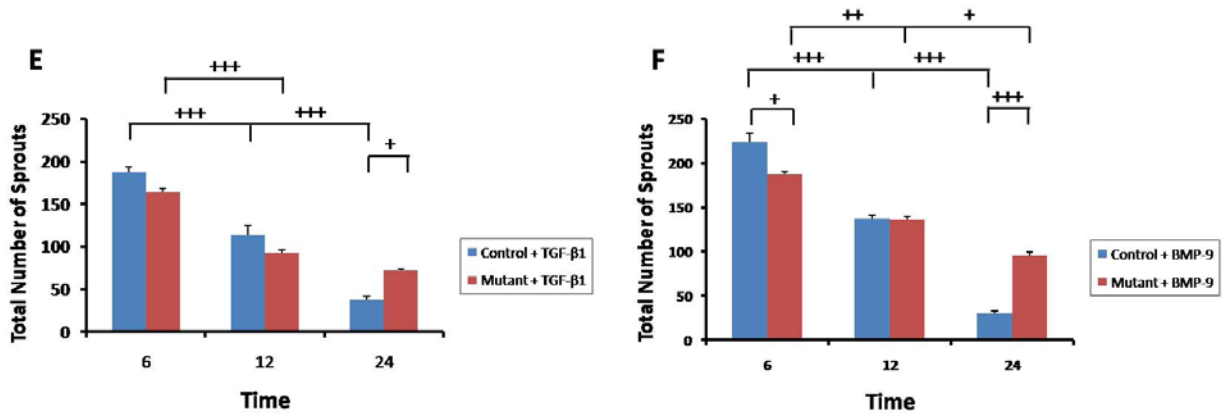

Figure 2-8. Continued.

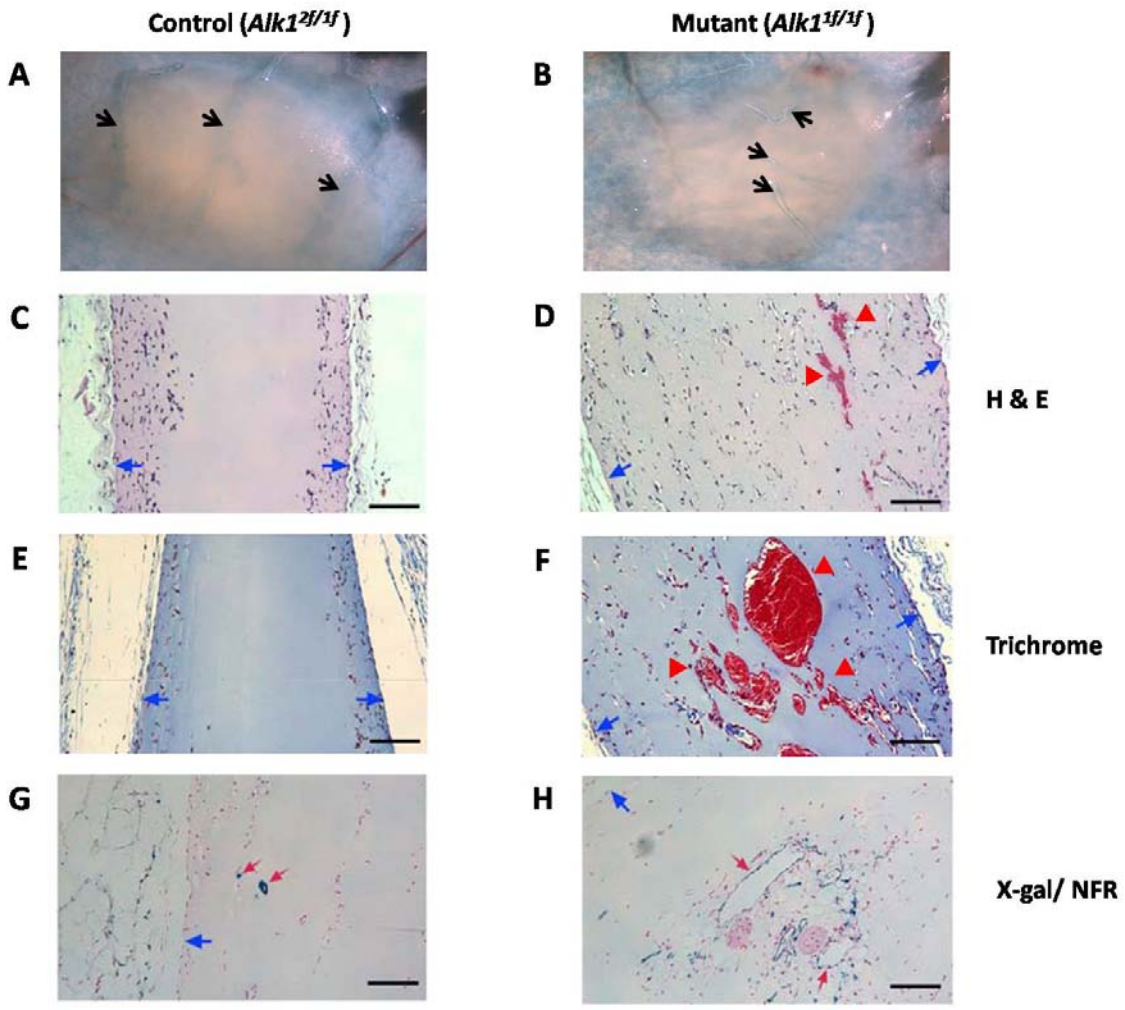

Figure 2-9. *in vivo Alk1*-deletion also resulted in higher migratory and pro-angiogenic properties of ECs. Whole mount Matrigel plugs from A) and G) control $R26^{+/+}$; $Alk1^{2f/2f}$; $Flk1^{+/lacZ}$ and B) and H) mutant $R26^{+/CreER}$; $Alk1^{2f/2f}$; $Flk1^{+/lacZ}$ mice were stained with X-gal. Representative histological sections of Matrigel plugs in the TM-treated control and mutant skin are shown in C, E, G and D, F, H, respectively. A) Macroscopic examination revealed all vessels were formed between the skin layer and Matrigel plug in the control (n=6). B) However, in the mutants, several nascent vessels invaded the Matrigel plug (n=5). Newly formed vessels are indicated by black arrows. In H & E staining, C) migrating control cells were confined to the edges of Matrigel plugs, whereas D) migrating mutant cells were found much more broadly. E) and F) Similar findings in C and D were observed by trichrome staining, which showed the Matrigel in blue. D) and F) Several disorganized blood vessel structures, denoted by red arrowheads, were only shown in Matrigels from the mutants. G) Nuclear fast red (NFR) staining following whole mount X-gal staining showed the appearance of few and small nascent blood vessels in the controls. H) Meanwhile, mutants displayed enlarged lumen and irregular shapes. Red arrows indicate X-gal positive vascular ECs. C) - H) Margins of Matrigel plugs are represented by blue arrows.

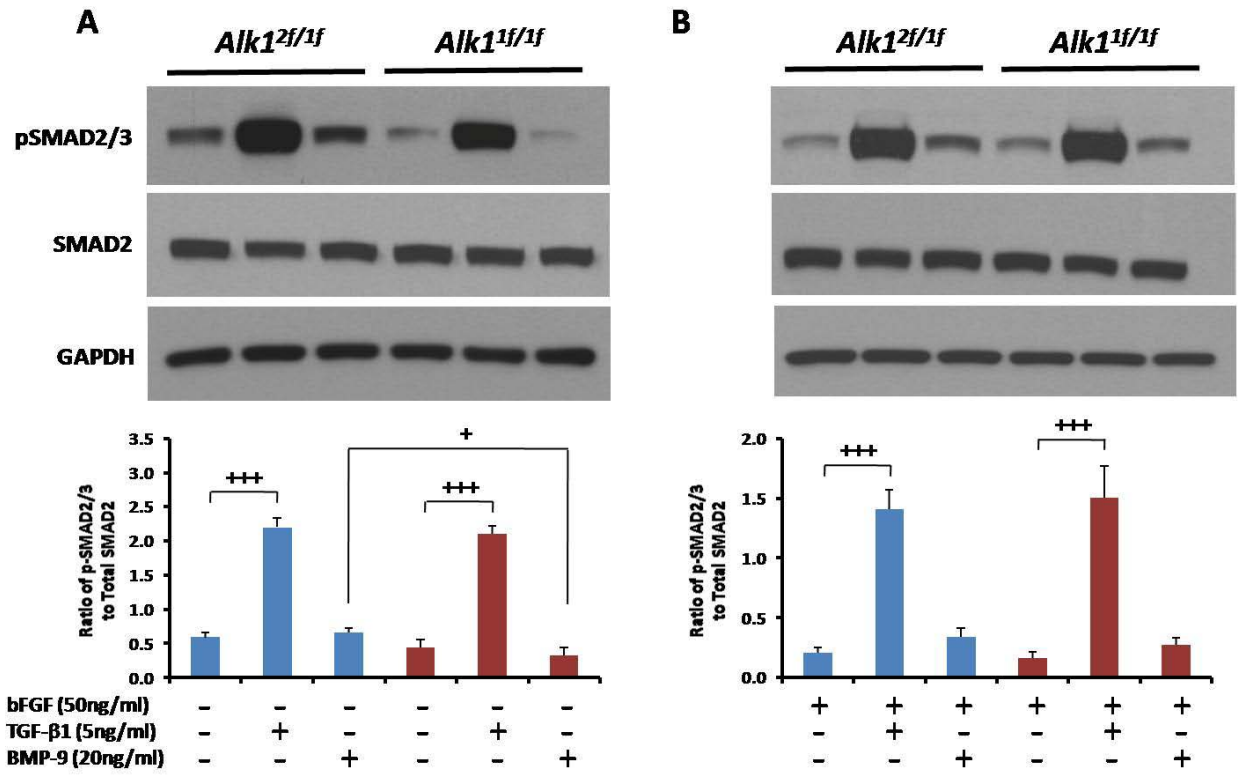

Figure 2-10. ALK1 signaling in pulmonary ECs was not specific for SMAD-dependent nor the ERK MAPK pathways. After overnight serum starvation, both *Alk1*$^{2f/1f}$ and *Alk1*$^{1f/1f}$ ECs were incubated with either TGF-β1 (5 ng/ml) or BMP-9 (20 ng/ml) in the absence A), C) and E) or presence B), D) and F) of bFGF (50 ng/ml) for 30 minutes. Protein lysates were resolved on a 8% SDS-polyacrylamide gel, transferred on a blotting membrane, and then immunoblotted with various antibodies. The level of induced phosphorylation was calculated by the ratio of phosphorylated proteins to total proteins. A) and B) Activation of TGF-β1-specific SMAD2/3 pathway was detected by phosphorylated-SMAD2/3. C) and D) Stimulation of BMP-9-specific SMAD1/5/8 pathway was revealed by phosphorylated-SMAD1/5/8. E) and F) Induction of ERK1/2 MAPK pathway was shown by its phosphorylation. Note that all Western blots are representatives of three independent experiments. GAPDH was used as a loading control. All total and phosphorylated protein amounts were normalized to the amount of GAPDH. After normalization, the level of induced phosphorylation was calculated. Data in all graphs represent means of values measured by densitometry from three separate blots. Error bars are SEM (+ $p<0.05$, ++ $p<0.01$ and +++ $p<0.001$).

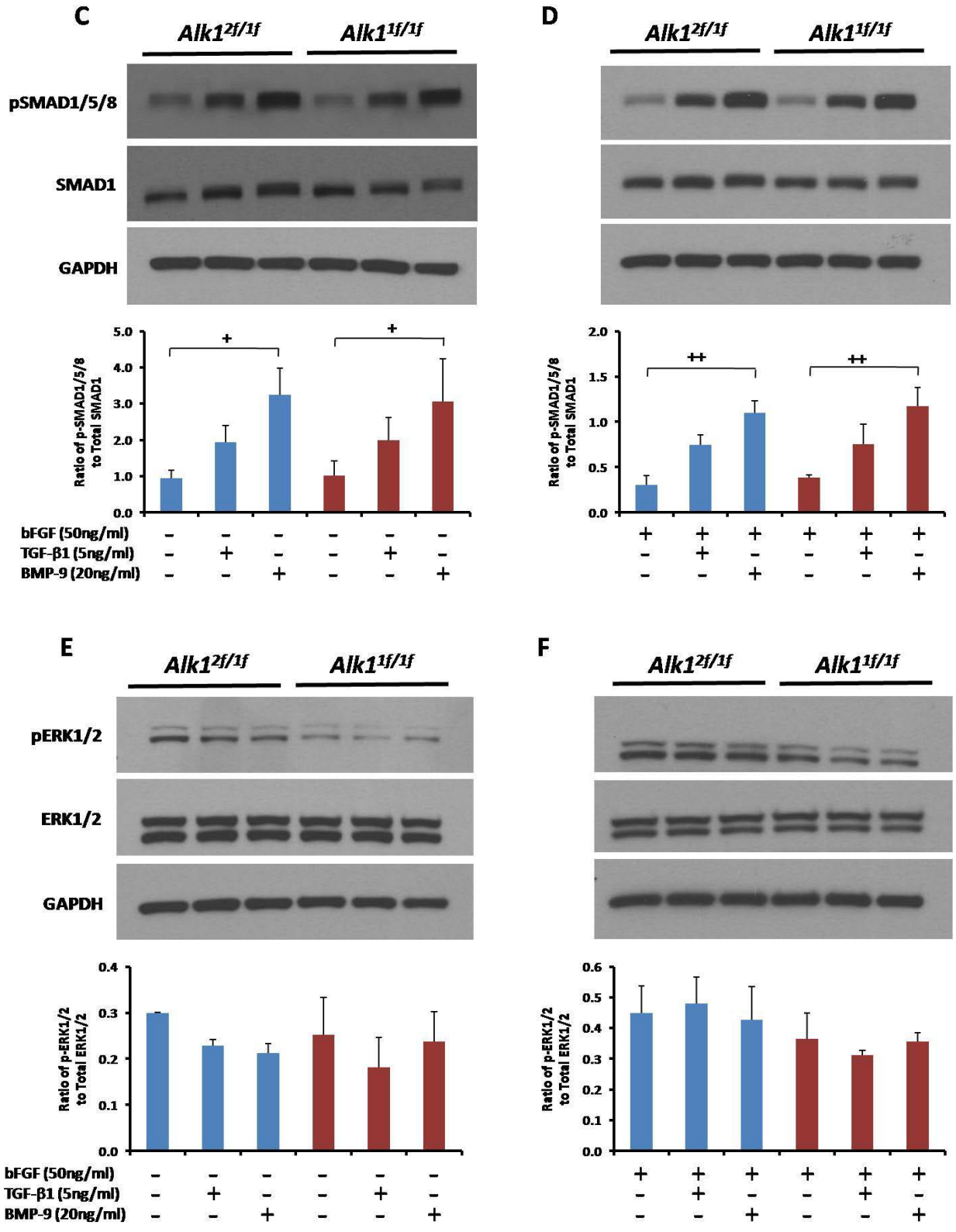

Figure 2-10. Continued.

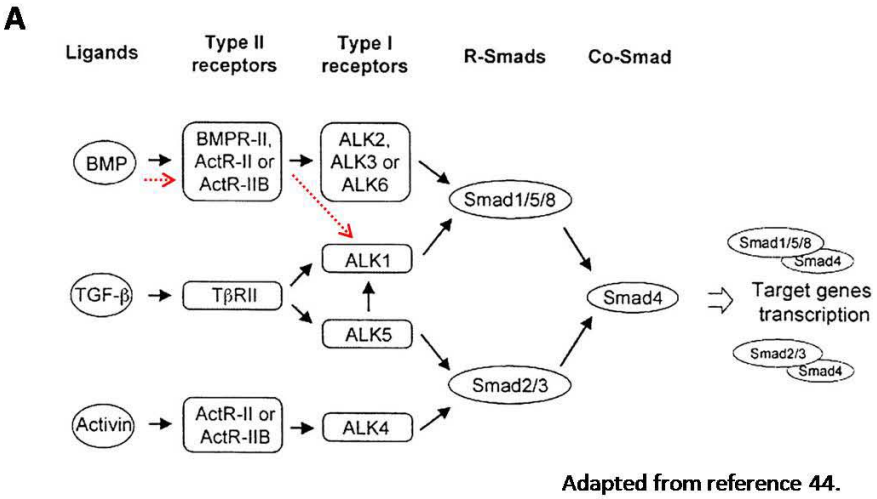

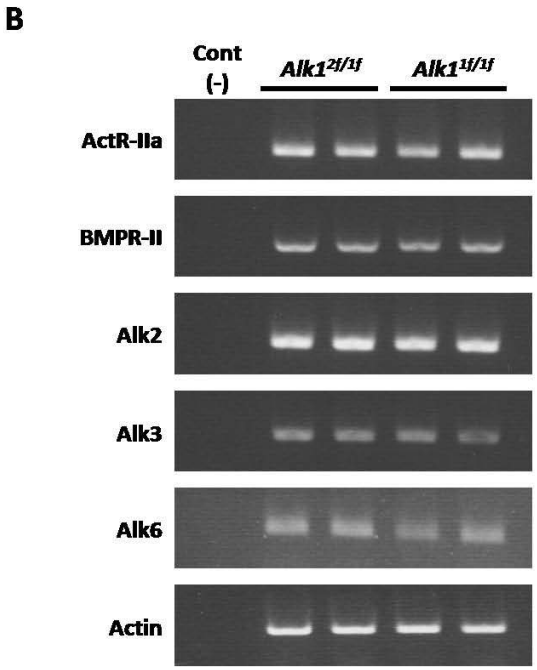

Figure 2-11. BMP-specific SMAD1/5/8 pathway for ALK1 signaling was compensated by other TGF-β type I receptors in pulmonary ECs. A) Diversity and complexity in TGF-β superfamily signaling through combinations among its type II, type I receptors and SMADs. Black arrows in solid line show a traditional view for the ALK1 signaling. The new insight in EC-specific ALK1 signal transduction mediated by BMP-specific pathway is indicated by the red dotted arrows. B) RT-PCR analysis confirmed the presence of compensatory pathways for the BMP pathway by the existence of TGF-β type II (ActRIIa and Bmpr2) and type I receptors (Alk2, 3 and 6). Note that total RNAs were extracted from two different cultures of each EC line. Negative control indicated the absence of RT reaction. Actin was used as a control showing that the same amounts of RNAs from each culture were used for the RT reaction.

CHAPTER 3
NOVEL PHYSIOLOGICAL EFFECT(S) OF ARTERIOVENOUS MALFORMATIONS (AVMS) ON TUMOR VASCULATURE

Background

Tumor Angiogenesis

In solid tumor biology, new blood vessel formation during tumor growth, also known as tumor angiogenesis, is an important process not only for understanding tumorigenesis but also designing anti-tumor therapies. The progression and metastasis of various solid tumors largely depend on their own vascular network. To support actively proliferating cells, tumors require their own blood supply that provides nutrients and oxygen as well as removes metabolic wastes (142). Therefore, as they grow beyond limited size, tumors turn on an angiogenic switch (142, 143). In contrast to physiological angiogenesis in which the balance between pro- and anti-angiogenic factors is strictly regulated and nascent vessels become rapidly stabilized, tumor-induced pathological angiogenesis causes locally unbalanced pro-angiogenic molecules to be overproduced and as a consequence new vessels are steadily formed (143). The constantly increased vascularity without stabilization leads to abnormal tumor vasculature in which blood vessels are irregular in shape, dilated and sinuous (143, 144). Furthermore, these tumor blood vessels exhibit disorganization of arterioles, venules and capillaries, are very leaky and hemorrhagic (143). Blood flow within the tumor vasculature is neither even nor unidirectional (144). In a recent review, it is argued that despite many differences between tumor and normal blood vessels there has been little attention on this matter (144). The tumor vasculature is categorized into six distinct subtypes during tumor angiogenesis. Based on its developing order, structure and function, the six different types are mother vessels (MV), capillaries, glomeruloid microvascular proliferations (GMP), vascular malformations (VM), feeder arteries (FA) and draining veins (DV).

Antiangiogenic Strategies Targeting Cancers

In the early 1970s, the concept of antiangiogenic therapy to treat solid tumors arose based on the necessity of angiogenesis for tumor growth, thus, inhibition of angiogenesis would be antitumorigenic by impeding progression of tumors (145). Since then, innumerable studies have been conducted to understand the underlying molecular mechanisms of angiogenesis in efforts to find positive and negative angiogenic factors. The vascular endothelial growth factor (VEGF) receptors and ligands family is the most-characterized activator. Researchers have learned much about the central role of the VEGF family in developmental, physiological, and pathological angiogenesis. The inhibition of the VEGF tyrosine kinase signaling pathway is the most tested and substantiated angiogenesis-based anticancer strategy (146-148). The first FDA-approved antiangiogenic drug in 2004 was a humanized anti-VEGF monoclonal antibody (bevacizumab) for the treatment of metastatic colorectal cancer, in combination with chemotherapy. This has been followed by various approaches designed to block the VEGF pathway including anti-VEGF receptor monoclonal antibodies, chimeric soluble VEGF receptors (VEGF-trap), and VEGF receptor tyrosine kinase inhibitors (TKIs) (23, 149, 150).

Lessons from Numerous VEGF/VEGFR Inhibitor-Based Clinical Trials

A great number of preclinical and clinical studies have proved that angiogenesis is an important therapeutic target for several types of solid tumors. In some cases, such advances provided new insight about the clinical application of anti-VEGF therapy. It was originally anticipated that blockade of tumor angiogenesis would inhibit the blood supply to tumors, thereby starving and cause them to shrink. However, based on clinical trials, the antitumor effects of anti-VEGF strategy are most likely due to the normalization of the tumor vasculature. It appears that suppression of VEGF signaling causes trimming of the abnormal tumor vasculature followed by remodeling of the remaining vasculature (23, 149, 151). The tumor

microenvironment becomes more accessible to efficient delivery of chemotherapeutic agents and oxygenated, heightening sensitivity to radiation therapy. Thus, the anti-VEGF-based monotherapy was not as successful as expected in many clinical studies, however, its antitumor efficacy was considerably improved when used in combination with a conventional therapy such as chemotherapy and radiation.

Like other cancer drugs, concerns about resistance to antiangiogenic therapies have emerged from some preclinical and clinical trials. Recurrent tumor growth was reported after initial tumor regression during long term treatment (152, 153). It was reported that established tumor blood vessels became resistant to anti-VEGF-mediated angiogenesis suppression due to the heterogeneity of tumor vasculature (154, 155), and made them intensely aggressive (143). Consequently, these suggest that angiogenic pathways in the tumor vasculature are very complicated and cannot be clearly explained by any one given pathway. Thus, researchers and clinicians realize that the most successful strategies must be combination therapy targeting multiple pro-angiogenic factors as well as different signaling pathways (23, 143, 148, 149, 151).

Emerging Novel Antiangiogenic Targets

Many genetic studies in mice have suggested that normal embryonic vascular development depends not only on the VEGF signaling pathway, but other signaling pathways as well. Since embryonic and adult (physiological and pathological) angiogenesis uses similar mechanisms, it seems logical that these other signaling pathways may also play important roles during tumor angiogenesis. Members of fibroblast growth factor (FGF) family are commonly studied pro-angiogenic proteins that are seen as potential antiangiogneic therapeutic targets (35, 156). Recently, the implication of axonal guidance receptors and ligands in angiogenesis has been emphasized. Examples include the Roundabout receptor (Robo4)/Slit ligand, Ephrin receptor/Ephrin ligand (EphA2 or EphB4), Unc5 receptor (Unc5B)/Netrin ligand (Netrin-1) and

Notch receptor/Delta-like ligand 4 (Dll4) families (13, 51). They were initially identified as important molecules in neuronal guidance during development (13, 51, 148), but there is evidence that dysregulation of these may be involved in tumor angiogenesis. Inhibition of Robo4 (157), the ephrins (158), Dll4 (58, 159) and activation of Unc5B receptor leads to a decrease in the experimental tumor growth and angiogenesis.

Interestingly, the results from studies in which Dll4-induced Notch signaling was blocked suggested a new concept for the angiogenesis-based tumor therapy (58, 159). It was found that when Dll4 was activated by VEGF signaling, it acted as a negative regulator to block VEGF-induced tumor angiogenesis (58). Thus, there is an inverse relationship between the Dll4/Notch activity and tumor vascularity. This was consistent with the previous conception of anti-VEGF therapy that in order to induce antitumor effects, tumor angiogenesis must be blocked. However, it was shown that blocking Dll4 resulted in increased tumor vascular density, consequently, reducing tumor growth (58, 159). Such an enigma was explained by the notion that unregulated angiogenesis due to blockade of Dll4 led to the formation of non-productive or -functional blood vessels in the tumor vasculature (58, 159). Furthermore, this approach was also antitumorigenic even in anti-VEGF therapy resistant tumors (58). These findings suggest a new angiogenesis-based therapeutic approach to tumor therapy in which induction of disorganized and non-productive blood vessels in the tumor vasculature would be an excellent alternative of anti-VEGF-mediated tumor therapies.

A Novel Anti-Tumor Effect of *Alk1* Deletion-Induced AVMs on Tumor Vasculature

Activin receptor-like kinase 1 (ALK1) is one of the type I receptor members from the TGF-β superfamily (89, 90). It is a transmembrane receptor containing a serine/threonine kinase activity. ALK1 is primarily expressed in vascular endothelial cells (ECs) (105-107). During murine embryonic and neonatal stages, it is predominantly expressed in arterial ECs, but its

expression is diminished in most blood vessels during adulthood. Expression of Alk1 is continuous in the lungs and initiated by wounding- or tumorigenesis-induced angiogenesis in adults (106). There have been numerous studies showing that ALK1 plays an important role in normal embryonic vascular development and postnatal vascular maintenance and remodeling. Homozygous germline null mutation of the *Alk1* gene was embryonic lethal between E10.5-11.5 due to severe vascular abnormalities (97). In humans, heterozygous mutations cause hereditary hemorrhagic telangiectasia (HHT), a dominantly inherited vascular disease. Major symptoms of HHT patients are epistaxis (spontaneous and recurrent nosebleeds), mucocutaneous telangiectases (focal dilation of blood vessels), and arteriovenous malformations (AVMs) in internal organs, including the brain, lung, liver and intestine, which result from the fragility of disorganized peripheral microvessels and direct connections between arteries and veins without proper capillary beds (38, 44, 65, 66).

HHT is a unique vascular disease in which mechanisms of adult vascular maintenance and pathological or physiological functions of AVMs can be investigated. Recently, we developed a new conditional knockout (cKO) mouse model using the Cre/LoxP system, specifically utilizing the CreER system. In this model, global homozygous *Alk1*-deletion could be induced by tamoxifen (TM) treatment at any given adult stage. We found that upon homozygous *Alk1*-deletion, blood vessels that formed in the wounding area were disorganized, dilated, tortuous and showed AVMs. Furthermore, these vascular lesions developed only in sites where both *Alk1* was deleted and ongoing angiogenesis was present. Another previous study described *Alk1*-deficient vascular endothelial cells formed excessive, irregular, and enlarged abnormal vascular structures in the Matrigel plug.

The formation of AVMs can be problematic because 1) the lack of capillaries prevents the proper exchange of appropriate nutrients and removal of wastes between the blood and surrounding tissue normally required, and 2) the dilated vessel walls are fragile and prone to rupturing. Based on such respects, we speculated that inducing these types of abnormal blood vessels within the tumor-feeding vasculature would result in insufficient supplies for tumor growth, thereby inhibiting their progression. To test this possibility, we injected Lewis lung carcinoma (LLC) cells into TM-treated control and mutant mice and examined how *Alk1*-deletion affects tumorigenesis. First, in subcutaneous tumor cell injections after a TM treatment, none of *Alk1*-deleted mutant mice developed tumors, whereas solid tumors formed under the skin of all control mice. Second, the growth of established solid tumors in the thigh of mice was significantly inhibited in the mutant mice after TM injection, as compared to those in the control mice. By latex dye injection into the systemic circulation of the mice, we found the formation of AVMs in the tumor feeder peripheral vessels. Further histological analyses revealed that tumors from the mutant mice displayed disrupted blood vessel surrounded by many necrotic tumor cells. Thus, creation of abnormal blood vessels during tumor angiogenesis resulted in the prevention of initiation and progression of tumorigenesis. This was most likely due to the lack of capillaries, AV shunts within AVMs and disruption of tumor-feeding blood vessels, suggesting that inhibition of the ALK1 signaling might be a new angiogenesis-based therapeutic approach to target the tumor vasculature.

Results

Initiation of Tumorigenesis Was Suppressed in *Alk1*-Deleted Adult Mutant Mice

Hyperactive tumor angiogenesis is largely responsible for the growth of solid tumors. Thus, considerable angiogenesis is initiated in the tissues bearing tumor masses. For the appropriate functions of a microvascular system, the local vascular network should be highly

organized into arterioles, capillaries and venules. Blood vessels within AVM lesions are disorganized, fragile and lack capillaries, eventually developing AV shunts. Consequently, arterial blood flows directly into veins, bypassing opportunities for feeding to take place. Based on such facts and our preliminary data, we hypothesized that in conditions of tumor-induced angiogenesis, blocking or deleting ALK1 signaling would lead to the development of abnormal blood vessels that would not adequately feed and allow progression of a tumor.

To test this hypothesis, we employed the same mouse model which was used in the preliminary study. In this model, to circumvent lethality of homozygous *Alk1*-deletion but still delete the *Alk1* gene at a desired adult stage, we applied the Cre/LoxP system in combination with the CreER system. In this conditional knockout (cKO) mouse ($R26^{+/CreER}$; $Alk1^{2f/2f}$), the transmembrane domain (exons 4 to 6) of the *Alk1* gene on both alleles is flanked by LoxP sequences, denoted as *2f*, and CreER cDNA is introduced into the ROSA26 locus, which allows ubiquitous expression of Cre recombinase. Upon TM treatment, Cre is active, recognizes the LoxP sites and deletes the transmembrane domain, resulting in *1f*-null alleles. As controls, $R26^{+/+}$; $Alk1^{2f/2f}$ mice were used, in which the *Alk1* cKO alleles are unaffected by TM because Cre is not present. Hereafter, mice containing $R26^{+/+}$; $Alk1^{2f/2f}$ will be indicated as controls, while $R26^{+/CreER}$; $Alk1^{2f/2f}$ mice will be denoted as mutants. All *in vivo* experiments were conducted in mice between 2 to 3 months of age.

First, we investigated how *Alk1*-deficiency affects the early stage of solid tumor development. Since globally *Alk1*-null mice died between 9 to 21 days after TM injection, the *in vivo* tumorigenesis studies needed to be performed within this time frame. Previously, we confirmed that a single intraperitoneal TM (2.5 mg/25 g bodyweight) injection was sufficient and efficient for deleting the *Alk1* gene in $R26^{+/CreER}$; $Alk1^{2f/2f}$ mice. On what is designated day zero,

both control (n=5) and mutant (n=7) mice were injected with TM (Figure 3-1A). On the following day, Lewis lung carcinoma (LLC) cells (2×10^5 cells) were subcutaneously injected into their dorsal region, and then tumor formation was monitored daily. Between four to five days later, tumors were apparent in almost all control mice, whereas no obvious tumor mass was observed in mutant mice, even more than a week later. On the ninth day post-TM administration, mice were sacrificed and LLC-implanted skins were collected and macroscopically examined (Figure 3-1A).

Initially, there was no significant difference in eating behaviors and bodyweights between control and mutant mice during the study. However, between eight to nine days after TM injection, *Alk1*-deleted mutant mice started to show distinctive appearance. Their skin and extremities were pale implying poor blood circulation in the peripheral vasculature. Additionally, the feces were very dark in color indicating possible internal bleedings. As expected an autopsy confirmed some hemorrhagic sites in the lungs and GI tracts in mutant mice. Surprisingly, only control mice developed apparent solid tumors under the skin (Figure 3-1B-G). The tumors developed several feeding blood vessels surrounding as well as within them (Figure 3-1B-D). However, in the mutants, less, discontinuous, irregular, thick blood vessels formed and hemorrhages were found in the area where tumor cells were inoculated (Figure 3-1E-G). Therefore, these data demonstrated that the initiation of tumor growth was suppressed by *Alk1*-deletion in the adult mice most likely due to abnormal tumor angiogenesis by the *Alk1*-deficiency.

Progression of Tumorigenesis Was Significantly Inhibited in *Alk1*-Deleted Adult Mutant Mice

Next, we tested whether *Alk1*-deletion delayed the progression of already established tumors. To induce the establishment of solid tumors, we injected LLC cells (1×10^5 cells) into

the right thigh of control (n=4) and mutant (n=8) mice (Figure 3-2A). Before injection, diameters of both right and left thighs were measured as around 8 mm. Twelve days later, diameter of tumor-injected right legs reached around 10 mm (Figure 3-2B), while the size of uninjected left legs barely changed. On that day, TM was administered into the mice and the size of tumors was measured daily (Figure 3-2B). By two days post-TM treatment, the growth of tumors in both control and mutant mice continued but with no difference in their size. On the day three, the increase in the size of tumors within mutants was lower than that of controls. Until the seventh day after TM injection, the tumor growth in control mice steadily increased, while that of mutant mice relatively slowed down. Between seven to eight days, the tumor growth in mutants plateaued. However, in controls, the tumors continued to enlarge and due to the enormous size of their tumors, the study had to be terminated. In the statistical analysis, the rate of tumor growth was significantly higher in control mice (0.78 mm ± 0.034) as compared to that of mutant mice (0.46 mm ± 0.024) (P<0.0001) (Figure 3-2B). In addition to the diameter measurement, size of tumors was further evaluated three-dimensionally (width, thickness and height) during the autopsy. Tumors from control mice (Figure 3-2C-E) were larger than those of mutant mice (Figure 3-2F-H) in all measurements. As a note, there was no difference in size of the uninjected left thighs between mice.

AVMs Were Resulted From *Alk1*-Deficiency in Peripheral Tumor-Feeding Blood Vessels

To visualize microcirculation of tumor-feeding blood vessels of superficial muscular tumors, we injected the latex dye into the arterial blood flow via the left ventricle of the heart right before the autopsy. Through this method only arteries are visible because the dye is too viscous to pass through the capillaries. In the controls, single-lined arteries were well-branched or sprouted into smaller arterioles, but not capillaries nor veins of tumor-feeding vasculature visualized. In terms of vascular morphology, a thick artery of the control became narrowed down

until their ends, and then diverged into several smaller vessels (Figure 3-3B). However, in the mutant, excessive, irregular, and disorganized vessels were observed around the tumor mass in the right thigh, and the end of an artery was blunt and looked discontinuous (Figure 3-3C). And the overall appearance of numerous blood vessels was abnormal, appearing entangled and convoluted (Figure 3-3C). It is noteworthy that we did not observe such abnormal vessels in counterpart tumor-uninjected left legs of the same *Alk1*-deleted mice (Figure 3-3A). This data supported our speculation that ALK1-deficiency would specifically target the tumor vasculature where there is active angiogenesis.

Importantly, when we further evaluated these tumor-feeding microvessels with high magnification, the existence of AVMs was apparent (Figure 3-3D). The ends of arteries were connected directly to veins through a thin vessel. Moreover, veins were remarkably dilated and wavy (Figure 3-3D). Such observations indicate that within the microcirculation of the tumor vasculature, arterial blood enters into veins through the AVMs, thus veins become enlarged and tortuous due to the high arterial blood pressure. Consequently, without properly functioning capillary beds, the arterial blood is directly intermingled with venule blood flows (arterio-venous shunts; AV shunts), rather than delivering supplies into tumor masses. This leads to an impediment of local vascular circulation, indeed starving the tumors and arresting their progression. Therefore, *Alk1*-deletion disrupted tumor angiogenesis and inhibited tumor growth by inducing AVMs in established tumor-feeding vasculature.

Alk1-Deletion during Tumor Angiogenesis Caused Disruption of Tumor Vascular Network

The blood vessels within the tumor masses were further examined by various histological analyses. In hematoxylin and eosin (H & E) staining, tumor sections from *Alk1*-deleted mutant mice showed much more intact muscle tissues (Figure 3-4B), whereas in the control, healthy muscle tissues were displaced by LLC cells and barely present (Figure 3-4A). A closer

examination of only tumors cells revealed several tiny well-developed and -maintained blood vessels in the control (Figure 3-4C). However, we found that blood cells largely dispersed in spaces between tumor cells in the mutants (Figure 3-4D). Importantly, unlike tumor cells surrounding blood vessels in the control, most tumor cells around these blood smears were necrotic.

Next, we performed immunohistochemistry to evaluate vascular integrity of the tumor vasculature. Platelet endothelial cell adhesion molecule (PECAM), also known as CD31, is a mediator for endothelial cell-cell interactions. The endothelial cell layer is important for perfusion of molecules between blood vessels and local tissues. PECAM immunostaining was irregularly diffused in tumors of mutant mice (Figure 3-5B), while it delineated well the continuous inner layer of microvessels within tumors of the control mice (Figure 3-5A). Additionally, another widely used protein marker to examine the integrity of blood vessels is alpha smooth muscle actin (α-SMA). It stains the smooth muscle layer which allows vascular walls to be maintained and surrounds the endothelial layer. Consistent with the results from PECAM/CD31 staining, controls showed many well-shaped tumor microvessels (Figure 3-5C), but positive staining was widely scattered throughout the sections within mutants (Figure 3-5D). These data indicated that the integrity of tumor vessel walls was severely disrupted by *Alk1*-deficiency. Consequently, due to the leakage of blood through ruptured vessel walls, microvessels within the tumor mass were not capable of proper exchange of small molecules such as nutrients, oxygen and wastes, thereby hindering the tumor growth. Thus, *Alk1*-deletion during tumor angiogenesis inhibited tumor progression not only by causing AVMs in tumor-feeding blood vessels but also compromising vascular integrity of the established tumor vascular network.

Discussion

We investigated whether inducing vascular abnormalities in the tumor vasculature by targeting the Alk1 gene could be a novel approach to treat solid tumors. We found that Alk1-deletion inhibited the onset and progression of tumorigenesis by causing vascular disorganization, disruption and shunts. Heterozygous mutations of the ALK1 have been implicated in HHT, a dominantly inherited vascular disease. Haploinsufficiency of ALK1 results in thinning of blood vessel walls and loss of capillary beds, leading to a dilated, fragile, disorganized and tortuous vascular network. Consequently, such abnormal blood vessels are prone to rupture, hemorrhagic and involve several AV shunts. In our preliminary study, it was demonstrated that both Alk1-deletion and wound-induced angiogenesis were necessary and sufficient for the development of these vascular lesions in the adult mice. Based on this promising data, we wanted to test whether such results could be recapitulated during tumor-induced angiogenesis upon the Alk1-deletion. As expected, formation of abnormal blood vessels, characterized by dilation and appearance of excessive, tortuous vessels and AVMs, resulted from Alk1-deficient tumor angiogenesis.

LLC cells injected under the skin could not establish solid tumors in *Alk1*-null mutant mice but showed few newly formed abnormal blood vessels and hemorrhages. However, in all control mice, they developed tumors as well as new blood vessels. This observation indicated that suppression of the onset of tumor growth was mainly due to the failure to induce functional blood vessels. However, we could not rule out the possibility that such suppression was due to other factors rather than impaired angiogenesis. One possibility is that as *Alk1*-null mutant mice died very quickly upon TM treatment, the observed inhibition of tumorigenesis could be due to a general defect such as impaired nutrient supply rather than intrinsic resistance to tumorigenesis. Furthermore, *Alk1*-deletion also inhibited the progression of tumor growth. Unlike tumors

established in the controls persistently growing, the growth rate of tumors in the mutants was gradually decreased four days later and almost ceased a week after the TM treatment. Due to the considerable size of tumors in control mice, we could not continue to monitor progression or regression of tumors beyond the eighth day post-TM in control and mutant mice. By latex dye injection, we found AVMs in the tumor-feeding peripheral vasculature only in the mutant. Moreover, our immunohistochemical analysis demonstrated that vascular endothelial and smooth muscle layers of tumor microvessels in the mutant were severely disrupted and vascular integrity of the tumor vasculature was compromised.

To support their growth and metastasis, solid tumors require new blood vessel formation for the establishment of their own vasculature, termed as tumor angiogenesis. Thus, the basic concept of antiangiogenic tumor therapy is that blocking tumor angiogenesis can inhibit the growth of tumors by preventing blood supplies to tumor tissues (145). There has been evidence from numerous preclinical and clinical studies to show that angiogenesis is an important therapeutic target to treat many solid tumors. Currently, blocking the VEGF tyrosine kinase signaling has been the most and best tested strategy for the antiangiogenesis therapy (146-148). However, numerous clinical applications of anti-VEGF therapy have made researchers and clinicians realize that targeting a single angiogenic pathway is not enough to achieve the desired antitumor effects. Additionally, emerging tumor vascular resistance against the anti-VEGF therapy emphasizes the urgent need of novel angiogenesis-based therapeutic targets such as angiogenic activators, inhibitors as well as different angiogenic signaling pathways (23, 143, 148, 149, 151).

In terms of alternative angiogenic pathways, data from recent reports show that despite increased blood vessel formation, blockade of Dll4-induced Notch signaling resulted in reduced

tumor growth (58, 159). In contrast to previous beliefs that there is an inverse correlation between vascular density and tumor growth, the increased tumor vascularity seen in blocking Dll4/Notch signaling was indeed antitumorigenic (58, 159). This data suggested that disorganization of newly formed tumor-feeding blood vessels by uncontrolled angiogenesis lead to vascular non-functionality or -productivity, resulting in the arrest and/or regression of tumors. Such results further support our hypothesis that abnormal blood vessels caused by *Alk1*-deficiency during tumor-induced angiogenesis are poorly functional due to disorganization of arteries, veins and lack of capillaries, thereby inhibiting the tumor growth. Our finding that development of AV shunts via AVMs in the tumor vasculature of *Alk1*-deleted mutant mice suggests a new mechanism for vascular non-functionality or -productivity. Most importantly, these AVMs were specifically formed in area of active tumor angiogenesis, suggesting that ALK1 blockage is more sensitive to active angiogenesis and can be targeted for tumor vasculature.

It is noteworthy that a recent review proposes the necessity of new strategies that are designed to target specific subsets of tumor blood vessels (144). The tumor vasculature was divided into six different categories, depending on their structural and functional characteristics: mother vessels (MV), capillaries, glomeruloid microvascular proliferations (GMP), vascular malformations (VM), feeder arteries (FA) and draining veins (DV). In a previous study, it was found that mouse tumors responded differently to anti-VEGF/VEGFR depending on their stages of tumorigenesis (160). Targeting VEGFR in endothelial cells showed efficacy for tumors in the early stages. However, it was not effective in late stage tumors due to the presence of mature blood vessels containing pericytes. Therefore, they argued that the anti-VEGF/VEGFR strategy might be effective for only tumor blood vessels appearing at the early stages of tumorigenesis,

such as MV and GMP (144). Tumor blood vessels existing at the late stages, such as FA and DV, are independent or resistant to the anti-VEGF/VEGFR approach. Consequently, it is important and necessary to find new therapeutic targets to specifically destroy these blood vessels (144). As shown in our histological analysis, *Alk1*-deletion obviously caused the destruction of vascular smooth muscle layers of tumor blood vessels. In that respect, inhibition of ALK1 signaling may be a feasible targeting strategy for these tumor blood vessels to treat the late stage tumors.

In summary, the ALK1-deficiency had an antitumor effect on the tumor vasculature. All of findings presented strengthen our hypothesis that blockage of the ALK1 signaling may be a new angiogenesis-based therapeutic approach in targeting blood vessels that support tumor growth. First, since *Alk1*-induced vascular abnormalities occur only where active angiogenesis is present in adults, inhibition of ALK1 may provide a way to specifically target blood vessels around and within tumor masses undergoing elevated and excessive angiogenesis. Second, we found that the pathological effects of AVMs, such as the lack of capillaries and appearance of AV shunts, could be antitumorigenic by causing non-functionality in the tumor blood vessels. Lastly, *Alk1*-deletion affected the vascular endothelial as well as the smooth muscle cell layers of blood vessels, resulting in fragile, leaky blood vessels as well as disruption of established microvessels. Thus, inhibition of the ALK1 signaling can be an effective strategy to target the tumor vascular network appearing at both early and late stages tumors.

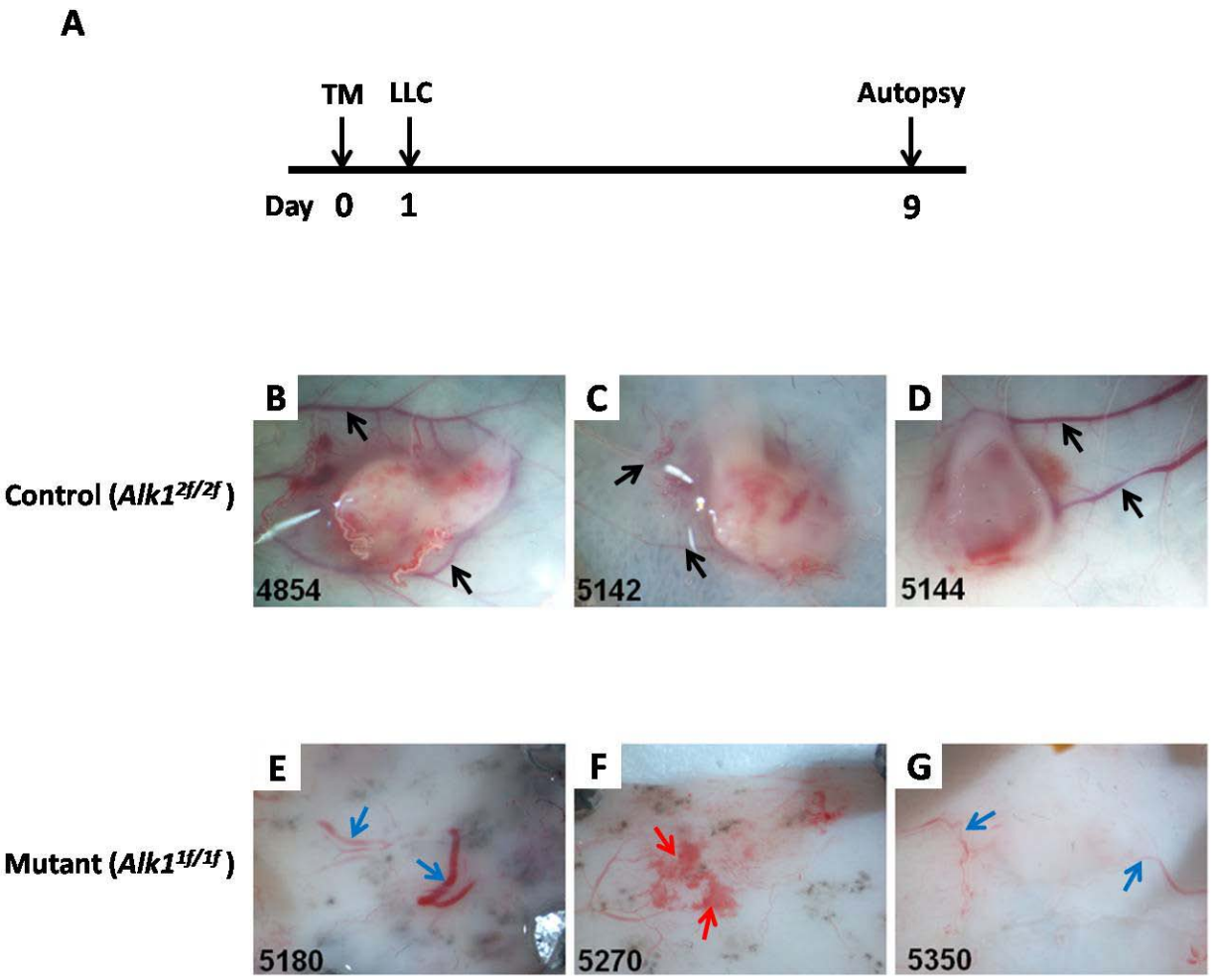

Figure 3-1. Initiation of tumor growth was repressed in $R26^{+/CreER}$; $Alk1^{1f/1f}$ mutant mice. A) Schematic diagram of the experimental plan. Tamoxifen (TM; 2.5 mg/25 g body weight) was administered one day before LLC cells (2×10^5 cells) injection. Nine days later representative pictures were taken at the autopsy. B) - D) Solid tumors formed under the skin of all $R26^{+/+}$; $Alk1^{2f/2f}$ control mice (n=5) showed well-developed tumor-feeding blood vessels, indicated by black arrows, around and within them. E) - G) No tumor formation was observed in *Alk1*-deleted mutant mice (n=7). Abnormal blood vessels and hemorrhages, represented by blue and red arrows respectively, were found in the area where tumor cells were injected.

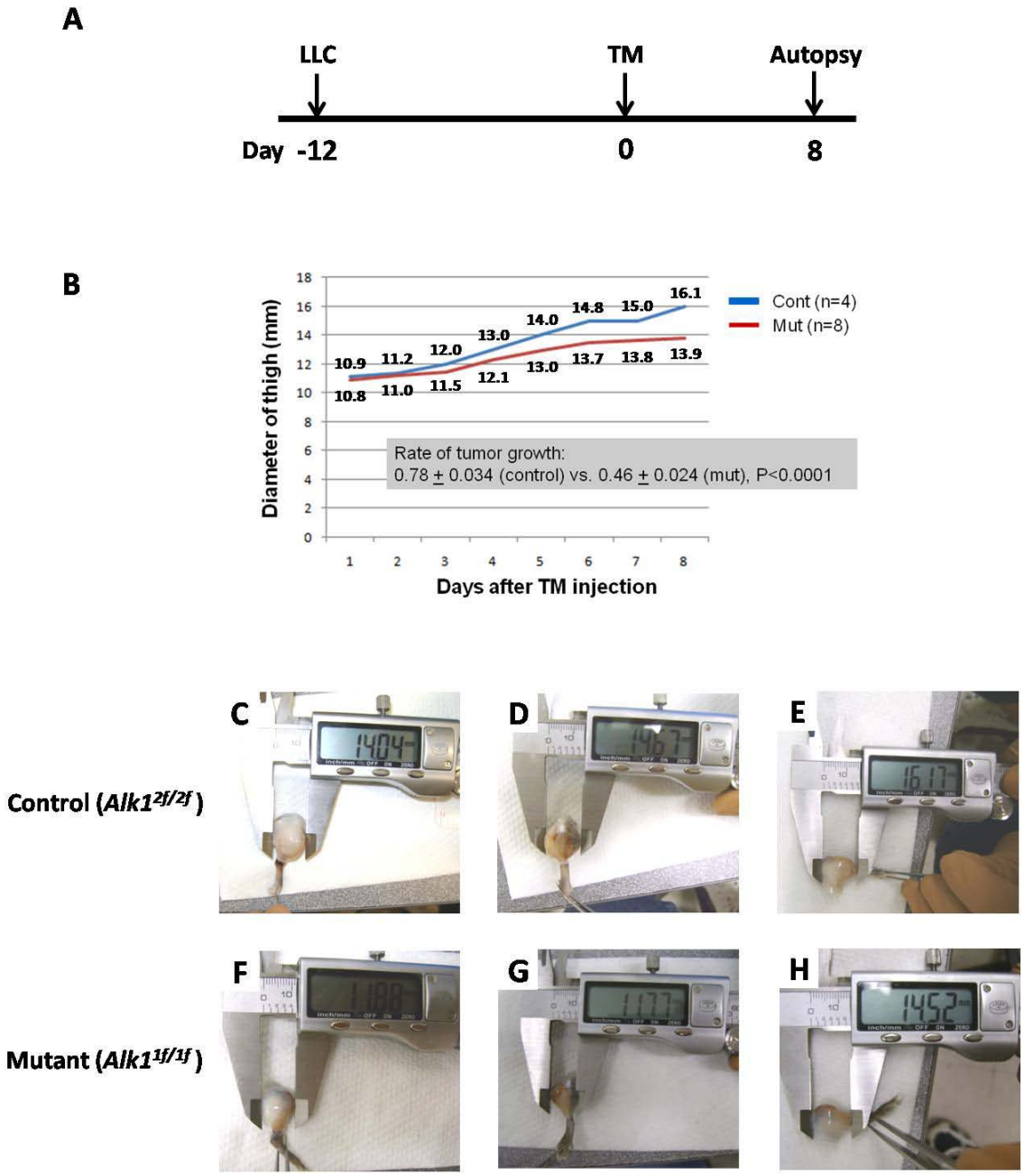

Figure 3-2. Tumor growth was significantly inhibited in *Alk1*-null mutant mice. A) LLC cells (1×10^5 cells) were intramusculary injected into the right legs of $Alk1^{2f/2f}$ control (n=4) and $Alk1^{1f/1f}$ mutant (n=8) mice and grown for twelve days. On the twelfth day after LLC cell inoculation, TM was injected into the peritoneum of both control and mutant mice. For eight days, diameters of their right thighs were daily measured. B) Rate of tumor growth in *Alk1*-deleted mutant mice (0.46 mm ± 0.024) was significantly lower than that in control mice (0.78 mm ± 0.034) (P<0.0001). At the autopsy, the size of tumor masses was evaluated by a three-dimensional measurement (width, thickness and height). In all measurements, C) - E) tumors from the $Alk1^{2f/2f}$ controls were considerably larger than F) - H) ones from the $Alk1^{1f/1f}$ mutants.

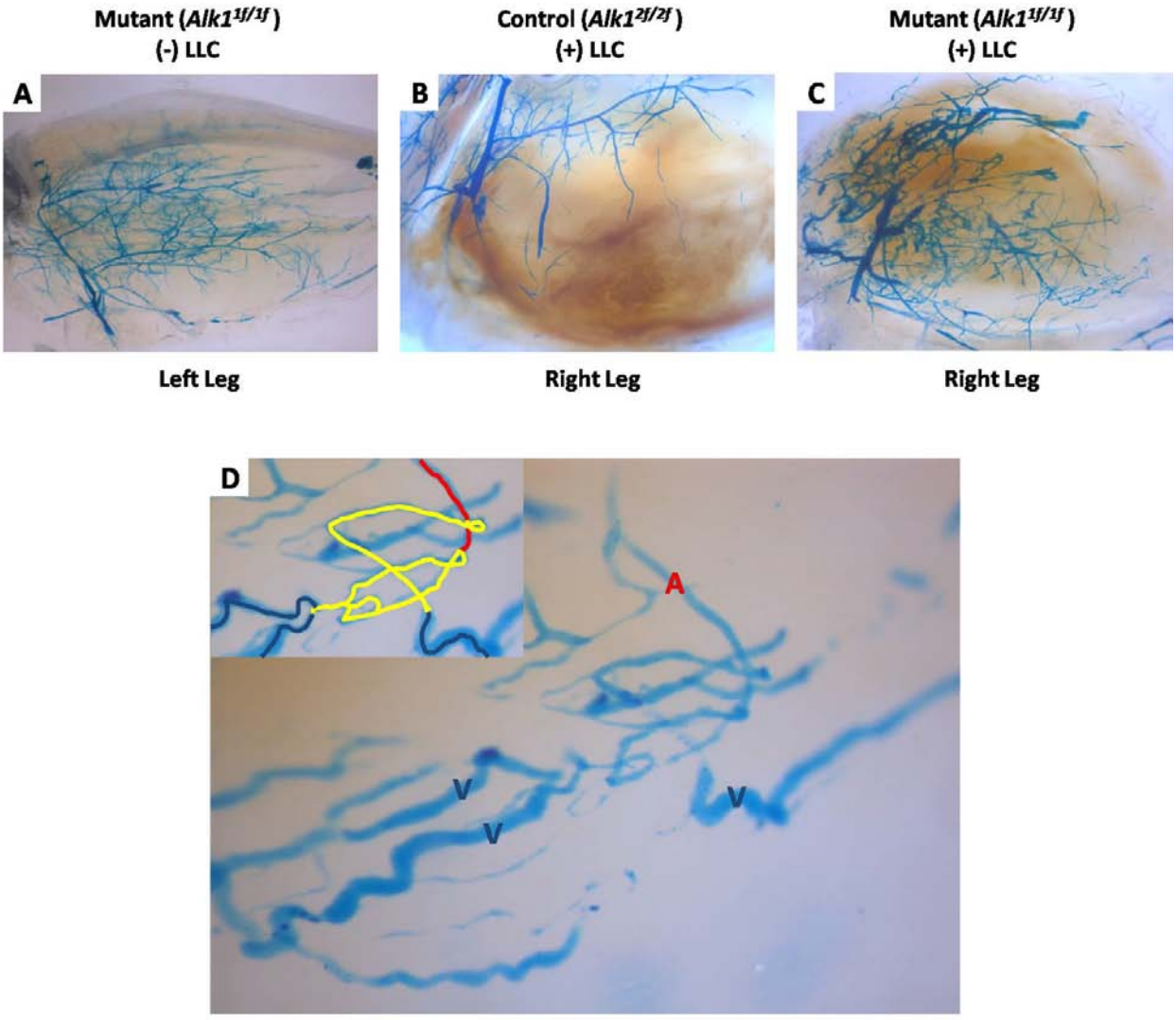

Figure 3-3. Latex day injection revealed *Alk1*-deletion caused AVMs in tumor-feeding blood vasculature. A) Left leg of a TM-injected mutant mouse maintained a highly organized vascular network in which only arteries were visualized by latex dye in the absence of tumor angiogenesis. B) In $Alk1^{2f/2f}$ control mice, similar to A, only arteries appeared as a single branches which diverged into smaller branches at their end. C) In the right leg which was from the same $Alk1^{1f/1f}$ mutant mouse in A, tumor-feeding blood vessels were excessive, disorganized, irregular and tortuous. D) A high magnification of C demonstrated direct connections between arteries and veins (AVMs) in the tumor vasculature of *Alk1*-null mice. Because of AV shunts within the AVMs, veins were dilated and convoluted, indicating the absence of intervening capillary beds. In the inset, the artery is delineated with a red solid line, while veins are lined dark blue. AVMs are represented as yellow lines. Note that in D, A = artery and V = vein.

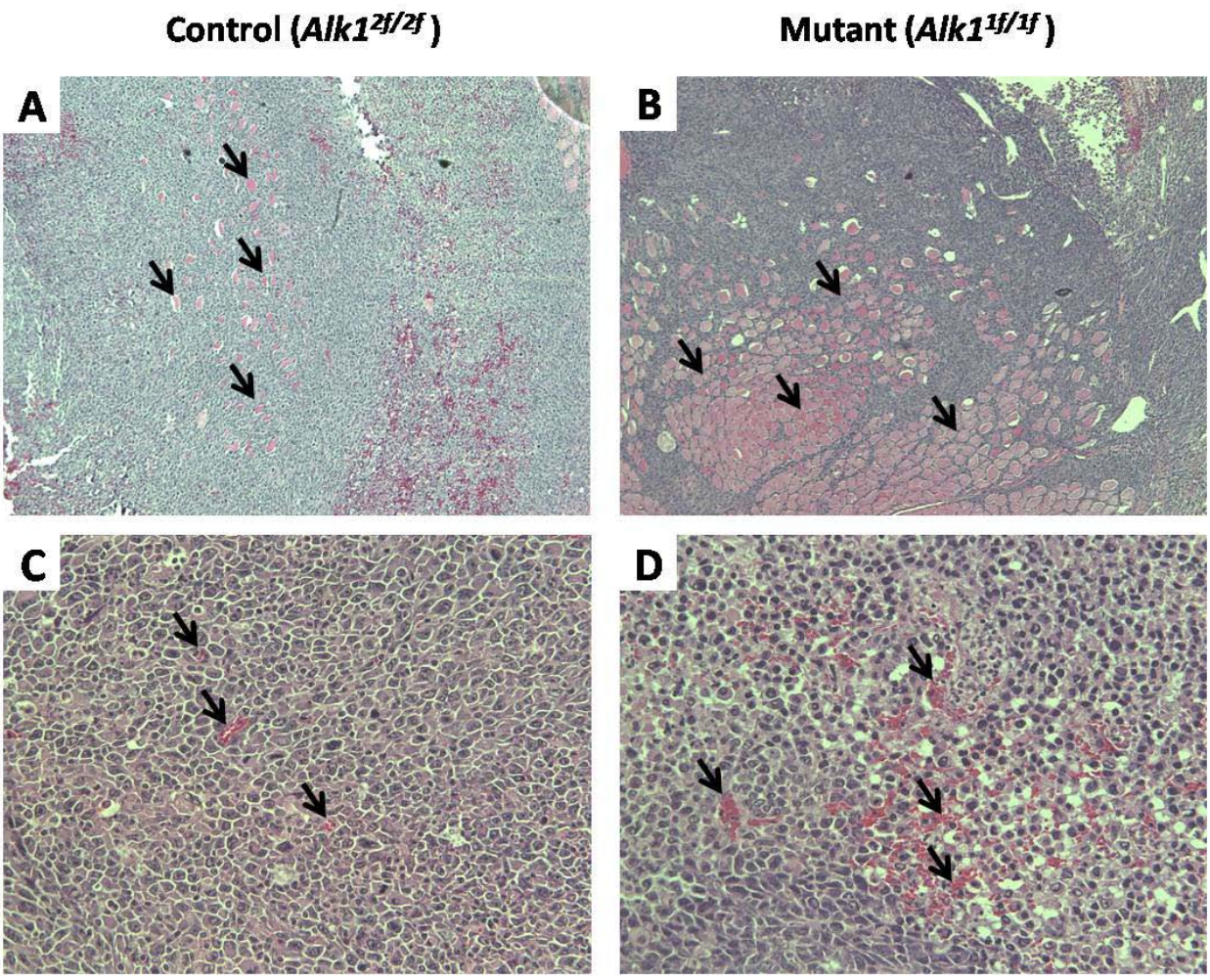

Figure 3-4. Tumor blood vessels were destroyed by *Alk1*-deficiency. Sections of muscle tumors were stained with hematoxylin and eosin (H & E). A) Tumors from control mice contained very little muscle tissues (50X). B) In mutant mice, intact muscle tissues were broadly observed (50X). Note that healthy muscle tissues in pink are pointed by black arrows in A and B. C) Growth of LLC cells was supported by several well-established microvessels in the control (200X). D) Due to the absence of microvessels, locally delivered blood leaked and was dispersed into tumor tissues in the mutant (200X). Unlike tumor cells in C, many of them underwent necrosis. Note that black arrows in C and D indicate blood cells within tumor tissues.

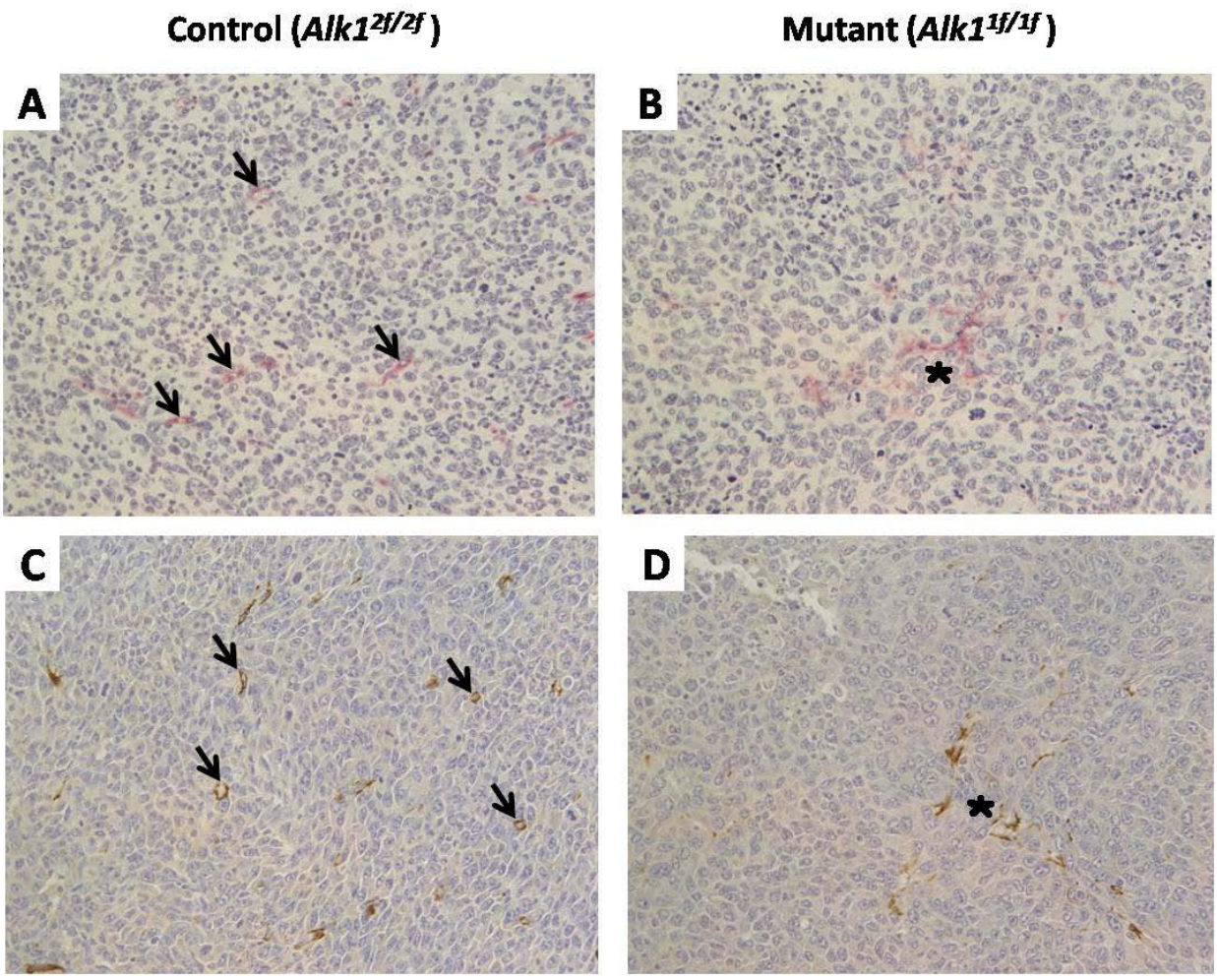

Figure 3-5. Tumor vascular integrity was disrupted by *Alk1*-deletion. Sections of muscle tumors were immunostained with A) and B) an endothelial-specific marker protein PECAM/CD31 or C) and D) a smooth muscle cell-specific marker protein α-SMA. A) The endothelium was well-maintained in tumor vessels of control mice was detected by PECAM/CD31-positive staining in light red (200X). B) PECAM/CD31-positive signals were disseminated in mutant mice, suggesting disruption of the endothelial layer of tumor vasculature (200X). C) Tumors of the controls presented nicely formed smooth muscle cell layers surrounding vascular endothelium (200X). D) In the mutants, diffused α-SMA staining implied that the smooth muscle cell layers of tumor-feeding blood vessels were also affected (200X). Note that black arrows in A and C indicate microvessels within the tumor mass. And asterisks in B and D demonstrates sites where microvessels were disrupted, thereby vascular endothelial and smooth muscle cells were scattered.

CHAPTER 4
CONCLUSIONS AND FUTURE STUDIES

The major pathological features of HHT are the dilation of microvessels and the formation of AVMs. In that respect, HHT is a unique vascular disease that may allow us to study underlying mechanisms for the maintenance of vascular integrity and the pathological or physiological effects of AVMs. Despite the identification of HHT disease-causing genes such as *ENG* (70-73), *ALK1* (74-76) and *SMAD4* (77) and intense efforts to understand their signaling, there are still many unanswered questions. Previously, based upon *in vivo* studies, we demonstrated that perturbation in the EC-specific ALK1 signaling was a major cause of HHT-like vascular lesions in mice (115, 161). And we recently found that combination of *Alk1*-deletion and ongoing angiogenesis were necessary and sufficient for *de novo* formation of vascular abnormalities in the established adult vasculature. The vasculature in the lung and GI tract were consistently affected by the *Alk1*-deletion in both embryonic and adult stages. It is noteworthy that *Alk1*-heterozygous mice did not develop such vascular lesions during adult angiogenesis.

In chapter 2, we investigated cellular and biochemical properties of ALK1-deficient pulmonary ECs in angiogenesis. The significance of this study was to determine the most pertinent molecular mechanism for the endothelial ALK1 signaling involved in the pathogenesis of HHT. Some questions of interest include: what are distinctive cellular traits including proliferation, migration and endothelial capillary-like assembly of *Alk1*-null ECs in response to pro-angiogenic cues? Is the ALK1 receptor specific for controlling the TGF-β subfamily signaling? Or, is it more relevant receptor for regulating the BMP subfamily pathway? What are downstream molecular pathway(s) responsible for mediating the ALK1 signaling in ECs? To address such important issues in a more manageable system, we established two new murine

pulmonary EC lines. Since we previously observed that the heterozygous deletion of the *Alk1* gene did not affect the adult vascular network in the presence or absence of angiogenesis, we isolated ECs from the mouse carrying the $R26^{+/CreER}$; $Alk1^{2f/1f}$ transgene. By utilizing the Cre/LoxP system, their genotypes could be switched by a single TM treatment from $Alk1^{2f/1f}$ (*Alk1*-null heterozygote) to $Alk1^{1f/1f}$ (*Alk1*-null homozygote).

In accordance with our *in vivo* data, there was no difference observed in cellular phenotypes including migration and tube formation between $Alk1^{2f/1f}$ and $Alk1^{1f/1f}$ ECs in the absence of pro-angiogenic factor(s). However, upon bFGF treatment, *Alk1*-null ECs displayed significantly increased migratory abilities. Moreover, they developed considerably excessive, disorganized, irregular and enlarged capillary-like structures on the Matrigel in response. These abnormal tube-like structures were due to rapid outgrowth of ALK1-deficient ECs at early time points and their resistance to regression at the later stages. To test whether antiangiogenic effects of TGF-β or BMP pathways on ECs were differentially exerted in angiogenesis in the presence or absence of the ALK1, cells were treated with TGF-β1 or BMP-9, respectively. It was found that a capillary-like network formed by *Alk1*-null ECs was significantly regressed by TGF-β1 from 6 hours, whereas more than 50% of such a network was sustained in response to BMP-9 at least up to 24 hours. This data indicated that TGF-β1-induced anti-angiogenic effects were present, while such effects from BMP-9 treatment were blunted in *Alk1*-null ECs. Western blot analysis further supported this data by demonstrating that the activation of ERK1/2 pathway was decreased by TGF-β1. However, such reduction was less after BMP-9 treatment. In contrast to previous studies that suggest the ALK1 signaling is SMAD1/5/8-dependent, the induction of this pathway was intact in our *Alk1*-null ECs. Thus, it suggests that ALK1 signaling is SMAD-

independent and that other molecular pathway(s) may be mediating the physiological effects of ALK1 in pulmonary ECs.

This study focused on finding a specific ligand and downstream molecular pathway for endothelial ALK1 signaling. In addition, identifying molecular target(s) of its signaling is also essential in elucidating the molecular mechanism relevant to the HHT pathogenesis. Recently, our laboratory performed a microarray analysis to investigate downstream genes which may be regulated by ALK1. By comparison of the transcript profiles between $Alk1^{2f/2f}$ control and $Alk1^{1f/1f}$ mutant lungs at neonatal and adult stages, we obtained a group of genes that were commonly up- or down-regulated at symptomatic conditions (e.g. vessel dilations and pulmonary hemorrhages) at both stages. The functions of these genes are known to be implicated in many pathways important for the normal vascular physiology such as TGF-β signaling, Notch/Delta signaling, vascular tone, vascular permeability and angiogenesis. Since the whole lungs displaying HHT-like phenotypes were used, this group of genes was supposed to reflect both causative and consequent gene expressions of pathological manifestation. To identify EC-specific ALK1 target genes that may contribute to pathological features seen in HHT, future studies should include such microarray analysis examining overlapping gene expression profiles between *in vivo* and *in vitro* HHT-like pathological conditions upon the ALK1-deficiency. Further investigations will provide a better characterization of the EC-specific ALK1 signaling. Therefore, the discovery of ALK1-specific molecular mechanism(s) will facilitate the development of the potential therapeutic target(s) to prevent or cure the clinical symptoms of the HHT.

In chapter 3, we tested whether creation of pathophysiological effects of HHT vascular lesions in the tumor vasculature could be a novel angiogenesis-based antitumor approach to treat

solid tumors. The clinical manifestation of HHT, such as spontaneous, recurrent bleedings from fragile microvessels and AV shunts via AVMs, are distinctive characteristics of a non-functional vascular network. Traditional angiogenesis-based antitumor therapy was based on the concept that blockage of angiogenic signaling pathways would inhibit tumor angiogenesis, preventing tumor growth. However, a recent *in vivo* investigation suggested a novel concept that increased induction of non-productive or -functional tumor vascularity by disrupting Notch/Dll4 signaling could be antitumorigenic (58), implying the importance of organization and functionality for the tumor vasculature. Thus, it led us to speculate that generation of ALK1 deficiency-causing non-productive HHT-like vascular abnormalities (paucity of capillaries and development of AV shunts) might inhibit the tumor growth.

We investigated effects of the *Alk1*-deletion on the initiation and progression of tumorigenesis induced by the LLC cell implantation *in vivo*. We observed that all of $R26^{+/+}$; $Alk1^{2f/2f}$ control mice developed solid tumors and nascent tumor-feeding blood vessels under the skin. By contrast, *Alk1*-null mutant mice showed no tumor formation, but did form new abnormal vessels and hemorrhages surrounding the site of tumor cell inoculation. Such observations demonstrate that in order for a solid tumor to develop, ALK1 is required for tumor angiogenesis. The ALK1-deficiency also affected the tumor growth by disrupting the established tumor vasculature. Upon deletion of the *Alk1* gene in mice by TM administration, the rate of tumor growth slowed down after three days and ceased growth at around a week. However, the tumor established in control mice rapidly and continuously grew. We examined whether such a difference was due to development of HHT-like vascular lesions in the tumor microvasculature. We found the existence of AVMs in the peripheral microcirculation of the tumor vasculature in only *Alk1*-deleted mutant mice. Histological and immunohistochemical examination of tumor

sections of the control displayed well-established and -maintained tumor feeder microvessels. On the other hand, those of the mutant contained blood smears, more intact muscle tissues, and necrotic tumor cells without blood vessel structures. Furthermore, PECAM/CD31 and α-SMA staining was diffused and scattered, indicating disruption of blood vessel wall integrity. Taken together, the onset and progression of the tumorigenesis was strongly influenced by ALK1's role in tumor angiogenesis and maintenance of the vasculature.

This study investigated the antitumor impact of the blockage ALK1 signaling by taking a genetic ablation approach. All findings of this study substantiated our hypothesis that vascular non-productivity and disruption resulting from the ALK1 deficiency in the tumor microcirculation may be antitumorigenic by compromising the blood supply to tumors. Based upon our promising *in vivo* data, various strategies are possible to target the ALK1 signaling for clinical applications. To avoid adverse effects, such as spontaneous formation of vascular lesions seen in HHT in the systemic blood vessels, pharmacological means targeting the ALK1 signaling should be local and specific. So far, as a pharmacological inhibitor for the ALK1 signaling, a ALK1-trap has been developed by Acceleron Pharma Inc (Cambridge, MA). The ALK1-trap is a soluble chimeric ALK1 receptor in which the ligand-binding domain of ALK1 is fused with the Fc region of an immunoglobulin. Therefore, its interaction with ALK1 ligands interrupts the ALK1 signaling by inhibiting association between the ALK1 ligand and its physiological ALK1 receptor. Although the underlying mechanism is unknown, it has been shown that ALK1-Fc can block the ALK1 signaling in a cell culture system and such blocking showed some inhibitory impacts on the tumor growth.

In the future investigations, it will be interesting to compare the efficacy of the ALK1-Fc to that of our genetic deletion approach *in vivo*. In addition, it will be important to examine

whether inhibitory effects of ALK1-Fc can cause the same vascular defects observed in our *Alk1*-deleted mice such as AVMs and vessel wall rupture. Better understanding of the ALK1 signaling will provide more molecular targets and more specific method in targeting its pathway. Thus, the follow-up studies to chapter 2 and 3 should be considered concomitantly. The identification of the HHT pathogenesis may offer specific and feasible targets within the tumor vasculature. We are hopeful that based on such a discovered molecular mechanism, various pharmacological approaches can be explored to modulate the ALK1 signaling. Examples of them include ALK1 ligand-binding proteins, such as dominant negative forms of ALK1 receptor lacking transmembrane and cytoplasmic kinase domains (ALK1-trap), diverse chemical serine/threonine kinase inhibitors inhibiting kinase activities of ALK1 and small interfering RNAs (siRNAs) blocking components of the ALK1 signaling. We hope and expect that inhibitors of ALK1 signaling will be an excellent alternative to current angiogenesis-based antitumor reagents and will be more efficacious in combination with other anti-angiogenic and/or -cancer drugs.

CHAPTER 5
MATERIALS AND METHODS

Transgenic Mice

All procedures performed on mice were reviewed and approved by the University of Florida Institutional Animal Care and Use Committee. The generation of *R26*$^{+/+}$*; Alk1*$^{2f/2f}$, *R26*$^{+/CreER}$*; Alk1*$^{2f/2f}$, and *R26*$^{+/CreER}$*; Alk1*$^{2f/1f}$ transgenic mouse lines was described previously (115). PCR genotyping was performed as previously detailed (115).

Overall Cell Culture Conditions

Murine pulmonary endothelial cells (pECs) were cultured in a specifically formulated endothelial cell medium (ECM) in which Dulbecco's modified eagle medium (DMEM; GIBCO) was supplemented with 20% fetal bovine serum (FBS; HyClone), 0.5% heparin (200 mg/ml; Sigma), 1% endothelial mitogen (10 mg/ml; Biomedical Technologies Inc), 1% nonessential amino acids (Mediatech), 1% sodium pyruvate (100 mM; Invitrogen) and 0.4% penicillin-streptomycin (Invitrogen). All culture plates (Falcon) and flasks (Falcon) used for the pEC culture were coated with 1:5 diluted bovine fibronectin stabilized solution (1 mg/ml; Bomedical Technologies Inc) and then incubated at 37°C for 30 minutes before each use.

Lewis lung carcinoma (LLC) cells were maintained in minimum essential medium (MEM)-α (Invitrogen) which was supplemented with 10% FBS, 0.25% L-Asparagine (Sigma), 1% L-Glutamine (200 mM; Invitrogen), sodium bicarbonate (added up to pH 7.2-7.4; 7.5% (w/v); Invitrogen) and 1% penicillin/streptomycin (Invitrogen). Both EC and LLC cell cultures were incubated at 37°C with 5% CO_2.

Establishment of *Alk1*$^{2f/1f}$ and *Alk1*$^{1f/1f}$ Pulmonary Endothelial Cells (pECs)

An eight-week-old mouse carrying the *R26*$^{+/CreER}$*; Alk1*$^{2f/1f}$ transgene was euthanized by an overdose of 100% isofluran and followed by cervical dislocation. Whole lungs were removed

and washed in HEPES followed by another washing in DMEM. Lung tissues were finely minced using a sterile scalpel. The chopped tissues were subjected to serial digestion using 2 ml of a 1X trypsin solution [0.25% trypsin, 0.5 M EDTA (pH 8.0) in DMEM] at 37°C, with frequent shaking, for three times at 8 minutes each. Trypsin digestion was inactivated by adding 6 ml of normal ECM. After a 10 minute incubation at room temperature, the supernatant was carefully collected and plated into 2 wells of a 6-well culture plate.

For immortalization, when the culture reached 50% confluency post isolation, they were transfected with SV40 DNA (4.0 µg) using Lipofectamine (Invitrogen) and following the manufacturer's protocol. To obtain homozygous *Alk1*-null (*Alk1*$^{1f/1f}$) pECs, immortalized parental heterozygous *Alk1*-null (*Alk1*$^{2f/1f}$) pECs were treated with 1 µM 4-hydroxytamoxifen (Sigma) for two consecutive days.

Sorting pECs by Fluorescent-Activated Cell Sorting (FACS)

At close to 100% confluency, the EC culture was incubated with 10 µg of Dio-Ac-LDL (200 µg/ml; Biomedical Technologies Inc) diluted in ECM at 37°C/5% CO_2 for 4 hours. Cells were then briefly washed twice with DMEM containing 10% FBS and Hanks' balanced salt solution (HBSS, Invitrogen) once. To obtain a single cell suspension, cells were trypsinized and washed in DMEM containing 10% FBS three times. The final cell suspension was diluted in the phenol red-free DMEM/F12 medium (DMEM and Ham's F-12, 50:50 mix, 1X; Mediatech) at the appropriate concentration (3×10^6 cells/ml). The cell suspension was sorted using the BD FACSAria Cell-Sorting System (BD Biosciences) at wavelengths of 484 nm (excitation) and 507 nm (emission). Endothelial marker-positive sorted cells were washed in DMEM with 10% FBS five times. Lastly, cells were diluted in ECM supplemented with 1% endothelial cell growth supplement (ECGS; BD Biosciences) at a concentration of 2.5×10^4 cells/cm^2.

Genomic DNA PCR Analysis

For genotyping of parental *Alk1*$^{2f/1f}$ and TM-treated *Alk1*$^{1f/1f}$ pECs, genomic DNA was extracted from each cell culture grown at 100% confluency in a well of a 6-well culture plate. Cells were lysed in lysis buffer [50 mM Tris (pH 8.0), 0.5% TritonX-100] containing proteinase K (1 mg/ml) at 55°C for overnight. On the next day, the lysed cells were centrifuged at 12,000 rpm for 10 minutes. The PCR reaction mixture was comprised of the following components: 5 µl of 5X buffer (Promega), 3 µl of $MgCl_2$ (25 mM; Promega), 0.5 µl of dNTPs (25 pM; Promega), 0.5 µl of each primer (25 pM; Integrated DNA Technologies Inc), 1 µl of genomic DNA and 12 µl of H_2O. The final mixture was covered with mineral oil to prevent evaporation. Before the addition of a *Taq* polymerase (500U; Promega), the mixture was boiled at 94°C for 10 minutes. 2 µl of a *Taq* polymerase was added at 72°C. A 35 cycle PCR reaction was run consisting of the following conditions: denaturing at 94°C for 45 seconds, priming at 60°C for 45 seconds and extending at 72°C for 1 minute. The last cycle remained at 72°C for 10 minutes. The PCR products were separated on a 3% Agarose gel (Lonza). The primers used for detecting the *Alk1*-cKO (*2f*) or *Alk1*-null (*1f*) alleles are summarized in the Table 5-1.

RT-PCR Analysis

To confirm the expression of endothelial biomarker genes, parental *Alk1*$^{2f/1f}$ and TM-treated *Alk1*$^{1f/1f}$ pECs were cultured until 100% confluency in a 25cm^2 culture flask. Total RNAs from cultures were extracted using the NucleoSpin RNA purification kit (Clontech). All experimental steps followed the manufacturer's protocol. 2 µg of RNA was used for reverse transcription (RT) reaction. The cDNAs were synthesized using SuperScript III First-Stand synthesis kit (Invitrogen) according to recommendations and guidelines from the company. After the RT reaction, 2 µl of cDNA was used for the PCR analysis. The PCR reaction mixture and hot-start PCR reaction were performed as detailed in the genomic DNA PCR analysis. Three

different PCR cycles were run. For the amplification of RNAs for Alk1, Smad1, Endothelin and Actin, a total of 27 cycles were run as the following: denaturing at 94°C for 45 seconds, priming at 60°C for 45 seconds and extending at 72°C for 1 minute. The PCR products were further processed at 72°C for 10 minutes. For Tie2, Flk1 and Endoglin, the PCR consisted of a denaturation at 94°C for 45 seconds, annealing at 60°C for 45 seconds and extension at 72°C for 1 minute 30 seconds for a total of 28 steps. Lastly, cDNAs for ActRIIa, Bmpr2, Alk2, Alk3, and Alk6 were amplified by the following PCR cycles: denaturing at 94°C for 45 seconds, priming at 55°C for 45 seconds and extending at 72°C for 1 minute 30 seconds. The primers used for RT-PCR analyses are summarized in the Table 5-2.

Western Blotting

Protein lysates extracted from pECs were subjected to Western blot analyses. The same number of *Alk1*$^{2f/1f}$ and *Alk1*$^{1f/1f}$ pECs were seeded into each well and grown in a 6-well culture plate. At 100% confluency, medium was changed from normal ECM to chemically defined growth factor- and serum-free ECM (Genlantis) for overnight serum starvation. On the next day, after removing defined ECM, the cultures were replenished with defined ECM containing bFGF (50 ng/ml; BD Biosciences) supplemented with either TGF-β1 (5 ng/ml; R & D Systems) or BMP-9 (20 ng/ml; R & D Systems) and incubated for 30 minutes at 37°C. This stimulation was terminated by briefly washing the cells with sterile PBS twice. Cells were lysed by adding 80 µl of 1X protein loading buffer [5X; 60 mM Tris-HCl (pH 6.8), 25% glycerol, 2% SDS, 14.4 mM β-mercaptoethanol, 0.1% bromophenol blue in H_2O] and collected in an eppendorf tube placed on ice. The whole protein lysates were boiled at 95 to 100°C for 5 minutes and cooled down on ice. After centrifugation at 13,000 rpm for 5 minutes, protein lysates were stored at -80°C until needed. 15 µl of each protein lysate was separated by SDS-PAGE on a 8% polyacrylamide (BioRad) protein gel. The fractionated proteins were transferred to PVDF membranes. After

blocking with a 5% non-fat milk blotting solution, membranes were incubated with a primary antibody against the protein of interest at 4°C overnight. On the following day, membranes were washed with a washing buffer [0.05% Igepal (Sigma) in PBS] and incubated with an appropriate horseradish peroxidase-linked secondary antibody at 4°C for 1 hour. Lastly, the protein was detected by a chemiluminescent Western blotting detection reagent (Amersham Pharmacia Biotech Inc).

The primary antibodies used for Western blot analyses are the followings: SMAD1 (1:500; Clone: 2C2; Chemicon International), phospho-SMAD1/5/8 (1:500; Cat #: 9511; Cell Signaling Technology), SMAD2 (1:500; Cat #: 3103; Cell Signaling Technology), phospho-SMAD2/3 (1:500; Cat #: 3101; Cell Signaling Technology), p44/42 MAPK (ERK1/2; 1:500; Cat #: 9102; Cell Signaling Technologies), phospho-p44/42 MAPK (phospho-ERK1/2; 1:500; Cat #: 9106; Cell Signaling Technology) and GAPDH (1:10,000; Cat #: ab8245; Abcam). The secondary antibodies used for Western blot analyses are the followings: HRP-labelled anti-mouse IgG (1:5,000; Cat #: NA931; Amersham) and HRP-linked anti-rabbit IgG (1:5,000; Cat #: NA934; Amersham).

in vitro Endothelial Migration Assay

For the 2D wound-induced migration assay, pECs were plated and grown in a 6-well culture plate. When cells reached 100% confluency, three wounding lines per well were created by scraping with a sterile tip. Then, cells were briefly washed with 1X HBSS (Invitrogen) two times and replenished with ECM or chemically defined growth factor- and serum-free ECM (Genlantis) containing bFGF (50 ng/ml) (BD Biosciences). Closing of these wounds was photographed at every 4 hours post-wound up to 12 hours. Based on a decrease in the width of each wound over time, ECs migration was calculated.

In the 3D modified Boyden chamber assay, 500 µL of ECM containing 20% FBS was added into each well in a 24-well culture plate. Migration chambers with 8 µm pore size (Biosciences) were then placed into each well. pECs (5×10^2 cells) were suspended in 500 µl of ECM containing 2% FBS and seeded into each migration chamber. After 48 hours incubation, medium was removed and migration chambers were stained with crystal violet dye. The chambers were allowed to air-dry overnight. Subsequently, stained cells in six randomly chosen fields were counted under the microscope. Chemically defined growth factor- and serum-free ECM (Genlantis) containing bFGF (50 ng/ml) (BD Biosciences) with 10% FBS was added to the bottom chambers and 1% FBS to the upper chambers to get rid the effects of FBS on ECs migration.

in vitro Tube Formation Assay on Matrigel

The phenol red-free Matrigel (BD Biosciences) was thawed overnight at 4°C. 200 µl of Matrigel was added into each well in a pre-chilled 24-well plate. Then, Matrigel was solidified by incubation at 37°C for 1 hour. pECs (6×10^4 cells/well) were suspended in 500 µl of chemically defined growth factor- and serum-free ECM (Genlantis) containing bFGF (50 ng/ml; BD Biosciences) in combination with either TGF-β1 (5 ng/ml; R & D Systems) or BMP-9 (20 ng/ml; R & D Systems) and seeded into each well. The endothelial capillary-like network formation was photographed at various time points: 3, 6, 9, 12 and 24 hours after seeding. To obtain quantitative readouts for the statistical analysis, all pictures were processed by the MatLab imaging program. From the processed images, areas of tube-like structures, total length of tubes and the number of endothelial outgrowth from each nodule were calculated.

in vivo Matrigel Plug Angiogenesis Assay

One day before or on the same day of the Matrigel implantation, 100 µl of tamoxifen (25 mg/ml of corn oil; Sigma) was injected into the peritoneum of both $R26^{+/+}$; $Alk1^{2f/2f}$ control and

R26$^{+/CreER}$*; Alk1*$^{2f/2f}$ mutant mice. On the following day, 200 µl of high concentration Matrigel (9.6 mg/ml) (BD Biosciences) was thawed overnight at 4°C, then mixed with 200 µl of bFGF (250 ng/ml) (BD Biosciences) and kept on ice. For anesthesia, the recipient mice were placed into a chamber in which 4% isoflurane gas was applied. During the injection procedure, anesthesia was maintained at 2 to 3% isoflurane. Right before the Matrigel injection, the fur on the dorsal area of the mice was shaved. The resulting 400 µl solution was then subcutaneously injected into the skin of dorsal region of mice. Between 7 to 10 days post tamoxifen injection, mice were sacrificed and the skin bearing implanted-Matrigel plugs was excised. Samples were fixed in 4% paraformaldehyde for at least 24 hours at room temperature. After washing in PBS two times for 15 minutes each, fixed plugs were sequentially dehydrated with an increasing concentration of ethanol (70% for 20 minutes, 95% for 1 hour and 100% for 2 hours) and incubated in an organic solvent for 20 minutes. The Matrigel plugs were incubated in paraffin for 3 hours and subsequently embedded in paraffin, then were sectioned at 5 µm. For histological examination, sections were incubated at 60°C overnight and deparaffinized by incubation in an organic solvent (Citrisolv; Fisher Scientific) for 30 minutes. Sections were sequentially rehydrated with decreasing concentrations of ethanol (100% for 10 minutes, 95% for 10 minutes, 70% for 10 minutes and H_2O) and subjected to hematoxylin and eosin (H & E) staining.

X-Gal Staining

For the visualization of migrating ECs or nascent vessels in Matrigel plugs from above, expression of the *LacZ* gene under the control of *Flk1* promoter was examined by X-gal staining. *R26*$^{+/+}$*; Alk1*$^{2f/2f}$ control or *R26*$^{+/CreER}$*; Alk1*$^{2f/2f}$ mutant mice carrying the *Flk1*^{LacZ}-KI allele were sacrificed and Matrigel plugs along with the attached skin were isolated. The isolated plugs were fixed in a fixative solution [1% formaldehyde (Fisher Scientific), 0.2% glutaraldehyde (Sigma), 2 mM $MgCl_2$, 5 mM EGTA, and 0.02% NP-40 in PBS] at room temperature for 10 minutes.

Fixation was followed by washing thrice with PBS for 5 minute each, with rocking. Then, samples were placed in an X-gal staining solution [5 mM $K_3Fe(CN)_6$, 5 mM $K_4Fe(CN)_6$, 2 mM $MgCl_2$, 0.01% NaDeoxycholate, 0.02% NP-40, 100 mM phosphate buffer (pH 7.3), 0.5 mg/ml X-gal (Fisher Scientific) in distilled-deionized H_2O] and incubated overnight at 37°C. The next day, X-gal-stained Matrigel plugs were washed with PBS, subsequently examined and photographed under the microscope. After microscopic observation, plugs were fixed in 4% paraformaldehyde solution at room temperature for at least 24 hours. For the histological analysis, samples were sequentially dehydrated as described above and paraffin-embedded. 5 µm thick sections were deparaffinized and rehydrated as described above, then counterstained with nuclear fast red (NFR).

in vivo Subcutaneous Tumor Generation

Tumor formation under the skin was induced by the subcutaneous injection of LLC cells. 100 µl of tamoxifen (25 mg/ml; Sigma) was intraperitoneally administered into $R26^{+/+}$; $Alk1^{2f/2f}$ control and $R26^{+/CreER}$; $Alk1^{2f/2f}$ mutant mice. On the next day, LLC cells were suspended in sterile PBS at a concentration of 1×10^5 cells/10 µl. The mice were anesthetized as detailed in the *in vivo* Matrigel plug angiogenesis assay. Prior to tumor cell injection, the fur of mice in the area surrounding the injection site was shaved, then 20 µl of the LLC cell suspension (2×10^5 cells) was injected into each mouse. For following nine days, the behaviors of the mice and tumor growth were monitored daily. At day 9 post LLC cell inoculation, the mice were euthanized by an overdose of 100% isofluran and subsequent cervical dislocation. The tumor cell-implanted dorsal skin was excised and fixed in 4% paraformaldehyde for at least 48 hours at room temperature. After fixation, samples were washed in PBS for 15 minutes twice and stored in PBS at 4°C.

in vivo Intramuscular Tumor Generation

To study effects of *Alk1*-deletion on the established tumor vasculature, the *in vivo* intramuscular tumor model was employed. LLC cells were prepared as described previously. 10 µl of tumor cell suspension (1×10^5 cells) was injected into the right thigh of each $R26^{+/+}$; $Alk1^{2f/2f}$ control and $R26^{+/CreER}$; $Alk1^{2f/2f}$ mutant mouse. The implanted tumor cells were allowed to be grown for 12 days with daily observation. On day 12, the diameter of the right thigh of control and mutant mice was between 10 to 11 mm. After intraperitoneal administration of 100 µl of tamoxifen (25 mg/ml; Sigma), tumor growth was further monitored daily for 8 days. At day 20 post-LLC cell implantation, the mice were sacrificed and right legs were collected. Left legs were also harvested as an internal control. The foot and fur were removed, and then the whole thighs were fixed in 4% paraformaldehyde at room temperature for at least 48 hours. The thighs were incubated in a decalcification solution (Biochemical) for 3 days at room temperature with shaking, sliced at 1 to 2 mm thickness for better penetration, then further decalcified in fresh solution for 3 more days. Decalcified samples were then subjected to multiple brief tap water washings followed by two 30 minute washings with tap water on a rocker. Samples were stored in PBS at 4°C until needed.

Latex Dye Injection

To visualize the systemic vascular circulation, mice bearing intramuscular tumor were subjected to the latex dye injection (Blue latex, Catalog# BR80B, Connecticut Valley Biological Supply Co, Southampton, MA). Mice were anesthetized by intraperitoneal injection of Ketamine/Xylazine (100 mg/15 mg per 1 kg body weight). The chest cavity of the mouse was opened to expose the heart, and then latex dye was injected into the left ventricle of the heart. The hair-removed whole right legs were briefly washed in PBS and fixed in 4% paraformaldehyde at room temperature for at least 3 days. To obtain the whole-mount imaging,

after washing in PBS twice for 15 minutes, samples were sequentially dehydrated by increasing concentration of methanol (20% for 20 minutes, 50% for 20 minutes, 75% for 20 minutes, 90% for 60 minutes, 100% for 1 hour and 30 minutes) and cleared with an organic solvent (Benzyl alcohol:Benzyl benzoate = 1:1; Sigma).

Histology and Immunohistochemistry

After fixation in 4% paraformaldehyde solution between 24-48 hours, depending on the size, tumor samples were washed in PBS twice for 15 minutes each. Samples were dehydrated by an increasing ethanol series of 70% (2 times for 30 minutes/each), 95% (two times for 50 minutes/each) and 100% (three times for 1 hour/each), and then 100% organic solvent (two times for 30 minutes/each), which was followed by incubation in paraffin for 3 hours. The paraffin-embedded tissues were sectioned at 5 μm in thickness. The sectioned tissues were deparaffinized by heating at 60°C overnight and 40 minutes incubation in an organic solvent, then rehydrated through a degraded ethanol series (100% → 95% → 70% → H_2O) and stained with hematoxylin and eosin (H & E).

For immunohistochemistry, sectioned samples were processed as same as described in preparation for the H & E staining. The standard ABC method using a Vector immunodetection kit (Vector Laboratories) was performed. Briefly, the rehydrated sections were treated with 3% (v/v) hydrogen peroxide (H_2O_2) at room temperature for 10 minutes to block the endogenous peroxidase activity. After washing in PBS twice, the sections were incubated with blocking serum corresponding to the species from which the secondary antibody was raised at room temperature for 1 hour. Next, the incubation with a primary antibody for the protein of interest at room temperature for 1 hour and 30 minutes was followed by washing with PBS. A biotinylated secondary antibody was applied to the samples for 30 minutes at room temperature. Sections were treated with the peroxidase-conjugated biotin/avidin complex for 30 minutes at room

temperature. Two PBS washes were followed by procedures for the color development via applying a DAB substrate chromogenic solution (Vector laboratories). The primary antibodies used for the immunohistochemistry are the following: PECAM/CD31 (1:300; Cat #: CM 303; Biocare Medical) and α-SMA (1:800; Clone: 1A4; Sigma).

Statistics

Data were represented as mean ± SEM or SE. The differences between groups were determined by the mixed linear regression model, general linear regression model, or Two-Way ANOVA. A value of $p<0.05$ was considered statistically significant.

Table 5-1. Summary of primers used for genomic PCR analysis.

Genes	Forward Primers	Reverse Primers
Alk1 (2f; floxed)	CAGCACCTACATCTTGGGTGGAGA	ACTGTTCTTCCTCGGAGCCTTGTC
Alk1 (1f; null)	CAGCACCTACATCTTGGGTGGAGA	TCCTCTTGTCGTATATGTCCC

Table 5-2. Summary of primers used for RT-PCR analysis.

Genes	Forward Primers	Reverse Primers
Alk1	TCATGGTGCACAGTGGTGCTG	CAAATCCCGCTGCTTCTCCTG
Alk2	AGTCATGGTTCAGGGAGACG	TGCAGCACTGTCCATTCTTC
Alk3	TAAAGGCCGCTATGGAGAAG	CCAGGTCAGCAATA AGCAA
Alk6	CACTCCCATTCCTCATCAAA	TTCCAATCTGCTTCACCATC
ActRIIa	CGTTCGCCGTCTTTCTTATC	AGGATTTGAAGTGGGCTGTG
Bmpr2	GTTGACAGGAGACCGGAAACAG	GGAGACTCAGATATTTGCACAG
Smad1	GGTTCGAGACCGTGTATGAAC	CTCCTTCGTCAGGTCTCCATC
Endothelin	ACCAGAAGTTGACGCACAACC	CAATCTAACCTCTTCCATTAGCC
Endoglin	TGCACTCTGGTACATCTATTC	TGGATTGGGCAGTTCTGTAAA
Flk1	AGAACACCAAAAGAGAGGAACG	GCACACAGGCAGAAACCAGTAG
Tie2	CTCATCTGTGGACGCTGGATG	GGCACTGAGTGGATGAAGGAG
Actin	CCTGAACCCTAAGGCCAACCG	GCTCATAGCTCTTCTCCAGGG

LIST OF REFERENCES

1. Jain, R. K. (2003) Molecular regulation of vessel maturation. *Nat Med* 9, 685-693

2. Risau, W., and Flamme, I. (1995) Vasculogenesis. *Annu Rev Cell Dev Biol* 11, 73-91

3. Folkman, J. (1995) Seminars in Medicine of the Beth Israel Hospital, Boston. Clinical applications of research on angiogenesis. *N Engl J Med* 333, 1757-1763

4. Folkman, J. (1995) Angiogenesis in cancer, vascular, rheumatoid and other disease. *Nat Med* 1, 27-31

5. Pepper, M. S. (1996) Positive and negative regulation of angiogenesis: from cell biology to the clinic. *Vasc Med* 1, 259-266

6. Reynolds, L. P., Killilea, S. D., and Redmer, D. A. (1992) Angiogenesis in the female reproductive system. *Faseb J* 6, 886-892

7. Risau, W. (1997) Mechanisms of angiogenesis. *Nature* 386, 671-674

8. Patan, S., Haenni, B., and Burri, P. H. (1996) Implementation of intussusceptive microvascular growth in the chicken chorioallantoic membrane (CAM): 1. pillar formation by folding of the capillary wall. *Microvasc Res* 51, 80-98

9. Pepper, M. S., Mandriota, S. J., Vassalli, J. D., Orci, L., and Montesano, R. (1996) Angiogenesis-regulating cytokines: activities and interactions. *Curr Top Microbiol Immunol* 213 (Pt 2), 31-67

10. Pepper, M. S., Montesano, R., Mandriota, S. J., Orci, L., and Vassalli, J. D. (1996) Angiogenesis: a paradigm for balanced extracellular proteolysis during cell migration and morphogenesis. *Enzyme Protein* 49, 138-162

11. Pepper, M. S. (1997) Transforming growth factor-beta: vasculogenesis, angiogenesis, and vessel wall integrity. *Cytokine Growth Factor Rev* 8, 21-43

12. Carmeliet, P. (2000) Mechanisms of angiogenesis and arteriogenesis. *Nat Med* 6, 389-395

13. Bicknell, R., and Harris, A. L. (2004) Novel angiogenic signaling pathways and vascular targets. *Annu Rev Pharmacol Toxicol* 44, 219-238

14. Lawson, N. D., Scheer, N., Pham, V. N., Kim, C. H., Chitnis, A. B., Campos-Ortega, J. A., and Weinstein, B. M. (2001) Notch signaling is required for arterial-venous differentiation during embryonic vascular development. *Development* 128, 3675-3683

15. Baron, M., Aslam, H., Flasza, M., Fostier, M., Higgs, J. E., Mazaleyrat, S. L., and Wilkin, M. B. (2002) Multiple levels of Notch signal regulation (review). *Mol Membr Biol* 19, 27-38

16. Iso, T., Hamamori, Y., and Kedes, L. (2003) Notch signaling in vascular development. *Arterioscler Thromb Vasc Biol* 23, 543-553

17. Ogawa, K., Pasqualini, R., Lindberg, R. A., Kain, R., Freeman, A. L., and Pasquale, E. B. (2000) The ephrin-A1 ligand and its receptor, EphA2, are expressed during tumor neovascularization. *Oncogene* 19, 6043-6052

18. Cheng, N., Brantley, D. M., and Chen, J. (2002) The ephrins and Eph receptors in angiogenesis. *Cytokine Growth Factor Rev* 13, 75-85

19. Pola, R., Ling, L. E., Silver, M., Corbley, M. J., Kearney, M., Blake Pepinsky, R., Shapiro, R., Taylor, F. R., Baker, D. P., Asahara, T., and Isner, J. M. (2001) The morphogen Sonic hedgehog is an indirect angiogenic agent upregulating two families of angiogenic growth factors. *Nat Med* 7, 706-711

20. Lee, S. H., Schloss, D. J., Jarvis, L., Krasnow, M. A., and Swain, J. L. (2001) Inhibition of angiogenesis by a mouse sprouty protein. *J Biol Chem* 276, 4128-4133

21. Kidd, T., Brose, K., Mitchell, K. J., Fetter, R. D., Tessier-Lavigne, M., Goodman, C. S., and Tear, G. (1998) Roundabout controls axon crossing of the CNS midline and defines a novel subfamily of evolutionarily conserved guidance receptors. *Cell* 92, 205-215

22. Huminiecki, L., Gorn, M., Suchting, S., Poulsom, R., and Bicknell, R. (2002) Magic roundabout is a new member of the roundabout receptor family that is endothelial specific and expressed at sites of active angiogenesis. *Genomics* 79, 547-552

23. Hicklin, D. J., and Ellis, L. M. (2005) Role of the vascular endothelial growth factor pathway in tumor growth and angiogenesis. *J Clin Oncol* 23, 1011-1027

24. Shibuya, M., Yamaguchi, S., Yamane, A., Ikeda, T., Tojo, A., Matsushime, H., and Sato, M. (1990) Nucleotide sequence and expression of a novel human receptor-type tyrosine kinase gene (flt) closely related to the fms family. *Oncogene* 5, 519-524

25. Matthews, W., Jordan, C. T., Gavin, M., Jenkins, N. A., Copeland, N. G., and Lemischka, I. R. (1991) A receptor tyrosine kinase cDNA isolated from a population of enriched primitive hematopoietic cells and exhibiting close genetic linkage to c-kit. *Proc Natl Acad Sci U S A* 88, 9026-9030

26. Hiratsuka, S., Minowa, O., Kuno, J., Noda, T., and Shibuya, M. (1998) Flt-1 lacking the tyrosine kinase domain is sufficient for normal development and angiogenesis in mice. *Proc Natl Acad Sci U S A* 95, 9349-9354

27. Dunk, C., and Ahmed, A. (2001) Vascular endothelial growth factor receptor-2-mediated mitogenesis is negatively regulated by vascular endothelial growth factor receptor-1 in tumor epithelial cells. *Am J Pathol* 158, 265-273

28. Millauer, B., Wizigmann-Voos, S., Schnurch, H., Martinez, R., Moller, N. P., Risau, W., and Ullrich, A. (1993) High affinity VEGF binding and developmental expression suggest Flk-1 as a major regulator of vasculogenesis and angiogenesis. *Cell* 72, 835-846

29. Zeng, H., Dvorak, H. F., and Mukhopadhyay, D. (2001) Vascular permeability factor (VPF)/vascular endothelial growth factor (VEGF) peceptor-1 down-modulates VPF/VEGF receptor-2-mediated endothelial cell proliferation, but not migration, through phosphatidylinositol 3-kinase-dependent pathways. *J Biol Chem* 276, 26969-26979

30. Dvorak, H. F. (2002) Vascular permeability factor/vascular endothelial growth factor: a critical cytokine in tumor angiogenesis and a potential target for diagnosis and therapy. *J Clin Oncol* 20, 4368-4380

31. Ogawa, S., Oku, A., Sawano, A., Yamaguchi, S., Yazaki, Y., and Shibuya, M. (1998) A novel type of vascular endothelial growth factor, VEGF-E (NZ-7 VEGF), preferentially utilizes KDR/Flk-1 receptor and carries a potent mitotic activity without heparin-binding domain. *J Biol Chem* 273, 31273-31282

32. Kaipainen, A., Korhonen, J., Mustonen, T., van Hinsbergh, V. W., Fang, G. H., Dumont, D., Breitman, M., and Alitalo, K. (1995) Expression of the fms-like tyrosine kinase 4 gene becomes restricted to lymphatic endothelium during development. *Proc Natl Acad Sci U S A* 92, 3566-3570

33. Paavonen, K., Puolakkainen, P., Jussila, L., Jahkola, T., and Alitalo, K. (2000) Vascular endothelial growth factor receptor-3 in lymphangiogenesis in wound healing. *Am J Pathol* 156, 1499-1504

34. Matsumura, K., Hirashima, M., Ogawa, M., Kubo, H., Hisatsune, H., Kondo, N., Nishikawa, S., Chiba, T., and Nishikawa, S. (2003) Modulation of VEGFR-2-mediated endothelial-cell activity by VEGF-C/VEGFR-3. *Blood* 101, 1367-1374

35. Ornitz, D. M., and Itoh, N. (2001) Fibroblast growth factors. *Genome Biol* 2, REVIEWS3005

36. Bottcher, R. T., and Niehrs, C. (2005) Fibroblast growth factor signaling during early vertebrate development. *Endocr Rev* 26, 63-77

37. Cao, R., Brakenhielm, E., Pawliuk, R., Wariaro, D., Post, M. J., Wahlberg, E., Leboulch, P., and Cao, Y. (2003) Angiogenic synergism, vascular stability and improvement of hind-limb ischemia by a combination of PDGF-BB and FGF-2. *Nat Med* 9, 604-613

38. Marchuk, D. A., Srinivasan, S., Squire, T. L., and Zawistowski, J. S. (2003) Vascular morphogenesis: tales of two syndromes. *Hum Mol Genet* 12 Spec No 1, R97-112

39. Derynck, R., and Zhang, Y. E. (2003) Smad-dependent and Smad-independent pathways in TGF-beta family signalling. *Nature* 425, 577-584

40. Massague, J. (1998) TGF-beta signal transduction. *Annu Rev Biochem* 67, 753-791

41. Chang, H., Brown, C. W., and Matzuk, M. M. (2002) Genetic analysis of the mammalian transforming growth factor-beta superfamily. *Endocr Rev* 23, 787-823

42. Roberts, A. B., and Sporn, M. B. (1993) Physiological actions and clinical applications of transforming growth factor-beta (TGF-beta). *Growth Factors* 8, 1-9

43. Piek, E., Heldin, C. H., and Ten Dijke, P. (1999) Specificity, diversity, and regulation in TGF-beta superfamily signaling. *Faseb J* 13, 2105-2124

44. Bertolino, P., Deckers, M., Lebrin, F., and ten Dijke, P. (2005) Transforming growth factor-beta signal transduction in angiogenesis and vascular disorders. *Chest* 128, 585S-590S

45. Heldin, C. H., Miyazono, K., and ten Dijke, P. (1997) TGF-beta signalling from cell membrane to nucleus through SMAD proteins. *Nature* 390, 465-471

46. Attisano, L., and Wrana, J. L. (1998) Mads and Smads in TGF beta signalling. *Curr Opin Cell Biol* 10, 188-194

47. Kretzschmar, M., and Massague, J. (1998) SMADs: mediators and regulators of TGF-beta signaling. *Curr Opin Genet Dev* 8, 103-111

48. ten Dijke, P., and Hill, C. S. (2004) New insights into TGF-beta-Smad signalling. *Trends Biochem Sci* 29, 265-273

49. Massague, J. (2000) How cells read TGF-beta signals. *Nat Rev Mol Cell Biol* 1, 169-178

50. Itoh, S., Itoh, F., Goumans, M. J., and Ten Dijke, P. (2000) Signaling of transforming growth factor-beta family members through Smad proteins. *Eur J Biochem* 267, 6954-6967

51. Sullivan, D. C., and Bicknell, R. (2003) New molecular pathways in angiogenesis. *Br J Cancer* 89, 228-231

52. Uyttendaele, H., Ho, J., Rossant, J., and Kitajewski, J. (2001) Vascular patterning defects associated with expression of activated Notch4 in embryonic endothelium. *Proc Natl Acad Sci U S A* 98, 5643-5648

53. Mailhos, C., Modlich, U., Lewis, J., Harris, A., Bicknell, R., and Ish-Horowicz, D. (2001) Delta4, an endothelial specific notch ligand expressed at sites of physiological and tumor angiogenesis. *Differentiation* 69, 135-144

54. Shutter, J. R., Scully, S., Fan, W., Richards, W. G., Kitajewski, J., Deblandre, G. A., Kintner, C. R., and Stark, K. L. (2000) Dll4, a novel Notch ligand expressed in arterial endothelium. *Genes Dev* 14, 1313-1318

55. Zimrin, A. B., Pepper, M. S., McMahon, G. A., Nguyen, F., Montesano, R., and Maciag, T. (1996) An antisense oligonucleotide to the notch ligand jagged enhances fibroblast growth factor-induced angiogenesis in vitro. *J Biol Chem* 271, 32499-32502

56. Liu, Z. J., Shirakawa, T., Li, Y., Soma, A., Oka, M., Dotto, G. P., Fairman, R. M., Velazquez, O. C., and Herlyn, M. (2003) Regulation of Notch1 and Dll4 by vascular endothelial growth factor in arterial endothelial cells: implications for modulating arteriogenesis and angiogenesis. *Mol Cell Biol* 23, 14-25

57. Taylor, K. L., Henderson, A. M., and Hughes, C. C. (2002) Notch activation during endothelial cell network formation in vitro targets the basic HLH transcription factor HESR-1 and downregulates VEGFR-2/KDR expression. *Microvasc Res* 64, 372-383

58. Noguera-Troise, I., Daly, C., Papadopoulos, N. J., Coetzee, S., Boland, P., Gale, N. W., Lin, H. C., Yancopoulos, G. D., and Thurston, G. (2006) Blockade of Dll4 inhibits tumour growth by promoting non-productive angiogenesis. *Nature* 444, 1032-1037

59. Pandey, A., Shao, H., Marks, R. M., Polverini, P. J., and Dixit, V. M. (1995) Role of B61, the ligand for the Eck receptor tyrosine kinase, in TNF-alpha-induced angiogenesis. *Science* 268, 567-569

60. Stein, E., Lane, A. A., Cerretti, D. P., Schoecklmann, H. O., Schroff, A. D., Van Etten, R. L., and Daniel, T. O. (1998) Eph receptors discriminate specific ligand oligomers to determine alternative signaling complexes, attachment, and assembly responses. *Genes Dev* 12, 667-678

61. Brose, K., Bland, K. S., Wang, K. H., Arnott, D., Henzel, W., Goodman, C. S., Tessier-Lavigne, M., and Kidd, T. (1999) Slit proteins bind Robo receptors and have an evolutionarily conserved role in repulsive axon guidance. *Cell* 96, 795-806

62. Huminiecki, L., and Bicknell, R. (2000) In silico cloning of novel endothelial-specific genes. *Genome Res* 10, 1796-1806

63. Waite, K. A., and Eng, C. (2003) From developmental disorder to heritable cancer: it's all in the BMP/TGF-beta family. *Nat Rev Genet* 4, 763-773

64. Tsuchida, K., Nakatani, M., Uezumi, A., Murakami, T., and Cui, X. (2008) Signal transduction pathway through activin receptors as a therapeutic target of musculoskeletal diseases and cancer. *Endocr J* 55, 11-21

65. Shovlin, C. L., Guttmacher, A. E., Buscarini, E., Faughnan, M. E., Hyland, R. H., Westermann, C. J., Kjeldsen, A. D., and Plauchu, H. (2000) Diagnostic criteria for hereditary hemorrhagic telangiectasia (Rendu-Osler-Weber syndrome). *Am J Med Genet* 91, 66-67

66. Abdalla, S. A., and Letarte, M. (2006) Hereditary haemorrhagic telangiectasia: current views on genetics and mechanisms of disease. *J Med Genet* 43, 97-110

67. Bideau, A., Plauchu, H., Brunet, G., and Robert, J. (1989) Epidemiological investigation of Rendu-Osler disease in France: its geographical distribution and prevalence. *Popul* 44, 3-22

68. Kjeldsen, A. D., Vase, P., and Green, A. (1999) Hereditary haemorrhagic telangiectasia: a population-based study of prevalence and mortality in Danish patients. *J Intern Med* 245, 31-39

69. Dakeishi, M., Shioya, T., Wada, Y., Shindo, T., Otaka, K., Manabe, M., Nozaki, J., Inoue, S., and Koizumi, A. (2002) Genetic epidemiology of hereditary hemorrhagic telangiectasia in a local community in the northern part of Japan. *Hum Mutat* 19, 140-148

70. McAllister, K. A., Grogg, K. M., Johnson, D. W., Gallione, C. J., Baldwin, M. A., Jackson, C. E., Helmbold, E. A., Markel, D. S., McKinnon, W. C., Murrell, J., and et al. (1994) Endoglin, a TGF-beta binding protein of endothelial cells, is the gene for hereditary haemorrhagic telangiectasia type 1. *Nat Genet* 8, 345-351

71. McDonald, M. T., Papenberg, K. A., Ghosh, S., Glatfelter, A. A., Biesecker, B. B., Helmbold, E. A., Markel, D. S., Zolotor, A., McKinnon, W. C., Vanderstoep, J. L., and et al. (1994) A disease locus for hereditary haemorrhagic telangiectasia maps to chromosome 9q33-34. *Nat Genet* 6, 197-204

72. Heutink, P., Haitjema, T., Breedveld, G. J., Janssen, B., Sandkuijl, L. A., Bontekoe, C. J., Westerman, C. J., and Oostra, B. A. (1994) Linkage of hereditary haemorrhagic telangiectasia to chromosome 9q34 and evidence for locus heterogeneity. *J Med Genet* 31, 933-936

73. Shovlin, C. L., Hughes, J. M., Tuddenham, E. G., Temperley, I., Perembelon, Y. F., Scott, J., Seidman, C. E., and Seidman, J. G. (1994) A gene for hereditary haemorrhagic telangiectasia maps to chromosome 9q3. *Nat Genet* 6, 205-209

74. Johnson, D. W., Berg, J. N., Gallione, C. J., McAllister, K. A., Warner, J. P., Helmbold, E. A., Markel, D. S., Jackson, C. E., Porteous, M. E., and Marchuk, D. A. (1995) A second locus for hereditary hemorrhagic telangiectasia maps to chromosome 12. *Genome Res* 5, 21-28

75. Vincent, P., Plauchu, H., Hazan, J., Faure, S., Weissenbach, J., and Godet, J. (1995) A third locus for hereditary haemorrhagic telangiectasia maps to chromosome 12q. *Hum Mol Genet* 4, 945-949

76. Johnson, D. W., Berg, J. N., Baldwin, M. A., Gallione, C. J., Marondel, I., Yoon, S. J., Stenzel, T. T., Speer, M., Pericak-Vance, M. A., Diamond, A., Guttmacher, A. E., Jackson, C. E., Attisano, L., Kucherlapati, R., Porteous, M. E., and Marchuk, D. A. (1996) Mutations in the activin receptor-like kinase 1 gene in hereditary haemorrhagic telangiectasia type 2. *Nat Genet* 13, 189-195

77. Gallione, C. J., Repetto, G. M., Legius, E., Rustgi, A. K., Schelley, S. L., Tejpar, S., Mitchell, G., Drouin, E., Westermann, C. J., and Marchuk, D. A. (2004) A combined syndrome of juvenile polyposis and hereditary haemorrhagic telangiectasia associated with mutations in MADH4 (SMAD4). *Lancet* 363, 852-859

78. Govani, F. S., and Shovlin, C. L. (2009) Hereditary haemorrhagic telangiectasia: a clinical and scientific review. *Eur J Hum Genet*

79. Guttmacher, A. E., Marchuk, D. A., and White, R. I., Jr. (1995) Hereditary hemorrhagic telangiectasia. *N Engl J Med* 333, 918-924

80. Sadick, H., Sadick, M., Gotte, K., Naim, R., Riedel, F., Bran, G., and Hormann, K. (2006) Hereditary hemorrhagic telangiectasia: an update on clinical manifestations and diagnostic measures. *Wien Klin Wochenschr* 118, 72-80

81. Sabba, C., Gallitelli, M., Pasculli, G., Suppressa, P., Resta, F., and Tafaro, G. E. (2006) HHT: a rare disease with a broad spectrum of clinical aspects. *Curr Pharm Des* 12, 1217-1220

82. Braverman, I. M., Keh, A., and Jacobson, B. S. (1990) Ultrastructure and three-dimensional organization of the telangiectases of hereditary hemorrhagic telangiectasia. *J Invest Dermatol* 95, 422-427

83. te Veldhuis, E. C., te Veldhuis, A. H., van Dijk, F. S., Kwee, M. L., van Hagen, J. M., Baart, J. A., and van der Waal, I. (2008) Rendu-Osler-Weber disease: update of medical and dental considerations. *Oral Surg Oral Med Oral Pathol Oral Radiol Endod* 105, e38-41

84. Sabba, C. (2005) A rare and misdiagnosed bleeding disorder: hereditary hemorrhagic telangiectasia. *J Thromb Haemost* 3, 2201-2210

85. Pau, H., Carney, A. S., and Murty, G. E. (2001) Hereditary haemorrhagic telangiectasia (Osler-Weber-Rendu syndrome): otorhinolaryngological manifestations. *Clin Otolaryngol Allied Sci* 26, 93-98

86. Cottin, V., Chinet, T., Lavole, A., Corre, R., Marchand, E., Reynaud-Gaubert, M., Plauchu, H., and Cordier, J. F. (2007) Pulmonary arteriovenous malformations in hereditary hemorrhagic telangiectasia: a series of 126 patients. *Medicine (Baltimore)* 86, 1-17

87. Peery, W. H. (1987) Clinical spectrum of hereditary hemorrhagic telangiectasia (Osler-Weber-Rendu disease). *Am J Med* 82, 989-997

88. Begbie, M. E., Wallace, G. M., and Shovlin, C. L. (2003) Hereditary haemorrhagic telangiectasia (Osler-Weber-Rendu syndrome): a view from the 21st century. *Postgrad Med J* 79, 18-24

89. ten Dijke, P., Ichijo, H., Franzen, P., Schulz, P., Saras, J., Toyoshima, H., Heldin, C. H., and Miyazono, K. (1993) Activin receptor-like kinases: a novel subclass of cell-surface receptors with predicted serine/threonine kinase activity. *Oncogene* 8, 2879-2887

90. ten Dijke, P., Yamashita, H., Ichijo, H., Franzen, P., Laiho, M., Miyazono, K., and Heldin, C. H. (1994) Characterization of type I receptors for transforming growth factor-beta and activin. *Science* 264, 101-104

91. Attisano, L., Carcamo, J., Ventura, F., Weis, F. M., Massague, J., and Wrana, J. L. (1993) Identification of human activin and TGF beta type I receptors that form heteromeric kinase complexes with type II receptors. *Cell* 75, 671-680

92. Lux, A., Attisano, L., and Marchuk, D. A. (1999) Assignment of transforming growth factor beta1 and beta3 and a third new ligand to the type I receptor ALK-1. *J Biol Chem* 274, 9984-9992

93. Scharpfenecker, M., van Dinther, M., Liu, Z., van Bezooijen, R. L., Zhao, Q., Pukac, L., Lowik, C. W., and ten Dijke, P. (2007) BMP-9 signals via ALK1 and inhibits bFGF-induced endothelial cell proliferation and VEGF-stimulated angiogenesis. *J Cell Sci* 120, 964-972

94. David, L., Mallet, C., Mazerbourg, S., Feige, J. J., and Bailly, S. (2007) Identification of BMP9 and BMP10 as functional activators of the orphan activin receptor-like kinase 1 (ALK1) in endothelial cells. *Blood* 109, 1953-1961

95. David, L., Mallet, C., Keramidas, M., Lamande, N., Gasc, J. M., Dupuis-Girod, S., Plauchu, H., Feige, J. J., and Bailly, S. (2008) Bone morphogenetic protein-9 is a circulating vascular quiescence factor. *Circ Res* 102, 914-922

96. Chen, Y. G., and Massague, J. (1999) Smad1 recognition and activation by the ALK1 group of transforming growth factor-beta family receptors. *J Biol Chem* 274, 3672-3677

97. Oh, S. P., Seki, T., Goss, K. A., Imamura, T., Yi, Y., Donahoe, P. K., Li, L., Miyazono, K., ten Dijke, P., Kim, S., and Li, E. (2000) Activin receptor-like kinase 1 modulates transforming growth factor-beta 1 signaling in the regulation of angiogenesis. *Proc Natl Acad Sci U S A* 97, 2626-2631

98. Ota, T., Fujii, M., Sugizaki, T., Ishii, M., Miyazawa, K., Aburatani, H., and Miyazono, K. (2002) Targets of transcriptional regulation by two distinct type I receptors for transforming growth factor-beta in human umbilical vein endothelial cells. *J Cell Physiol* 193, 299-318

99. Urness, L. D., Sorensen, L. K., and Li, D. Y. (2000) Arteriovenous malformations in mice lacking activin receptor-like kinase-1. *Nat Genet* 26, 328-331

100. Srinivasan, S., Hanes, M. A., Dickens, T., Porteous, M. E., Oh, S. P., Hale, L. P., and Marchuk, D. A. (2003) A mouse model for hereditary hemorrhagic telangiectasia (HHT) type 2. *Hum Mol Genet* 12, 473-482

101. Cole, S. G., Begbie, M. E., Wallace, G. M., and Shovlin, C. L. (2005) A new locus for hereditary haemorrhagic telangiectasia (HHT3) maps to chromosome 5. *J Med Genet* 42, 577-582

102. Bayrak-Toydemir, P., McDonald, J., Akarsu, N., Toydemir, R. M., Calderon, F., Tuncali, T., Tang, W., Miller, F., and Mao, R. (2006) A fourth locus for hereditary hemorrhagic telangiectasia maps to chromosome 7. *Am J Med Genet A* 140, 2155-2162

103. ten Dijke, P., and Arthur, H. M. (2007) Extracellular control of TGFbeta signalling in vascular development and disease. *Nat Rev Mol Cell Biol* 8, 857-869

104. Rahimi, R. A., and Leof, E. B. (2007) TGF-beta signaling: a tale of two responses. *J Cell Biochem* 102, 593-608

105. Roelen, B. A., van Rooijen, M. A., and Mummery, C. L. (1997) Expression of ALK-1, a type 1 serine/threonine kinase receptor, coincides with sites of vasculogenesis and angiogenesis in early mouse development. *Dev Dyn* 209, 418-430

106. Seki, T., Yun, J., and Oh, S. P. (2003) Arterial endothelium-specific activin receptor-like kinase 1 expression suggests its role in arterialization and vascular remodeling. *Circ Res* 93, 682-689

107. Goumans, M. J., Valdimarsdottir, G., Itoh, S., Rosendahl, A., Sideras, P., and ten Dijke, P. (2002) Balancing the activation state of the endothelium via two distinct TGF-beta type I receptors. *Embo J* 21, 1743-1753

108. Goumans, M. J., Lebrin, F., and Valdimarsdottir, G. (2003) Controlling the angiogenic switch: a balance between two distinct TGF-b receptor signaling pathways. *Trends Cardiovasc Med* 13, 301-307

109. Fernandez, L. A., Sanz-Rodriguez, F., Blanco, F. J., Bernabeu, C., and Botella, L. M. (2006) Hereditary hemorrhagic telangiectasia, a vascular dysplasia affecting the TGF-beta signaling pathway. *Clin Med Res* 4, 66-78

110. Li, D. Y., Sorensen, L. K., Brooke, B. S., Urness, L. D., Davis, E. C., Taylor, D. G., Boak, B. B., and Wendel, D. P. (1999) Defective angiogenesis in mice lacking endoglin. *Science* 284, 1534-1537

111. Bourdeau, A., Dumont, D. J., and Letarte, M. (1999) A murine model of hereditary hemorrhagic telangiectasia. *J Clin Invest* 104, 1343-1351

112. Arthur, H. M., Ure, J., Smith, A. J., Renforth, G., Wilson, D. I., Torsney, E., Charlton, R., Parums, D. V., Jowett, T., Marchuk, D. A., Burn, J., and Diamond, A. G. (2000) Endoglin, an ancillary TGFbeta receptor, is required for extraembryonic angiogenesis and plays a key role in heart development. *Dev Biol* 217, 42-53

113. Satomi, J., Mount, R. J., Toporsian, M., Paterson, A. D., Wallace, M. C., Harrison, R. V., and Letarte, M. (2003) Cerebral vascular abnormalities in a murine model of hereditary hemorrhagic telangiectasia. *Stroke* 34, 783-789

114. Torsney, E., Charlton, R., Diamond, A. G., Burn, J., Soames, J. V., and Arthur, H. M. (2003) Mouse model for hereditary hemorrhagic telangiectasia has a generalized vascular abnormality. *Circulation* 107, 1653-1657

115. Park, S. O., Lee, Y. J., Seki, T., Hong, K. H., Fliess, N., Jiang, Z., Park, A., Wu, X., Kaartinen, V., Roman, B. L., and Oh, S. P. (2008) ALK5- and TGFBR2-independent role of ALK1 in the pathogenesis of hereditary hemorrhagic telangiectasia type 2. *Blood* 111, 633-642

116. Lampugnani, M. G. (1999) Cell migration into a wounded area in vitro. *Methods Mol Biol* 96, 177-182

117. Staton, C. A., Stribbling, S. M., Tazzyman, S., Hughes, R., Brown, N. J., and Lewis, C. E. (2004) Current methods for assaying angiogenesis in vitro and in vivo. *Int J Exp Pathol* 85, 233-248

118. Davis, G. E., and Senger, D. R. (2005) Endothelial extracellular matrix: biosynthesis, remodeling, and functions during vascular morphogenesis and neovessel stabilization. *Circ Res* 97, 1093-1107

119. Passaniti, A., Taylor, R. M., Pili, R., Guo, Y., Long, P. V., Haney, J. A., Pauly, R. R., Grant, D. S., and Martin, G. R. (1992) A simple, quantitative method for assessing angiogenesis and antiangiogenic agents using reconstituted basement membrane, heparin, and fibroblast growth factor. *Lab Invest* 67, 519-528

120. David, L., Mallet, C., Vailhe, B., Lamouille, S., Feige, J. J., and Bailly, S. (2007) Activin receptor-like kinase 1 inhibits human microvascular endothelial cell migration: potential roles for JNK and ERK. *J Cell Physiol* 213, 484-489

121. Liu, D., Wang, J., Kinzel, B., Mueller, M., Mao, X., Valdez, R., Liu, Y., and Li, E. (2007) Dosage-dependent requirement of BMP type II receptor for maintenance of vascular integrity. *Blood* 110, 1502-1510

122. Lamouille, S., Mallet, C., Feige, J. J., and Bailly, S. (2002) Activin receptor-like kinase 1 is implicated in the maturation phase of angiogenesis. *Blood* 100, 4495-4501

123. Roman, B. L., Pham, V. N., Lawson, N. D., Kulik, M., Childs, S., Lekven, A. C., Garrity, D. M., Moon, R. T., Fishman, M. C., Lechleider, R. J., and Weinstein, B. M. (2002) Disruption of acvrl1 increases endothelial cell number in zebrafish cranial vessels. *Development* 129, 3009-3019

124. Wu, X., Ma, J., Han, J. D., Wang, N., and Chen, Y. G. (2006) Distinct regulation of gene expression in human endothelial cells by TGF-beta and its receptors. *Microvasc Res* 71, 12-19

125. Carlson, T. R., Yan, Y., Wu, X., Lam, M. T., Tang, G. L., Beverly, L. J., Messina, L. M., Capobianco, A. J., Werb, Z., and Wang, R. (2005) Endothelial expression of constitutively active Notch4 elicits reversible arteriovenous malformations in adult mice. *Proc Natl Acad Sci U S A* 102, 9884-9889

126. Murphy, P. A., Lam, M. T., Wu, X., Kim, T. N., Vartanian, S. M., Bollen, A. W., Carlson, T. R., and Wang, R. A. (2008) Endothelial Notch4 signaling induces hallmarks of brain arteriovenous malformations in mice. *Proc Natl Acad Sci U S A* 105, 10901-10906

127. Gridley, T. (2007) Notch signaling in vascular development and physiology. *Development* 134, 2709-2718

128. Roca, C., and Adams, R. H. (2007) Regulation of vascular morphogenesis by Notch signaling. *Genes Dev* 21, 2511-2524

129. Tsuchida, K. (2004) Activins, myostatin and related TGF-beta family members as novel therapeutic targets for endocrine, metabolic and immune disorders. *Curr Drug Targets Immune Endocr Metabol Disord* 4, 157-166

130. Harrison, C. A., Gray, P. C., Vale, W. W., and Robertson, D. M. (2005) Antagonists of activin signaling: mechanisms and potential biological applications. *Trends Endocrinol Metab* 16, 73-78

131. Reissmann, E., Jornvall, H., Blokzijl, A., Andersson, O., Chang, C., Minchiotti, G., Persico, M. G., Ibanez, C. F., and Brivanlou, A. H. (2001) The orphan receptor ALK7 and the Activin receptor ALK4 mediate signaling by Nodal proteins during vertebrate development. *Genes Dev* 15, 2010-2022

132. Tsuchida, K., Nakatani, M., Yamakawa, N., Hashimoto, O., Hasegawa, Y., and Sugino, H. (2004) Activin isoforms signal through type I receptor serine/threonine kinase ALK7. *Mol Cell Endocrinol* 220, 59-65

133. Miyazono, K., Maeda, S., and Imamura, T. (2005) BMP receptor signaling: transcriptional targets, regulation of signals, and signaling cross-talk. *Cytokine Growth Factor Rev* 16, 251-263

134. Engel, M. E., McDonnell, M. A., Law, B. K., and Moses, H. L. (1999) Interdependent SMAD and JNK signaling in transforming growth factor-beta-mediated transcription. *J Biol Chem* 274, 37413-37420

135. Yu, L., Hebert, M. C., and Zhang, Y. E. (2002) TGF-beta receptor-activated p38 MAP kinase mediates Smad-independent TGF-beta responses. *Embo J* 21, 3749-3759

136. Bakin, A. V., Tomlinson, A. K., Bhowmick, N. A., Moses, H. L., and Arteaga, C. L. (2000) Phosphatidylinositol 3-kinase function is required for transforming growth factor beta-mediated epithelial to mesenchymal transition and cell migration. *J Biol Chem* 275, 36803-36810

137. Vinals, F., and Pouyssegur, J. (2001) Transforming growth factor beta1 (TGF-beta1) promotes endothelial cell survival during in vitro angiogenesis via an autocrine mechanism implicating TGF-alpha signaling. *Mol Cell Biol* 21, 7218-7230

138. de Caestecker, M. P., Parks, W. T., Frank, C. J., Castagnino, P., Bottaro, D. P., Roberts, A. B., and Lechleider, R. J. (1998) Smad2 transduces common signals from receptor serine-threonine and tyrosine kinases. *Genes Dev* 12, 1587-1592

139. Kretzschmar, M., Doody, J., Timokhina, I., and Massague, J. (1999) A mechanism of repression of TGFbeta/ Smad signaling by oncogenic Ras. *Genes Dev* 13, 804-816

140. Funaba, M., Zimmerman, C. M., and Mathews, L. S. (2002) Modulation of Smad2-mediated signaling by extracellular signal-regulated kinase. *J Biol Chem* 277, 41361-41368

141. Xu, X., Han, J., Ito, Y., Bringas, P., Jr., Deng, C., and Chai, Y. (2008) Ectodermal Smad4 and p38 MAPK are functionally redundant in mediating TGF-beta/BMP signaling during tooth and palate development. *Dev Cell* 15, 322-329

142. Papetti, M., and Herman, I. M. (2002) Mechanisms of normal and tumor-derived angiogenesis. *Am J Physiol Cell Physiol* 282, C947-970

143. Bergers, G., and Benjamin, L. E. (2003) Tumorigenesis and the angiogenic switch. *Nat Rev Cancer* 3, 401-410

144. Nagy, J. A., Chang, S. H., Dvorak, A. M., and Dvorak, H. F. (2009) Why are tumour blood vessels abnormal and why is it important to know? *Br J Cancer* 100, 865-869

145. Folkman, J. (1971) Tumor angiogenesis: therapeutic implications. *N Engl J Med* 285, 1182-1186

146. Ferrara, N., Gerber, H. P., and LeCouter, J. (2003) The biology of VEGF and its receptors. *Nat Med* 9, 669-676

147. Ferrara, N. (2004) Vascular endothelial growth factor: basic science and clinical progress. *Endocr Rev* 25, 581-611

148. Ferrara, N., and Kerbel, R. S. (2005) Angiogenesis as a therapeutic target. *Nature* 438, 967-974

149. Jain, R. K., Duda, D. G., Clark, J. W., and Loeffler, J. S. (2006) Lessons from phase III clinical trials on anti-VEGF therapy for cancer. *Nat Clin Pract Oncol* 3, 24-40

150. Morabito, A., De Maio, E., Di Maio, M., Normanno, N., and Perrone, F. (2006) Tyrosine kinase inhibitors of vascular endothelial growth factor receptors in clinical trials: current status and future directions. *Oncologist* 11, 753-764

151. Kerbel, R. S. (2006) Antiangiogenic therapy: a universal chemosensitization strategy for cancer? *Science* 312, 1171-1175

152. Klement, G., Baruchel, S., Rak, J., Man, S., Clark, K., Hicklin, D. J., Bohlen, P., and Kerbel, R. S. (2000) Continuous low-dose therapy with vinblastine and VEGF receptor-2 antibody induces sustained tumor regression without overt toxicity. *J Clin Invest* 105, R15-24

153. Kerbel, R., and Folkman, J. (2002) Clinical translation of angiogenesis inhibitors. *Nat Rev Cancer* 2, 727-739

154. Yu, J. L., Rak, J. W., Coomber, B. L., Hicklin, D. J., and Kerbel, R. S. (2002) Effect of p53 status on tumor response to antiangiogenic therapy. *Science* 295, 1526-1528

155. Casanovas, O., Hicklin, D. J., Bergers, G., and Hanahan, D. (2005) Drug resistance by evasion of antiangiogenic targeting of VEGF signaling in late-stage pancreatic islet tumors. *Cancer Cell* 8, 299-309

156. Rusnati, M., and Presta, M. (2007) Fibroblast growth factors/fibroblast growth factor receptors as targets for the development of anti-angiogenesis strategies. *Curr Pharm Des* 13, 2025-2044

157. Suchting, S., Heal, P., Tahtis, K., Stewart, L. M., and Bicknell, R. (2005) Soluble Robo4 receptor inhibits in vivo angiogenesis and endothelial cell migration. *Faseb J* 19, 121-123

158. Heroult, M., Schaffner, F., and Augustin, H. G. (2006) Eph receptor and ephrin ligand-mediated interactions during angiogenesis and tumor progression. *Exp Cell Res* 312, 642-650

159. Yan, M., and Plowman, G. D. (2007) Delta-like 4/Notch signaling and its therapeutic implications. *Clin Cancer Res* 13, 7243-7246

160. Bergers, G., Song, S., Meyer-Morse, N., Bergsland, E., and Hanahan, D. (2003) Benefits of targeting both pericytes and endothelial cells in the tumor vasculature with kinase inhibitors. *J Clin Invest* 111, 1287-1295

161. Seki, T., Hong, K. H., and Oh, S. P. (2006) Nonoverlapping expression patterns of ALK1 and ALK5 reveal distinct roles of each receptor in vascular development. *Lab Invest* 86, 116-129

BIOGRAPHICAL SKETCH

Eun-Jung Choi was born in 1976 in Seoul, the capital city of Korea. Upon graduating from high school in 1995, Eun-Jung entered the KONKUK University in Seoul where she majored in Animal Science. During her undergraduate study, Eun-Jung joined the laboratory of Poultry and Nutrition Sciences under Dr. Chang-Won Kang's mentoring for two years. In her senior year, Eun-Jung worked in National Institute of Animal Science in Suwon. And she earned her Bachelor of Science degree in Animal and Life Sciences in 2001. In the following year, Eun-Jung entered the Master Program in Molecular Genetics and Microbiology at the University of Florida College of Medicine. Eun-Jung joined Dr. Alfred S. Lewin's laboratory and studied the ribozyme-mediated gene therapy for eye diseases. She completed her master thesis titled "Comparison of the Effects of a Processing Sequence and a Nuclear Export Element on Ribozyme Activity in Transfected Cells" and received her Master of Science degree in 2004. In the same year, to pursue her Ph.D., Eun-Jung joined the Interdisciplinary Program in Biomedical Sciences at the University of Florida College of Medicine. Since 2005, Eun-Jung has been working in the laboratory of Dr. S. Paul Oh in the Department of Physiology and Functional Genomics. Under Dr. Oh's supervision, she did her graduate work engaged in the *in vitro* and *in vivo* studies elucidating the role of a TGF-β type I receptor, Activin receptor-Like Kinase 1 (ALK1). Eun-Jung completed her Ph.D. program in August of 2009.